STUDY OF
SPACECRAFT TRANSPONDER POWER AMPLIFIER

FINAL REPORT

AUGUST 1964

Prepared for

GODDARD SPACE FLIGHT CENTER

Under Contract No.

NAS 5-3423

TRW SPACE TECHNOLOGY LABORATORIES

THOMPSON RAMO WOOLDRIDGE INC.

STUDY OF
SPACECRAFT TRANSPONDER POWER AMPLIFIER
FINAL REPORT

4104-6001-RU-000

August 1964

Prepared for

GODDARD SPACE FLIGHT CENTER

Under Contract No. NAS5-3423

TRW SPACE TECHNOLOGY LABORATORIES
Thompson Ramo Wooldridge, Inc.
One Space Park • Redondo Beach, California

Prepared for
GODDARD SPACE FLIGHT CENTER
Under Contract NAS5-3423

Prepared R. R. Cagnon
R. R. Cagnon

Prepared K. E. Lytal
K. E. Lytal

Prepared S. D. McCaskey
S. D. McCaskey
Project Engineer

Approved R. C. Booton, Jr. for
R. C. Booton, Jr.
Director
Communication Laboratory

TRW SPACE TECHNOLOGY LABORATORIES
Thompson Ramo Wooldridge, Inc.
One Space Park · Redondo Beach, California

ABSTRACT

24939

This report covers a study program conducted to investigate the feasibility of a wideband, direct RF to RF conversion communication satellite transponder, utilizing a TWT in a re-entrant mode. After amplification by the TWT, the signal(s) are frequency translated and reamplified by the same TWT. Pre- and post-amplification is provided to establish system sensitivity and dc to RF conversion efficiency. The optimum transponder type and configuration was determined, fabricated, and evaluated. Analysis of the measured performance is presented with emphasis on the baseband distortion characteristics for both single and multiple signals. Unusual characteristics of the TWT as operated in the re-entrant mode are also analyzed and presented. The gain, output power, and noise figure obtained with the re-entrant transponder were established to be consistent with the basic requirements of a communication satellite. The major advantage offered is reduced transponder complexity and the extremely wide bandwidths which can be realized.

Author

CONTENTS

ILLUSTRATIONS

ILLUSTRATIONS (Continued)

ILLUSTRATIONS (Continued)

ILLUSTRATIONS (Continued)

ILLUSTRATIONS (Continued)

1.0 INTRODUCTION

Advanced communication satellite studies as performed by STL for NASA indicate the need to extend transponder bandwidth capabilities in order to provide an optimum balance between information rate, bandwidth, and reasonable satellite output power.

Present satellite transponder configurations for RELAY, SYNCOM, and TELSTAR use some form of a basic superheterodyne receiver followed by a frequency upconverter and a traveling wave tube (TWT) power amplifier. The majority of the amplification takes place at some low intermediate frequency. While this technique has the advantage of being well within the "state-of-the-art," it has several disadvantages for future advanced communication satellites. The two most prominent disadvantages of present configurations are:

1) Such systems presently appear to be bandwidth limited to 40 or 50 mc

2) Spurious responses inherent with the use of frequency conversion and multiplication equipment introduce a definite problem when more than one wideband channel is envisioned

It was the objective of this program to investigate a more advanced communication satellite transponder which takes advantage of RF amplification at or near the received or the transmitted frequency. This was accomplished by utilizing a TWT in a re-entrant mode, coupled with a low noise front end and an output power amplifier.

2.0 BASIC CONSIDERATIONS FOR A RE-ENTRANT TWT REPEATER FOR COMMUNICATION SATELLITES

2.1 TYPE OF REPEATER

The first consideration in the design of a communication satellite repeater is the type of repeater. By type, we mean here the basic method of transferring the information from the received carrier to the transmitted carrier. Four principal types can be identified.

1) The Linear Translator

The incoming carrier is simply translated to the transmitting frequency band by linear mixing with spacecraft local oscillators. Amplification can be accomplished partially at radio frequency and partially at intermediate frequency or entirely at radio frequencies. The modulating information remains essentially unchanged by the passage through the repeater.

2) The Frequency Multiplier

In this repeater, the received carrier is multiplied in frequency at some point in the amplifying chain. Generally, linear translations will also be involved. Because of the nonlinear multiplication, some form of angle modulation must be employed in the system. Also, since both signal and noise deviations are multiplied by the same factor as the carrier frequency, this type of repeater adversely affects the uplink noise contribution. On the other hand, input and output RF bandwidths can be different, allowing separate matching of up and downlinks to ground station characteristics.

3) The Modulation Converter

An extra degree of freedom exists in this repeater in that the up and downlink modulation forms need not be the same. Thus, the uplink might employ a bandwidth-conserving modulation and a high power transmitter, while the downlink

might use a modulation which efficiently trades bandwidth for limited satellite transmitter power. A particular example of this repeater is the SSB/FM system which transmits single sideband voice channels to the spacecraft and receives an FDM/FM carrier in return. In principle, a SSB/FM repeater can accomplish the conversion at intermediate frequency, thereby eliminating the weight and signal distortion added by baseband equipment.

4) The Demodulator-Modulator

This repeater demodulates the received information to baseband and then remodulates the transmitted carrier. Processing of the information can obviously be accomplished at baseband. In a system using PCM modulation, for example, the pulses can be regenerated, making the downlink the only contributor to system thermal noise. In multichannel telephony, individual groups of voice channels can be rearranged according to destination.

From this brief review of satellite repeater types, it is clear that the re-entrant TWT repeater is most appropriate for operation as a linear translator or perhaps a frequency multiplier. The other two types generally require a reduction to intermediate or baseband frequencies which would tend to negate the advantages of the re-entrant repeater. Henceforth, then, we shall assume that the repeater will function either as a linear translator or frequency multiplier.

2.2 POWER OUTPUT

The previous categorization of repeater types was premised on different behavior with respect to S/N ratio performance.[1] This is entirely appropriate for a communication satellite system in which the ultimate capacity is basically limited by thermal noise. Furthermore,

[1] J. A. Develet, Jr., "Selected Topics on Modulation Systems for an Active Wideband Communication Satellite," STL 8949-0006-NU-000, 23 April 1961.

for some time to come, such satellites will be limited in prime power and therefore transmitted power. Thus, the downlink will be the determining factor in system thermal noise performance. After specifying the modulation and repeater type, the choice of transmitter power output is the next important step.

In an overall communication satellite design, the available power for the transmitter is determined by the orbital characteristics, launch vehicle capability, power subsystem design, and requirements of other subsystems such as attitude control. Without a specific application for the re-entrant repeater at present, the best that can be specified here is a range of interest for power output. It appears that transmitter powers of three to thirty watts will satisfy most of the present and near future communication requirements. The lower limit is established by the expressed intent of using the repeater for the transmission of several hundred CCIR quality telephone channels or high-fidelity television. The upper limit arises from the payload capabilities of present boosters and the prime power requirements of the transmitter. The latter directly affects the weight of the power subsystem which comprises 50 to 60 percent of the total weight of current communication satellites.

In passing, it should be noted that an upper limit in power output is imposed by the necessity of avoiding excessive interference with ground microwave relay systems sharing the same frequency band. The CCIR is presently considering a recommendation that received ground power from satellite transmissions be limited to a specific power level.

2.3 NOISE FIGURE

The spacecraft noise figure directly affects the noise contribution of the uplink and therefore deserves careful attention. Again, this parameter should be specified in light of a complete system design; however, a range of values can be established as follows. First, assuming that the antenna illuminates only the earth, the lower limit is determined by the fact that the spacecraft antenna noise temperature will be essentially that of the earth which it views exclusively. If the antenna illuminates a larger area than the earth, its noise temperature may be less but at the expense of antenna gain. There is little point in reducing

the receiver noise temperature below that of the antenna, which is about 300°K. The corresponding noise figure is 3 db. The upper limit on the noise figure can be set by reference to good design practice and the state of the art in receivers. A conventional mixer or medium noise TWT should be able to achieve a noise figure in the vicinity of 10 db or noise temperature of 3000°K.

The repeater noise figure having been established in the range of 3 to 10 db (300-3000°K), a further refinement can be accomplished. In general, it is good system design practice to minimize the effect of uplink thermal noise. In Appendix C, an expression for this effect is derived for the usual communication satellite system. This is:

$$\frac{(S/N)_D}{(S/N)_T} = 1 + \frac{(S/N)_g}{(S/N)_s} \simeq 1 + \frac{P_s T_s}{P_g T_g} \qquad (2\text{-}1)$$

where

$\frac{(S/N)_D}{(S/N)_T}$ = uplink noise contribution

$(S/N)_s$ = predetection S/N ratio in satellite

$(S/N)_g$ = predetection S/N ratio in ground station due to downlink only

$P_{s,g}$ = transmitter power on satellite, ground

$T_{s,g}$ = noise temperature on satellite, ground

Equation (2-1) is valid provided:

1) The same ground antenna is used for transmitting and receiving so that increased gain at the higher frequency is offset by greater "free space" path loss

2) The satellite antenna is gain-limited by the requirement of illuminating the total area visible on the earth at both transmit and receive frequencies, or by virtue of being an isotropic radiator

3) The satellite repeater is a linear translator. However, the relation could be readily modified to take into account frequency multiplication

4) The transmitter powers and noise temperatures are total effective values including any line or other losses

The interesting conclusion to be drawn from (2-1) is that, for fixed ground station parameters and a fixed allowable uplink noise contribution, the transmitted power and total noise temperature are inversely proportional. That is, the greater the output power, the smaller the repeater noise figure should be. For the ranges developed above, a repeater with 30 watts of transmitter power should be associated with the 3 db noise figure, whereas a three-watt transmitter should be associated with the 10 db noise figure. Stated in general terms, the rule is that the better the downlink with regard to noise performance, the better the uplink must be to avoid degrading it.

2.4 GAIN

The basic requirement on repeater gain is simply that there be sufficient power amplification to raise the received power to the transmitted power level with a margin to allow for long-term degradation. The range of gain will depend on the input dynamic range since the output power will generally be held constant. The input dynamic range is determined by system design constraints, such as orbital altitude, maximum and minimum ranges, antenna patterns and look angles, minimum and maximum ground transmitter powers, power programming, etc. Usually, some form of automatic gain control or limiting will be required to provide a nearly constant output power in the face of input power variations.

An estimate of the gain required in a typical repeater may be developed by reference once again to (2-1). The minimum allowable signal received at the satellite can be determined by requiring that the uplink contribution be no more than 3 db, i.e., $(S/N)_s = (S/N)_g$. At this point we must make an assumption about the minimum (S/N) required. For phase-lock demodulation of wideband FDM/FM telephony, for example, the minimum (S/N) in the loop noise bandwidth, B_N, is

7 db.[2] With a 6 db margin included, then, the minimum allowable S/N ratio in the receiver loop bandwidth is 13 db. This corresponds to a S/N ratio, $(S/N)_s$, in an equal bandwidth at the spacecraft of 16 db, since 3 db has been allowed for uplink contribution. With the repeater noise figure and power output specified as above, the repeater gain for the minimum received signal is given by

$$G_m \simeq \frac{P_s}{40\, k\, T_s\, B_N} \qquad (2\text{-}2)$$

For example, using the previously determined values $P_s = 3$ watts and $T_s = 3000^{\circ}K$,

$$G_m = \frac{1}{5.52 \times 10^{-19}\, B_N}$$

or in decibels

$$G\,(db) = 182.6 - 10 \log B_N\,(cps) \qquad (2\text{-}3)$$

As an example, the STL phase-lock demodulator developed for RELAY has a noise bandwidth B_N of 25 mc. The indicated spacecraft gain for a system employing this demodulator is therefore 109 db. For the re-entrant TWT repeater, it is reasonable that the noise bandwidth may be 500 mc or more and hence require only 96 db or less of gain. It must be noted carefully that (2-2) and (2-3) give only a rough estimate of required gain. First, from (2-2), the gain is a function of the ratio of P_s over T_s. In the discussion of noise figure, it was observed that it is desirable to keep the product of P_s and T_s constant. Choosing the other extremes of the ranges of interest in these parameters would therefore have resulted in the factor 182.6 db in (2-3) being some 17 db greater. Another consideration which will increase the required repeater gain is the necessity of allowing a margin for long term degradation.

---

[2] J. A. Develet, Jr., "Coherent FDM/FM Telephone Communication," Proc. IRE, September 1962.

This gain margin should be from 10 to 20 db. Thus, the design gain for the repeater could be as much as 37 db greater than that called for by (2-3).

Another factor emerges from (2-2). With an additional 10 db gain allowed for margin, the repeater is, at least initially, capable of raising a signal only 5 db above the noise in a bandwidth equal to that of the phase-lock demodulator to full power output. The noise bandwidth of the repeater will not generally be the same as that of the phase-lock demodulator on the ground. However, there is no point in making the repeater gain greater than that required to saturate the transmitter with amplified receiver noise:

$$G_n = \frac{P_s}{k T_s B_{N,s}} \qquad (2\text{-}4)$$

Comparing (2-2) and (2-4), it is clear that for $B_{N,s} < 40\ B_{N,g}$, $G_m < G_n$ and (2-2) should be used to determine the maximum gain. The gain is maximum in the sense that the minimum allowable signal was postulated in deriving (2-2) and higher gain will degrade the S/N achievable at the output of the repeater. Stronger signals might in fact be used. For a multiple access satellite, it is conceivable that $B_{N,s} > 40\ B_{N,g}$ since several information bands are amplified simultaneously. In this case, (2-4) will establish the maximum gain. Again, assuming a 500 mc noise bandwidth $B_{N,s}$, this maximum gain is seen to be 112 to 129 db for the re-entrant repeater depending on the values chosen for P_s and T_s.

The dynamic range of the repeater may be defined as the difference between the minimum and maximum signals which will drive the transmitting TWT output to within a specified level of the nominal power output, say one decibel. The dynamic range will vary as the repeater components age. At the design end of life, the minimum signal can be taken as in (2-2) or $40\ k T_s B_{N,g}$. (As noted above, it is possible in a multiple access repeater that the noise level becomes the effective minimum signal.) The maximum signal will depend on the exact orbital and ground station characteristics and is difficult to state

in general. However, the repeater must provide the required gain reduction in the form of hard or soft limiting and/or automatic gain control to accommodate the maximum signal.

2.5 BANDWIDTH AND SPECTRUM UTILIZATION

The repeater bandwidth can be defined in several different terms. The total equivalent noise bandwidth concept was used above to study the noise figure and gain requirements. The noise bandwidth of the phase-lock demodulator which ultimately demodulates the FDM/FM telephony signal was also introduced. The repeater bandwidth can also be expressed as the band between points in the gain-frequency characteristic where the gain is down a specified amount from midband gain. One db and three db bandwidths are useful concepts. In an FM system, it would perhaps be more meaningful to refer to points on the phase- or delay-frequency characteristics since these are more significant determinants of system performance.

Of course, inherent in the specification of any of these bandwidths is the concept of spectrum occupied by the signal. Spectrum occupancy is often defined as the frequency range within which 99 percent of the signal energy resides. Another useful rule-of-thumb for the spectrum occupancy of FM systems is

$$\text{spectrum occupancy} = 2f_p + 2f_m \qquad (2\text{-}5)$$

where

f_p = peak frequency deviation

f_m = maximum modulation frequency

Spectrum utilization can be defined as the percentage of spectrum occupied by the signals in the total band allocation including guard bands. Guard bands between independent communication carriers are required because of many considerations: doppler shifts, oscillator instabilities, filter gain- and delay-frequency characteristics, direct interference, and intermodulation distortion.

In a multiple access satellite, spectrum utilization is of prime importance. For example, a source of poor spectrum utilization is the necessity of maintaining close control of transmission characteristics within filter passbands, thereby dictating less sharp cutoff slopes than otherwise. For example, the RF spectrum of a high deviation FDM/FM telephony signal is given by

$$W(f) = W(f_c) \exp\left[- (f - f_c)^2 / 2 f_{rms}^2 \right] \qquad (2\text{-}6)$$

Using the 99 percent criterion, the spectrum occupancy of this signal is $5.2\ f_{rms}$. In practice, however, it is found necessary to make the 1 db bandwidth more nearly equal to the other spectrum occupancy. For example, for a 300-channel FDM/FM system

$$2 f_p + 2 f_m = 9.8 f_{rms} \text{ -- } 10.8 f_{rms}$$

depending on the required channel quality at receiver threshold. The "extra" bandwidth results from the necessity of having a nearly constant delay-frequency characteristic to avoid intermodulation distortion.

2.6 BASEBAND DISTORTION

In general terms, baseband distortion is the variation of the received baseband signal from the original input baseband. However, for the re-entrant TWT repeater, the primary concern is with low nonlinearities of the repeater which affect the received baseband and not with distortion introduced by the modulation-demodulation process.

Nonlinear distortion can arise from any of the various nonlinearities that may be in the system; however, the effect of any particular nonlinearity may be more or less significant depending on the frequency, modulation, etc. The nonlinear phenomena of greatest interest here are differential gain and phase and AM to PM and FM to AM conversion. The following derivations of differential gain and phase are presented here as an aid in defining these terms and how they can be measured.

2.6.1 Differential Gain

Differential gain is defined by the IRE as the difference between (a) the ratio of the output amplitudes of a small, high frequency sine wave signal at two stated levels of a low frequency signal on which it is superimposed, and (b) unity.

That is, consider an input-output characteristic such as shown in Figure 2-1.

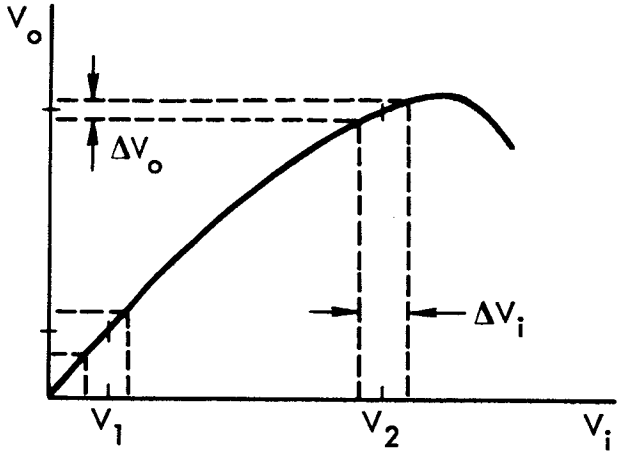

Figure 2-1. Input-Output Characteristics

where ΔV_i is the peak-to-peak input amplitude of the small signal

ΔV_o is the peak-to-peak output amplitude of the small signal

then, differential gain is

$$DG = \frac{\Delta V_o \text{ (of the small signal)} \,\big|\, V_i = V_1}{\Delta V_o \text{ (of the small signal)} \,\big|\, V_i = V_2} - 1$$

The differential gain can be measured by applying a signal to the system of the form:

$$V_i(t) = V(t) + v \cos \omega_h t$$

and recovering the amplitude of the high frequency term at ω_h

where

$V(t)$ is a large amplitude sweep signal with frequency $\omega_l < \omega_h$

v (which corresponds to ΔV_i above) is a constant amplitude small compared to $V(t)$

Then, expressing the input-output characteristic in a three-term power series,

$$V_o(t) = a_1 V_i(t) + a_2 V_i^2(t) + a_3 V_i^3(t)$$

the output, after filtering out the low frequency terms is

$$V_o'(t) = A_1 \cos \omega_h t + A_2 \cos 2\omega_h t + A_3 \cos 3\omega_h t$$

where

$$A_1 = v\left[a_1 + \frac{3}{4} a_3 v^2 + 2a_2 V(t) + 3a_3 V^2(t)\right]$$

$$A_2 = \frac{v^2}{2}\left[a_2 + 3a_3 V(t)\right]$$

$$a_3 = \frac{v^3}{4} a_3$$

A_1 is the envelope amplitude of the recovered high frequency term and represents ΔV_o as $V(t)$ sweeps over its range.

Thus, differential gain (DG) is determined by the ratio of the envelope values at two different points on the sweep.

$$DG = \frac{A_1 \Big|_{V(t) = V_1}}{A_1 \Big|_{V(t) = V_2}} - 1$$

The two points V_1 and V_2 are often chosen where the envelope is minimum and maximum respectively, giving the maximum differential gain over the sweep range.

Differential gain may be expressed in differential form by writing

$$\Delta V_o = \frac{\partial V_o}{\partial V_i} \Delta V_i$$

then

$$DG = \frac{\partial V_o / \partial V_i \Big| V_i = V_1}{\partial V_o / \partial V_i \Big| V_i = V_2} - 1$$

since ΔV_i is fixed

$$= \frac{a_1 + 2a_2 V_1 + 3a_3 V_1^2}{a_1 + 2a_2 V_2 + 3a_3 V_2^2} - 1$$

This differs from the previous expression in that the compression term $3/4\ a_3 v^2$ is not included. However, assuming the system is basically linear, this term is generally small compared to a_1 and may be safely neglected.

For an amplitude modulated signal, the effect of differential gain is to compress (or expand) the modulation. In addition, particularly for more complex signals such as FDM, harmonics and cross-product terms due to the higher order terms of the expansion (i.e., $V_i^2(t)$ and $V_i^3(t)$) will fall back in the output baseband and give rise to intermodulation noise. In FM systems, the distortion effects due to differential gain occur primarily in the baseband equipment.

2.6.2 Differential Phase

Differential phase (DP) is defined by the IRE as the difference in phase shift through the system for a small high frequency sinewave signal at two stated levels of a low frequency signal on which it is superimposed

$$DP = \phi \Big| V_1 - \phi \Big| V_2$$

where ϕ = phase shift of small, high frequency signal

V_1, V_2 = amplitude levels of the low frequency signal

For an FM system, the differential phase may readily be measured by the system shown in Figure 2-2.

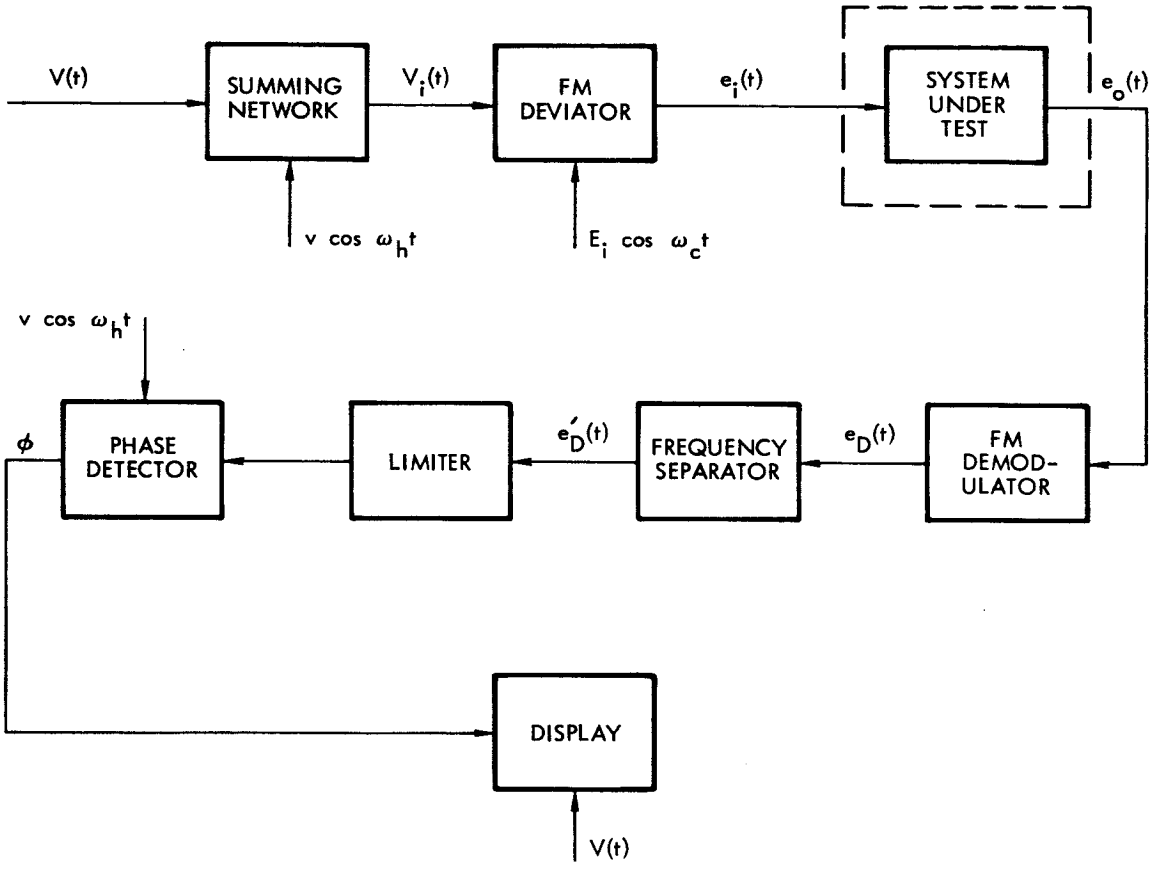

Figure 2-2. Test Setup for Measurement of Differential Phase (Envelope Delay)

The signal applied to the FM deviator is of the same form as that used to measure differential gain.

$$V_i(t) = V(t) + v \cos \omega_h t$$

Then, the signal out of the FM deviator $e_i(t)$ is

$$e_i(t) = E_i \cos \left[\omega_c t + \theta(t) \right]$$

where

$$\dot{\theta}(t) = k_1 \left[V(t) + v \cos \omega_h t \right] = \omega_i$$

E_i = amplitude of the FM signal

ω_c = FM carrier frequency

k_1 = modulator constant

ω_i = frequency deviation from carrier

Assuming a phase frequency characteristic for the system under test as shown in Figure 2-3,

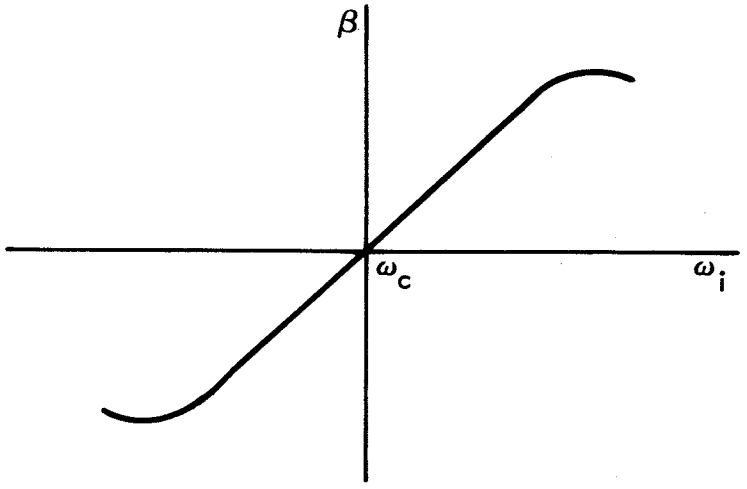

Figure 2-3. Phase Frequency Characteristic

a phase shift β is introduced at the output as a function of the input frequency deviation $\omega_i = \dot{\theta}(t)$, resulting in a signal at the output of the system of the form

$$e_o(t) = E_o \cos \left[\omega_c t + \theta(t) + \beta(\omega_i) \right]$$

The frequency deviation (time derivative of phase) seen at the FM demodulator is then

$$\omega_o = \dot{\theta}(t) + \dot{\beta}(\omega_i)$$

and the corresponding FM demodulator output is

$$e_D(t) = k_2 \omega_o = k_2 \left[\dot{\theta}(t) + \dot{\beta}(\omega_i) \right]$$

where

k_2 = demodulator constant

Writing $\dot{\beta}(\omega_i) = \frac{d}{dt} \beta(\omega_i) = \frac{d\beta(\omega_i)}{d\omega_i} \frac{d\omega_i}{dt}$

and

$$\frac{d\omega_i}{dt} = \ddot{\theta}(t) = k_1 \left[\dot{V}(t) - v \omega_h \sin \omega_h t \right]$$

the above expression for $e_D(t)$ becomes

$$e_D(t) = k_1 k_2 \left[V(t) + v \cos \omega_h t + \frac{d\beta(\omega_i)}{d\omega_i} \left(\dot{V}(t) - v\omega_h \sin \omega_h t \right) \right]$$

After filtering out the low frequency terms in $V(t)$ and $\dot{V}(t)$, the high frequency component of the output is

$$e_D'(t) = k_1 k_2 v \left[\cos \omega_h t - \omega_h \frac{d\beta(\omega_i)}{d\omega_i} \sin \omega_h t \right]$$

$$= A \cos (\omega_h t + \phi)$$

where

$$A = k_1 k_2 v \left[1 + \left(\omega_h \frac{d\beta}{d\omega_i} \right)^2 \right]^{1/2}$$

$$\phi = \tan^{-1}\left(\omega_h \frac{d\beta}{d\omega_i}\right)$$

Clearly, ϕ is the phase shift of the high frequency signal ω_h. The magnitude of ϕ is detected with a phase detector and displayed versus either the sweep amplitude $V(t)$ or the frequency deviation corresponding to $V(t)$.

$$DP = \phi \Big|_{V(t)=V_1} - \phi \Big|_{V(t)=V_2} = \phi \Big|_{\omega_i=\omega_1} - \phi \Big|_{\omega_i=\omega_2}$$

Usually, in any case of interest, the phase shift is small and $\tan\phi$ can be replaced by ϕ obtaining

$$\tan\phi \simeq \phi = \omega_h \frac{d\beta}{d\omega_i}$$

$\frac{d\beta}{d\omega}$ is called the envelope delay and is the variable generally plotted versus frequency rather than differential phase

It is seen that envelope delay is proportional to the derivative of phase with respect to frequency (slope of the phase-frequency characteristic) and it is the departure of this variable from a flat characteristic which causes distortion. Typically, the delay frequency characteristic can be resolved into a linear portion and a parabolic portion. This may be seen more clearly by expressing the phase frequency characteristic in a three-term power series

$$\beta = b_i \omega_i + b_2 \omega_i^2 + b_3 \omega_i^3$$

and envelope delay

$$\tau_d = \frac{d\beta}{d\omega_i} = b_1 + 2b_2\omega_i + 3b_3\omega_i^2$$

Thus, linear delay corresponds to second order phase distortion and parabolic delay corresponds to third order phase distortion. The

constant delay b_1 corresponds to linear phase and does not cause distortion of the baseband signal.

2.6.3 AM to PM and FM to AM Conversion

In FM systems, these two types of distortion are not too significant in themselves but are important when considered together. This may be seen for the re-entrant TWT repeater by considering an FDM signal of constant amplitude applied to the input of the TWT. The non-flat gain frequency characteristic of the tube will cause the output to have a varying amplitude (FM to AM). When this signal is fed back through the TWT, AM to PM conversion will transfer the amplitude variations back onto the FM and cause distortion of the output FM signal. Actually, since many signals are present at once, this process can occur within the tube and in an FDM/FM system can cause intelligible crosstalk. If complementary channel operation is used where the talker talks and listens in the same channel, the result is an echo.

3.0 RE-ENTRANT TRANSPONDER

3.1 GENERAL

A block diagram of the basic transponder configuration is shown in Figure 3-1. The system consists of a low noise tunnel diode pre-amplifier, the re-entrant loop TWT with its associated diplexer filter and down converter, and a power amplifier.

Assuming an output power of 3 to 4 watts, the considerations of Sections 2.3 and 2.4 indicate a required noise figure of 10 db and overall transponder gain of 100 to 110 db. Thus, allowing a gain of 35 db for the power amplifier and 15 db for the preamplifier, the re-entrant loop gain is determined to be 50 to 60 db. Therefore, for the re-entrant TWT, a low power tube with a small signal gain of 35 to 40 db and saturated power output of about 30 milliwatts will provide enough excess gain to accommodate the down converter and diplexer losses and still yield a usable output signal well below saturation. Although other assignments of gain and power distribution can obviously be made, the above assumptions are reasonable and the loop components were selected and evaluated on this basis.

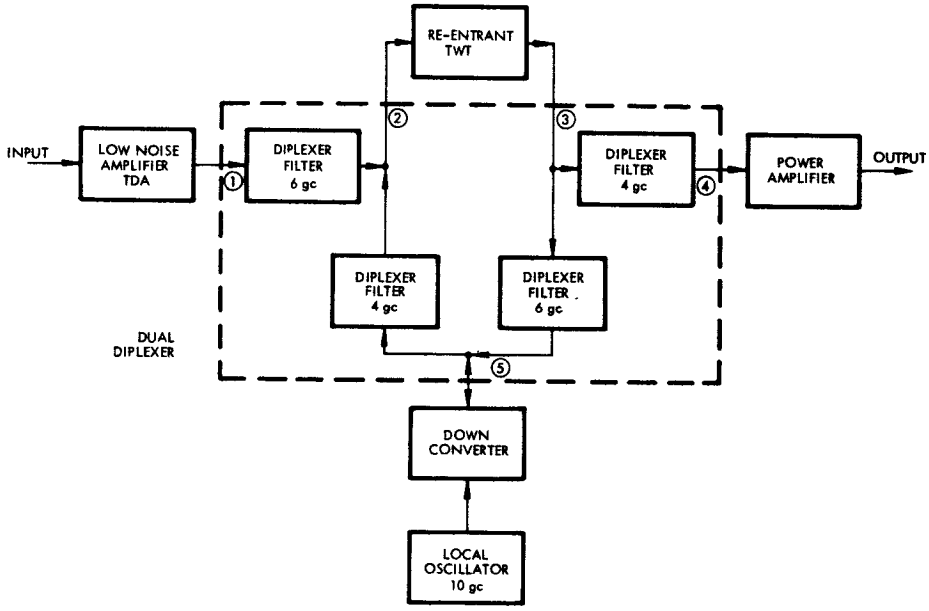

Figure 3-1. System Block Diagram

Multiple access is one of the most attractive possible applications of the re-entrant transponder. For this case it is necessary to operate the re-entrant TWT well below saturation to minimize distortion. This is also true of the power amplifier if all the signals are amplified by the PA. However, dc power and efficiency considerations make it undesirable to operate the PA much below saturation. Therefore, separate power amplifiers would likely be necessary for every one or two carriers. The relative inefficiency of operating the loop tube below saturation is of little consequence in this case.

As the transponder was not designed for any specific application, no effort was made to optimize the overall system. Rather, the objective was to design and package the transponder to be as versatile as possible and enable evaluation of the re-entrant loop over a wide range of input signals. To this end, the system was packaged to allow ready access to all the components. In addition, the loop was allowed to run at maximum gain and the losses required to limit overall gain inserted between the re-entrant loop and power amplifier and/or tunnel diode amplifier. The final package is pictured in Figures 3-2 to 3-4, and Figure 3-5 shows a drawing of the package.

3.2 RE-ENTRANT LOOP TWT

The major area of investigation in this project is the re-entrant loop portion of the transponder and selection of a suitable traveling wave tube. Due to the uncommon nature of this application, there was virtually no desired information available. In an effort to find a tube compatible with the requirements of a re-entrant loop, a survey of potentially usable TWT's was made and two selected for evaluation.

One of these tubes is a General Electric ZM-3110 which exhibits the following characteristics:

1)	Frequency	4 to 8 gc
2)	Small signal gain	30 db
3)	Noise figure	15 db

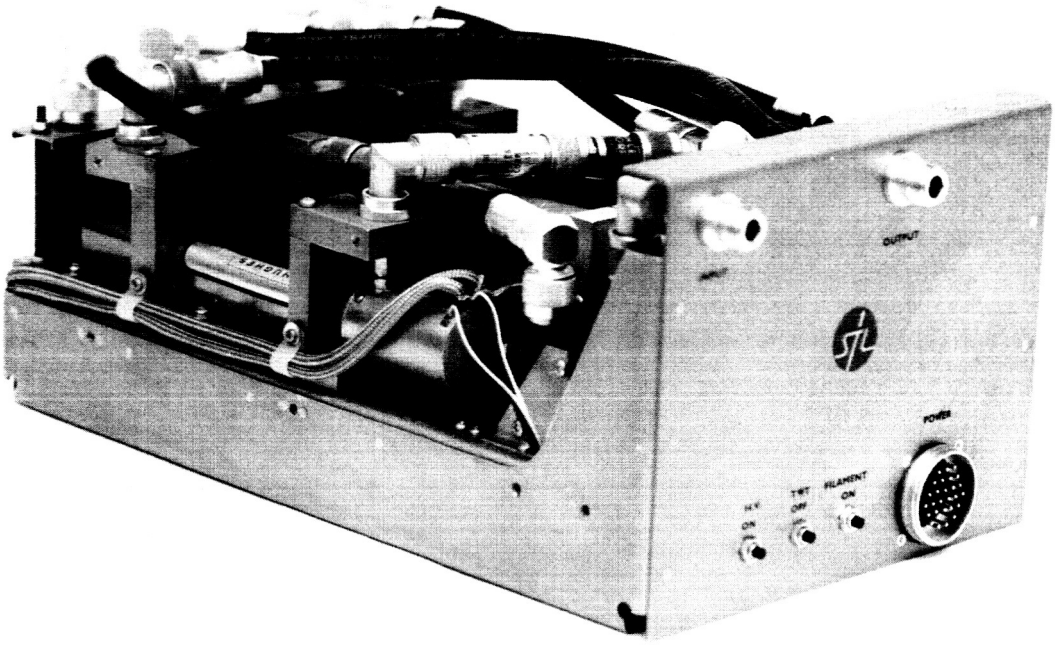

Figure 3-2. Re-entrant Transponder Configuration

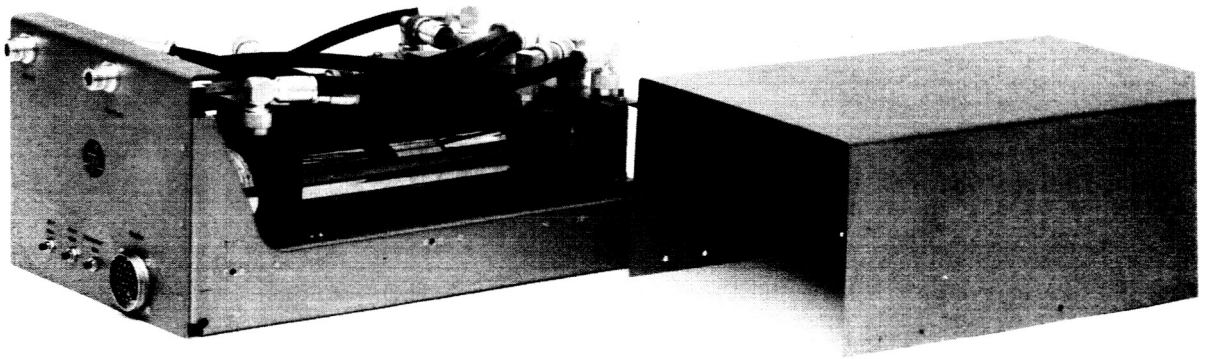

Figure 3-3. Re-entrant Transponder Configuration

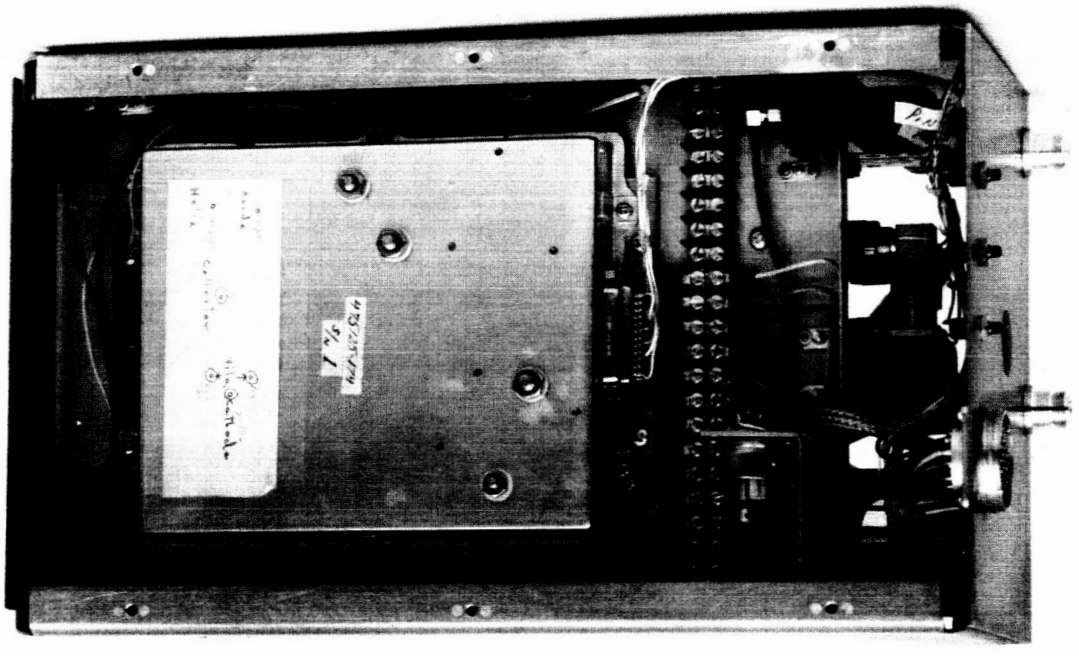

Figure 3-4. Re-entrant Transponder Configuration

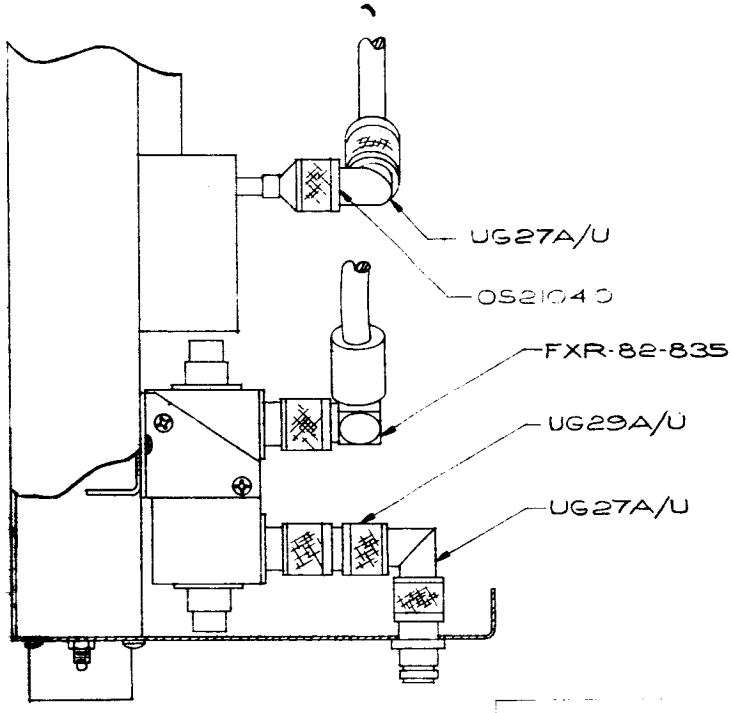

UG27A/U

UG23A/U

HIGH LEVEL TWT
POWER AMPLIFIER
HUGHES # 384-H

(TOP) STL CONVERTER
(BOTTOM) ATTENUATOR
WINCHELL 6 DB

TUNNEL DIODE
AMPLIFIER

UG30/

TABLE			
PIN NO.	DESCRIPTION	VOLTAGE	FUNCTION
1	LOCAL OSC.	+28	OSCILLATOR
2	LOCAL OSC.	+28	XTAL OVEN
3	LOCAL OSC.	-28	COMMON GRD
4	TUNNEL DIODE	+12	AMPLIFIER
7	TUNNEL DIODE	-12	AMPLIFIER
5	TIME DELAY REL.	6.3VAC	RELAY
6	TIME DELAY REL.	6.3VAC	RELAY
9	CONTROL BOX (HUGHES)	+15	CONTROL BOX
11	↑ ↑ ↑	-15	↕ ↕
20	↓ ↓ ↓	+31	↓
24	CONTROL BOX (HUGHES)	-31	CONTROL BOX
15	M.E.C. TV/T	5VAC	HEATER GRD
16	↑ ↑	—	CATHODE GRD
10		5VAC	HEATER
21		-22.2	GRID #1
25		31.7	GRID #2
22		58.2	GRID #3
24		329	GRID #4
18		836	HELIX
13	↓ ↓	900	COLLECTOR
27	M.E.C. TWT	—	GRD CAP
ALL OTHER PINS SPARES			

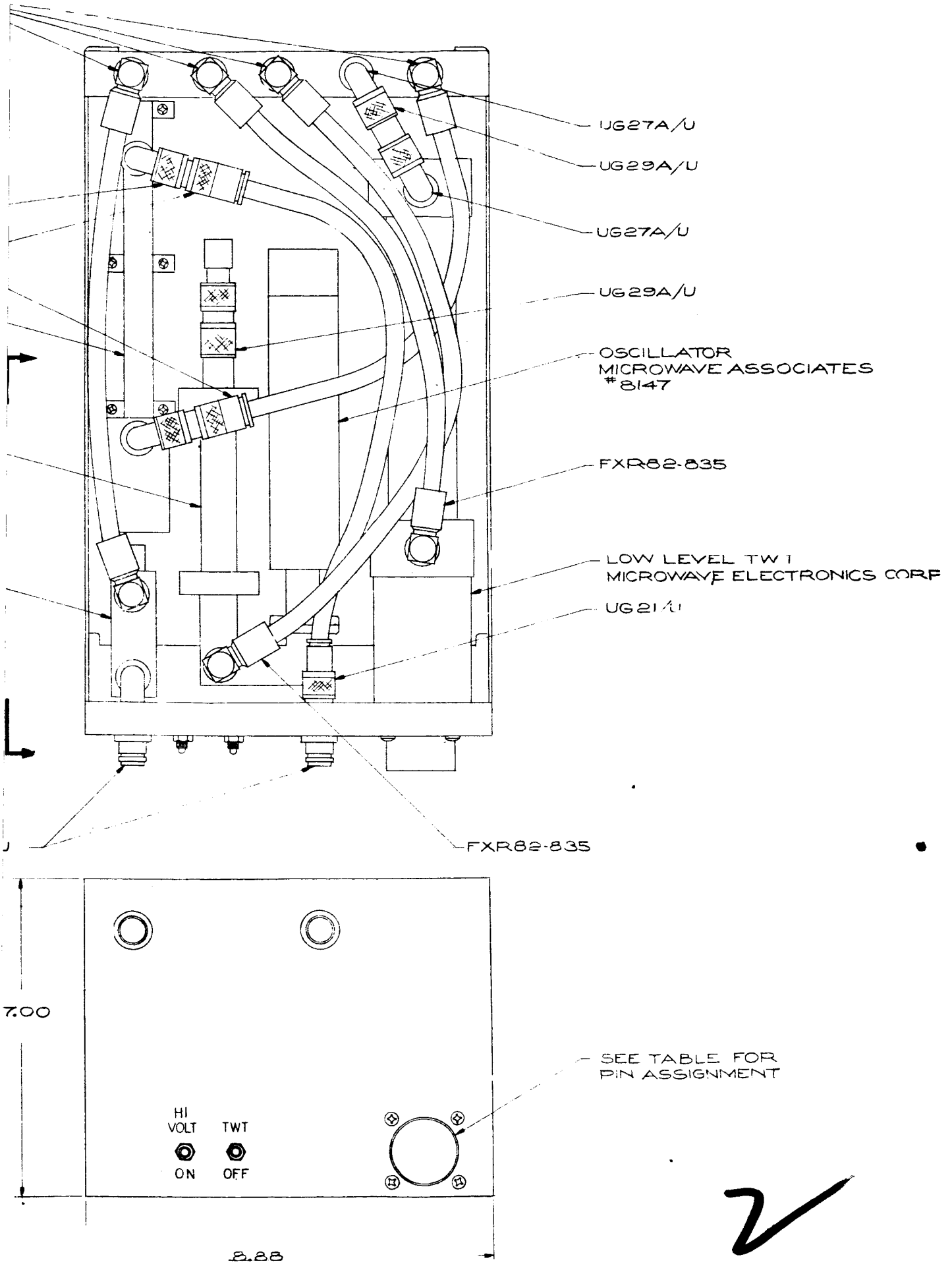

Figure 3-5. Re-entrant Transponder Outline Drawing

4)	Power output	10 mw
5)	Focusing	PPM

The second tube is a modified Microwave Electronic Corporation M-2112 (MEC-M-5184) ordered with the following specialized characteristics:

1)	Frequency	3.7 to 6.43 gc
2)	Small signal gain	35 db min (40 db objective)
3)	Gain variation	(see note 1)
4)	Noise figure	15 db max
5)	Focusing	PPM

Note 1: In any 50 mc segment in the frequency ranges of 3.70 to 4.20 and 5.91 to 6.43 gc, the total gain variation including gain fine structure, shall be $\pm$ 0.1 db maximum as an objective.

Results of the TWT evaluation are shown in Figures 3-6 through 3-24. The curves are paginated in a manner to facilitate comparison between the MEC-M-5184 and the GE ZM-3110: i.e., for those tests which were performed on both tubes, the results obtained with the M-5184 are followed by those for the ZM-3110.

Figures 3-6 to 3-9 show the power-in versus power-out and gain-frequency characteristics of the tubes respectively. In an effort to provide valid comparison between the two tubes, it is convenient to normalize the input power readings to a power we shall call P_S [3]. This is a reference input power level, equal to the saturated power output divided by the small signal power gain. This power level is less than the input power required to saturate the TWT by a factor equal to the gain compression, c, at saturation. The value of P_S is indicated in Figures 3-6 and 3-7 by the dashed lines for the different frequencies. The closeness of the curves in Figure 3-6 is indicative of a nearly flat gain-frequency characteristic which is also seen in Figure 3-8.

Noise figure versus frequency is shown in Figures 3-10 and 3-11. Figures 3-12 and 3-13 compare the gain and phase characteristics of the two tubes. Figure 3-12 shows that the gain of the M-5184 is exceptionally

[3] J. L. Putz, Private Communications, August 1963, General Electric Power Tube Division, Palo Alto, California.

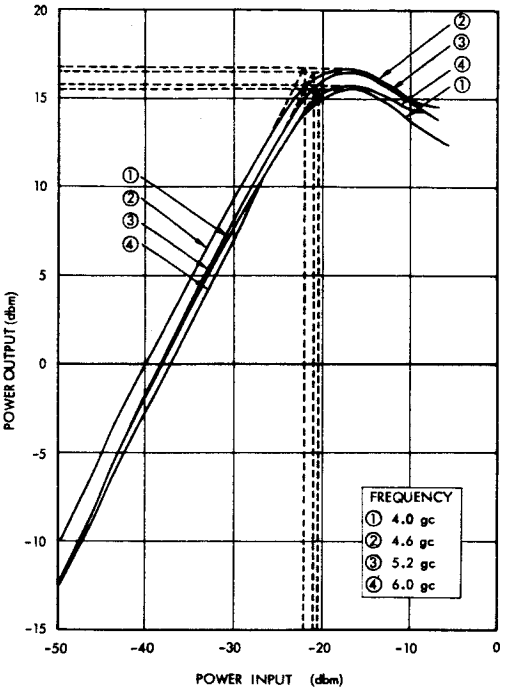

Figure 3-6. Power Output vs Power Input
TWT -- MEC M-5184, S/N 100

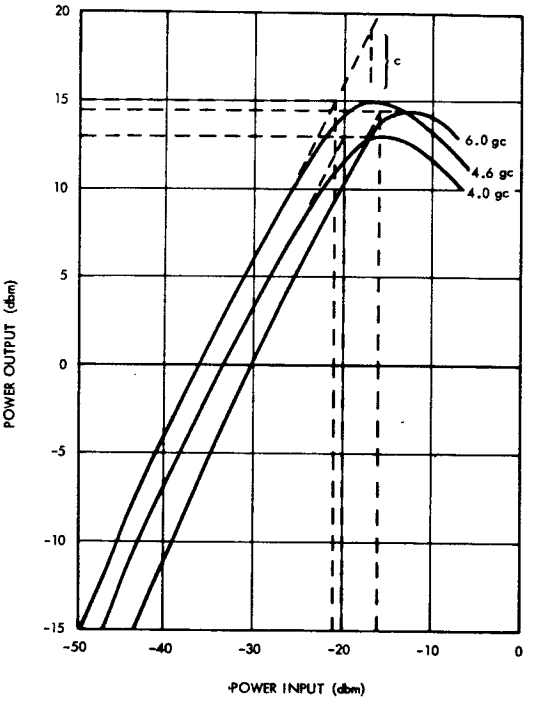

Figure 3-7. Power Output vs Power Input
TWT -- GE ZM-3110

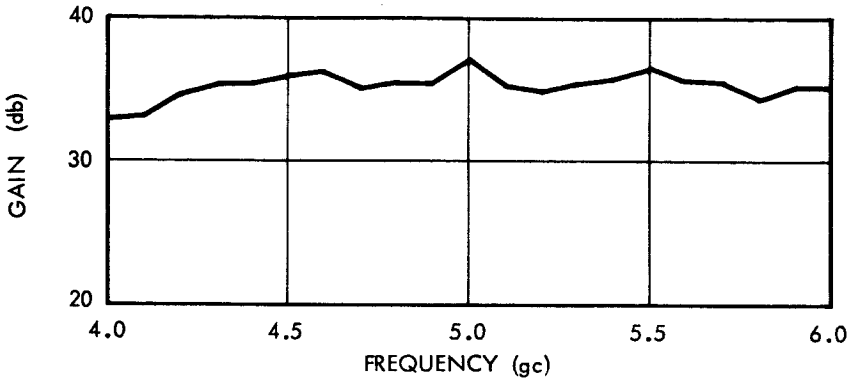

Figure 3-8. Saturation Gain vs Frequency
TWT -- MEC M-5184, S/N 100

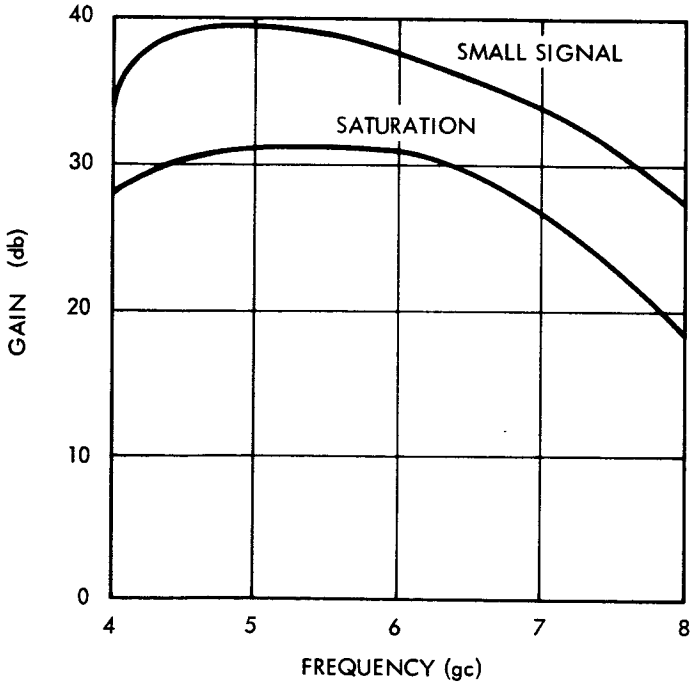

Figure 3-9. Gain vs Frequency
TWT -- GE ZM-3110

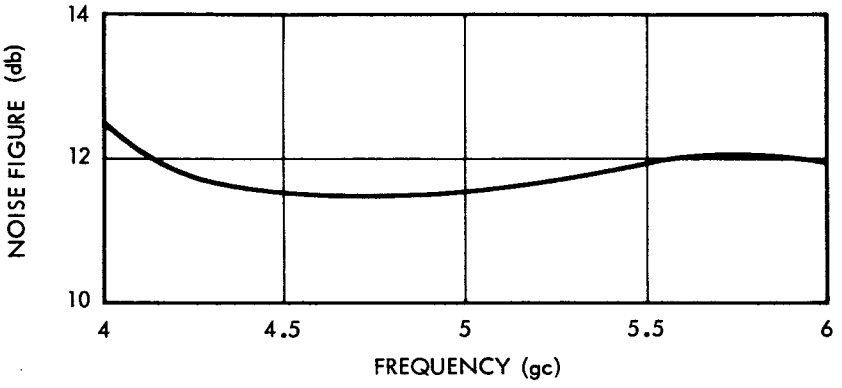

Figure 3-10. Noise Figure vs Frequency
TWT -- MEC M-5184, S/N 100

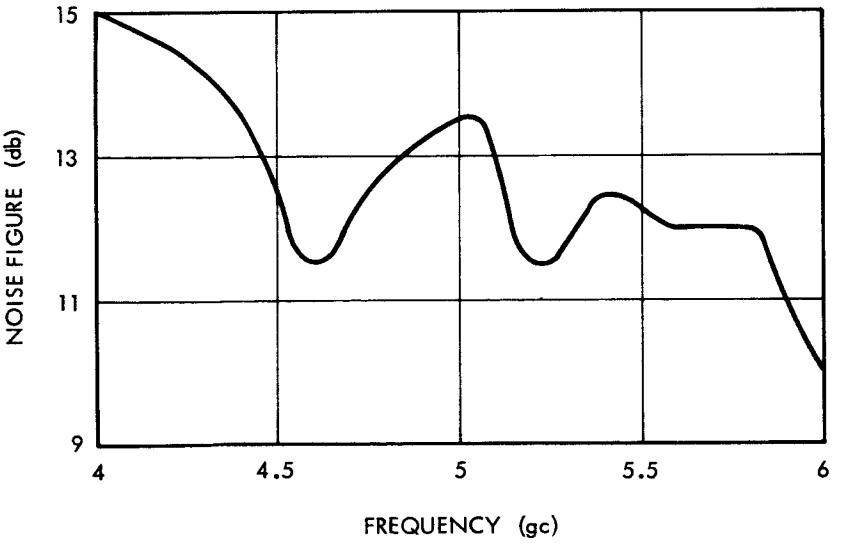

Figure 3-11. Noise Figure vs Frequency
TWT -- GE-3110, S/N 224

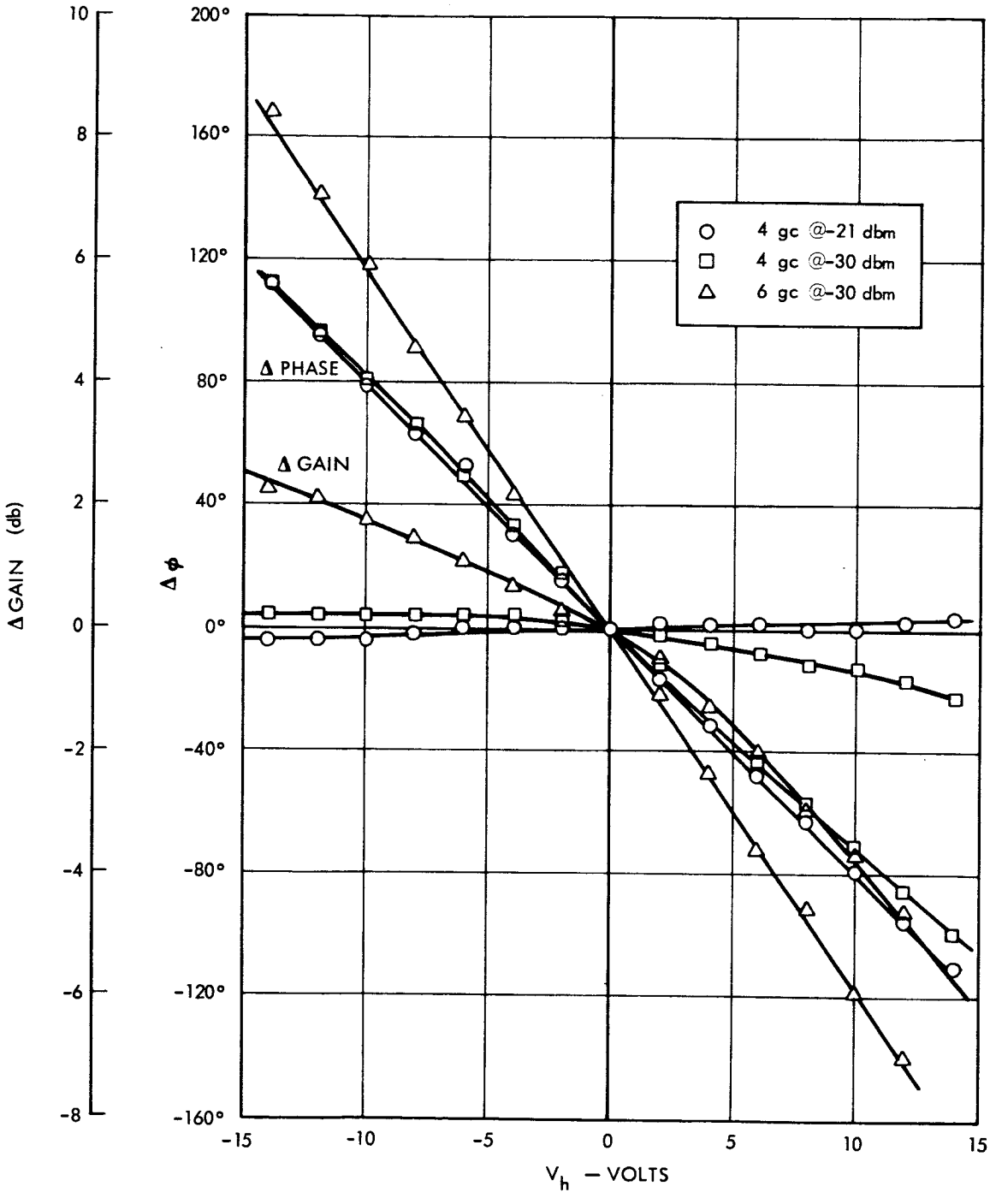

Figure 3-12. Gain and Phase Characteristic vs Helix Voltage TWT -- MEC M-5184, S/N 100

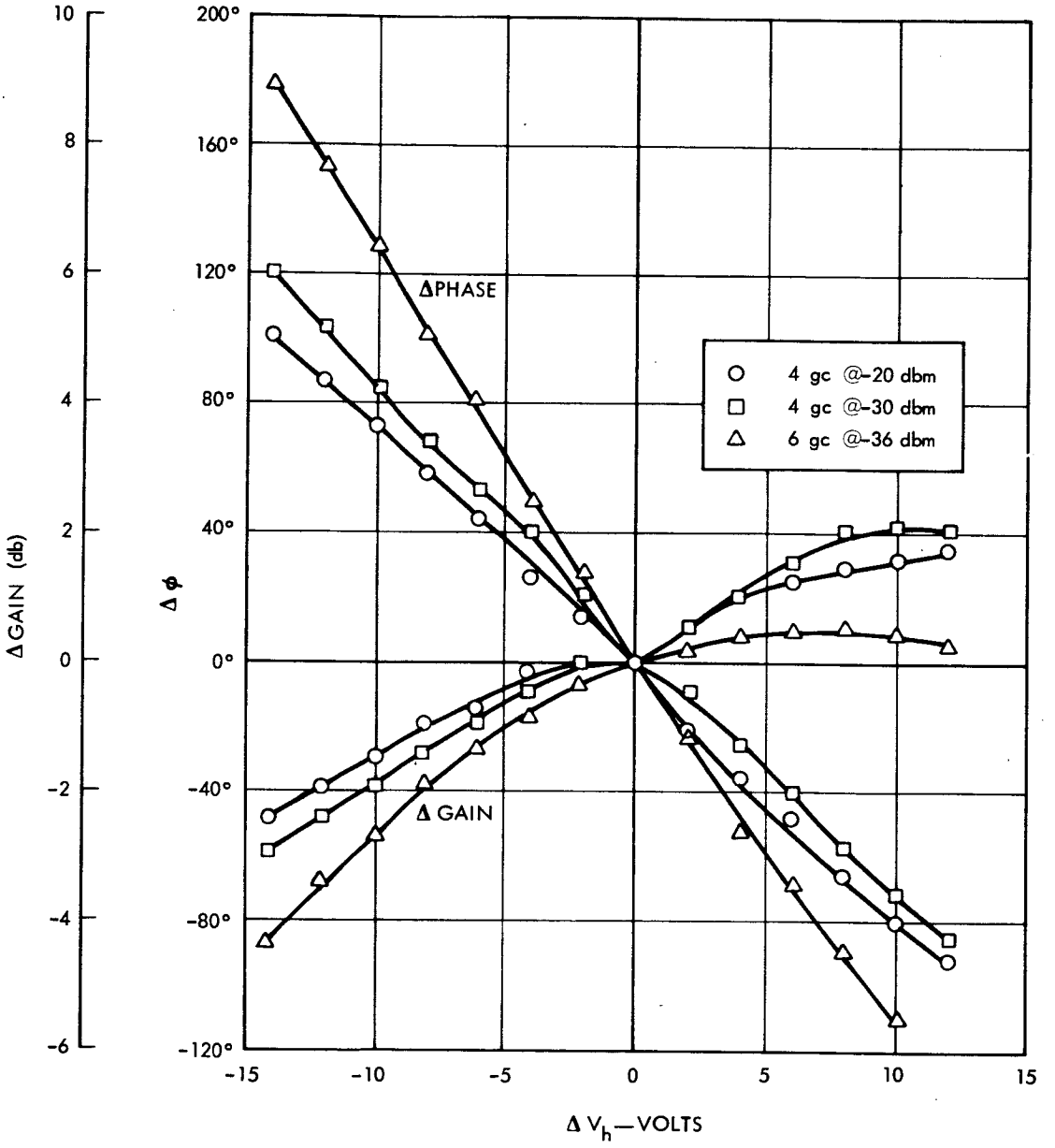

Figure 3-13. Gain and Phase Characteristic vs Helix Voltage TWT -- GE-3110, S/N 224

insensitive to helix voltage variations as opposed to the gain variation exhibited by the ZM-3110. The phase sensitivity to helix voltage variation is seen to be dependent upon input power as well as frequency.

Figures 3-14 and 3-15 show the relative phase shift experienced by a small signal due to the presence of an interfering signal as a function of the interfering signal input power. The relative phase shift experienced by a single signal due to a change in its input power is also plotted.

This effect is dependent upon the frequency placement of the two signals with relation to the gain-frequency characteristics of the particular TWT. To illustrate, note the difference in relationship between the curves representing the low level 6 gc signal in the presence of the 4 gc interfering signal and the curves representing the signal at 4 gc alone in Figures 3-14 and 3-15. Both sets of curves, however, indicate that the input power should be less than 10 db below P_S.

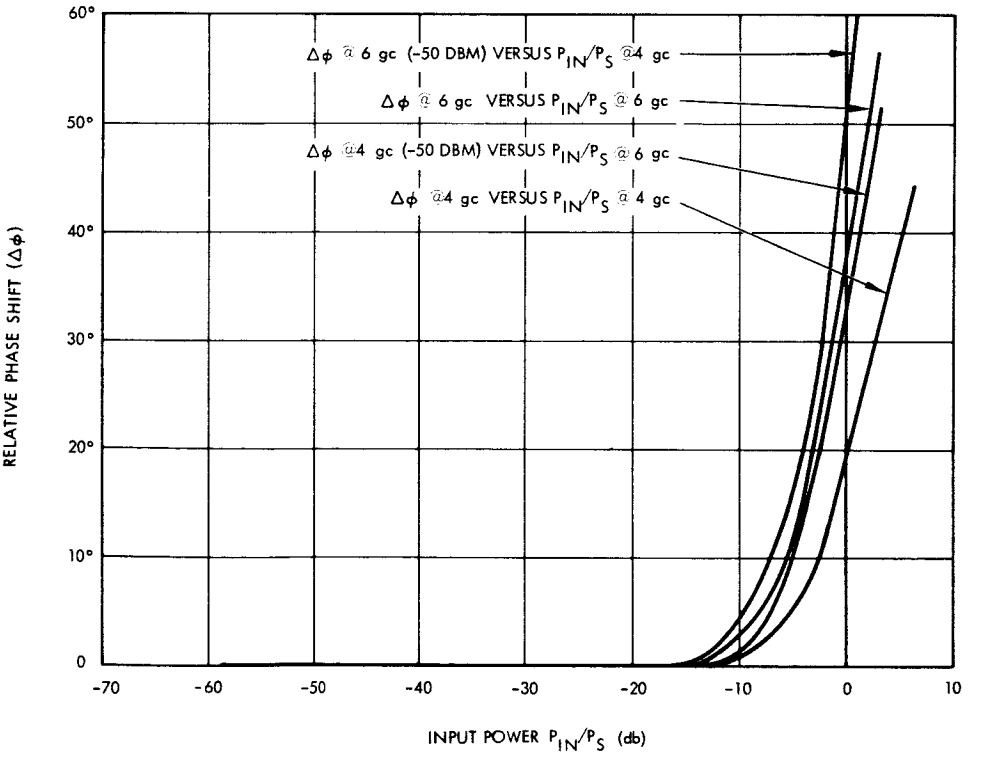

Figure 3-14. Relative Phase Shift vs Input Power TWT -- MEC M-5184, S/N 100

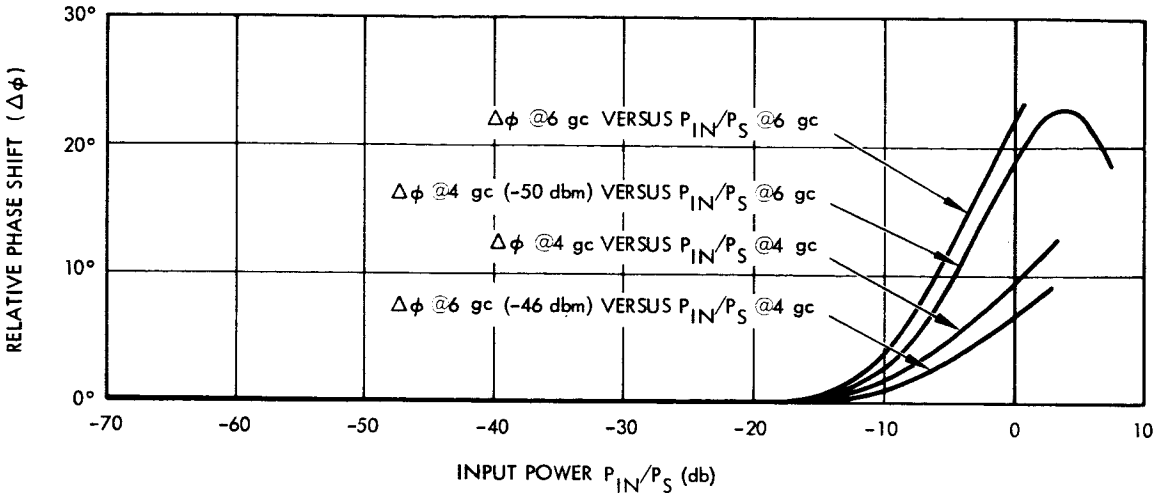

Figure 3-15. Relative Phase Shift vs Input Power
TWT -- GE-3110, S/N 224

The normalized time delay variation (envelope delay distortion) is shown in Figures 3-16 and 3-17 as a function of frequency over a 10 mc range. It is difficult to evaluate delay coefficients from these curves; however, it is seen that the total envelope delay is less than 10 nsec for both tubes.

Figures 3-18 and 3-19 compare the gain suppression of a small signal, due to the interaction effects of an interfering signal, as a function of the interfering signal input power. Physically, the suppression characteristics of a traveling wave tube are produced by the differential efficiency of beam interaction with strong and weak signals applied simultaneously to the helical slow wave structure of the tube. Thus, the gain to the small signal is reduced when it is applied in the presence of a strong signal of different frequency. This effect is somewhat dependent upon the frequency placement of the two signals with relation to the gain-frequency characteristic of the particular TWT.

An illustration of this frequency dependence can be noted from Figure 3-18. The curve showing the suppressing signal at 4 gc and the small signal at 6.0 gc (at a level of -31 dbm) falls off much faster than the curve which shows the same frequencies with their roles reversed, i.e., suppressing signal at 6.0 gc and small signal at 4.0 gc. A similar relationship holds for the other curves.

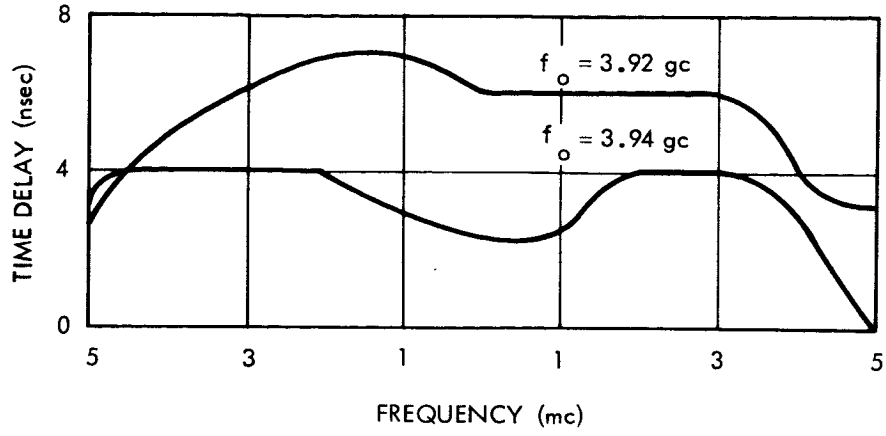

Figure 3-16. Envelope Delay vs Frequency Input Level P_S -9 db
TWT -- MEC M-5184, S/N 100

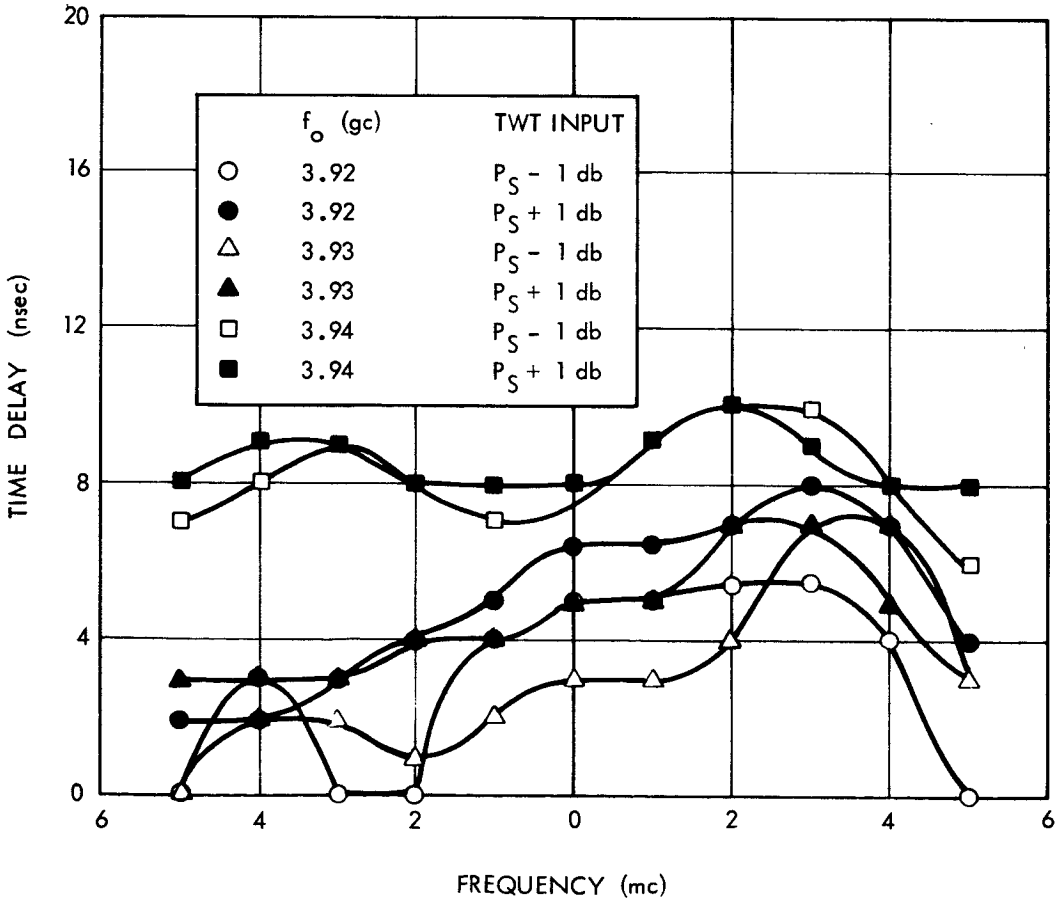

Figure 3-17. Envelope Delay vs Frequency
TWT -- GE-3110, S/N 224

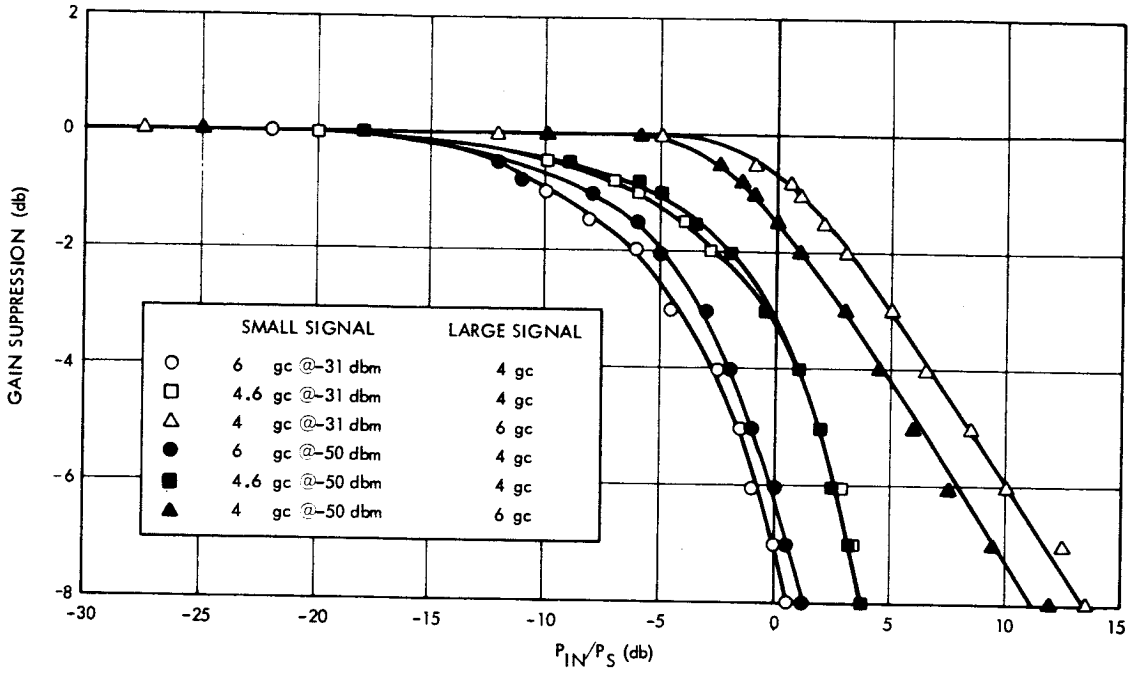

Figure 3-18. Gain Suppression Characteristics
TWT -- MEC M-5184, S/N 100

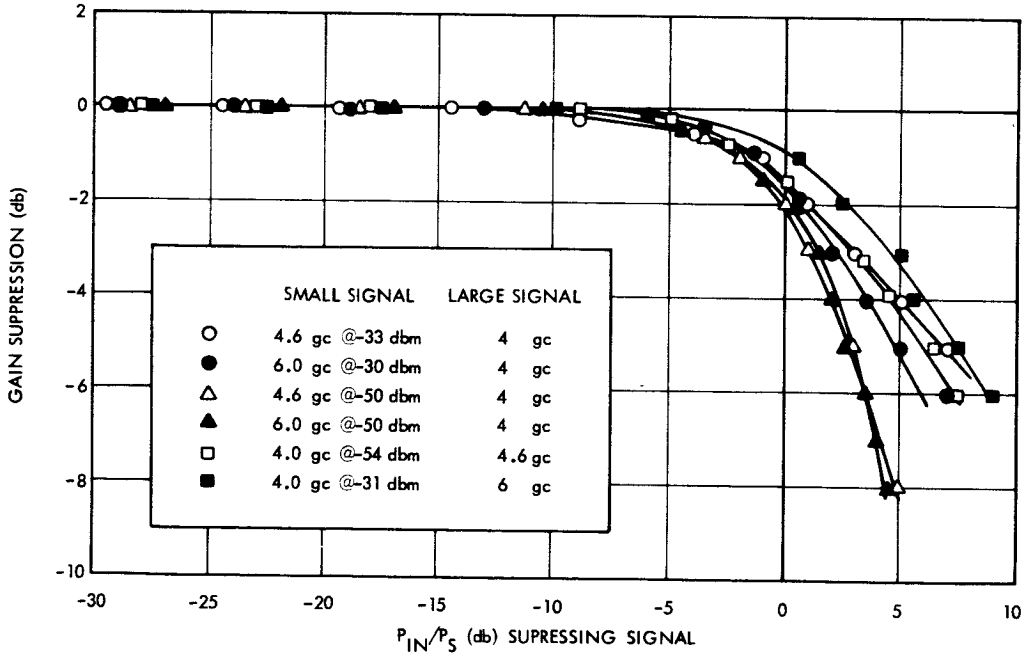

Figure 3-19. Gain Suppression Characteristics
TWT -- GE ZM-3110

The two tubes are seen to exhibit considerably different performance as regards small signal gain suppression. Taking 0.5 db as a maximum allowable gain suppression, Figure 3-19 shows that the recirculated input power to the loop must be kept less than 4 db below P_S for the ZM-3110, whereas the recirculated input must be less than 12 db below P_S for the M-5184. This 8 db difference more than offsets the difference in output powers between the two tubes for equal input powers relative to P_S.

Typical intermodulation curves for the two tubes are shown in Figures 3-20 to 3-23. In each set of curves, f_1 represents a constant input power at the frequency and power noted and f_o represents a variable input power relative to $P_S(f_o)$. The other curves are intermodulation products and are denoted by $f_o \pm n$, where $n = n\Delta f = n \left| f_o - f_1 \right|$. Δf equals 25 mc in all the figures shown. Figure 3-24 shows the intermodulation characteristics of the MEC M-5184 when f_o and f_1 are set at equal power levels and their levels varied together. The input power plotted in Figure 3-24 is the input power of each signal; the total input power to the tube is 3 db higher.

The significance of the intermodulation curves, particularly Figure 3-24, is that they establish the nonlinearity of the TWT power transfer characteristic. These curves are used to establish an initial operating point for the re-entrant loop and to calculate the resultant intermodulation noise.

The TWT evaluation results are summarized below in tabular form. The tests performed on the tubes are listed along with the figures pertinent to the test, and the tube which exhibits the best characteristics for application in a re-entrant loop.

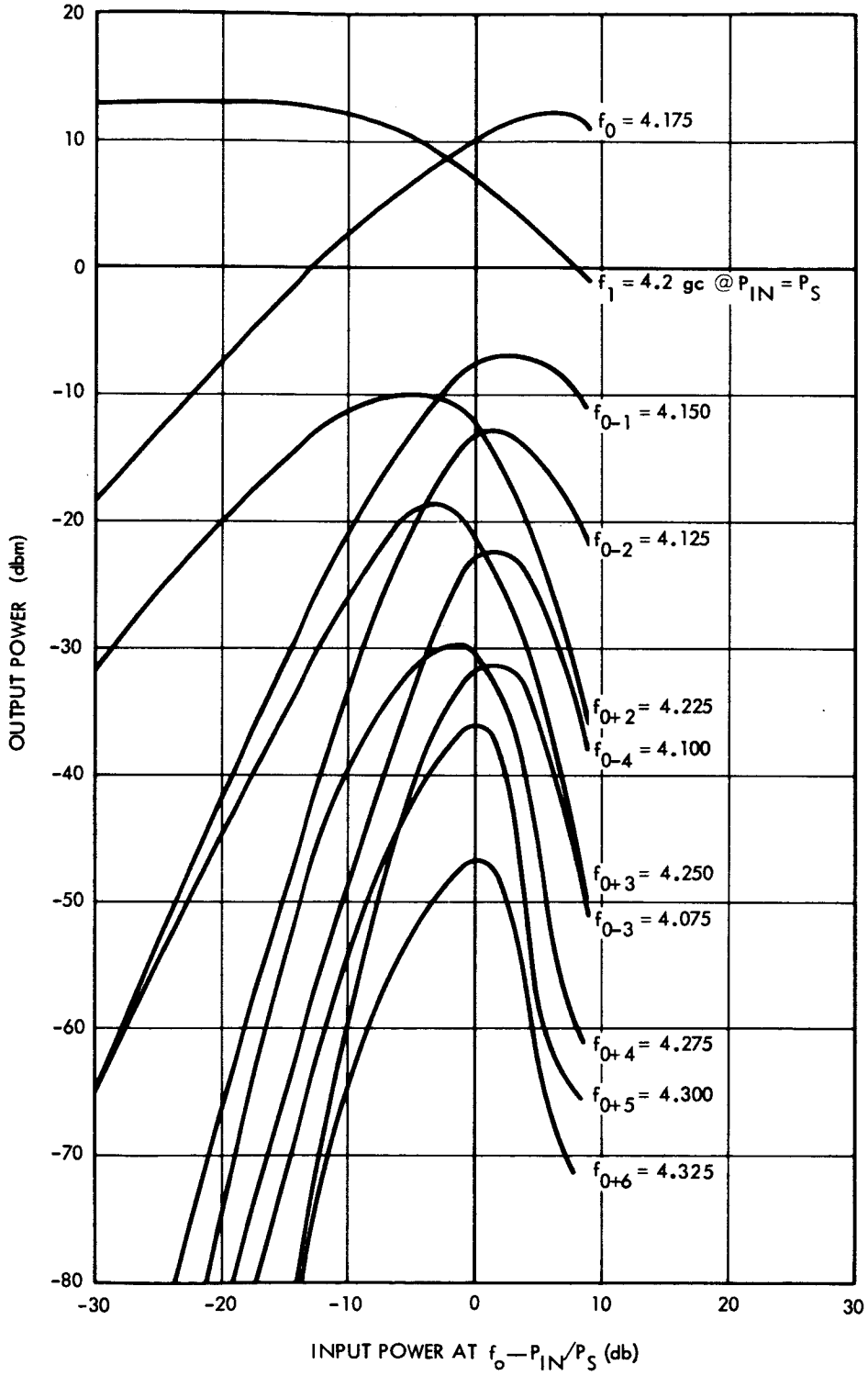

Figure 3-20. Intermodulation
TWT -- MEC M-5184, S/N 100

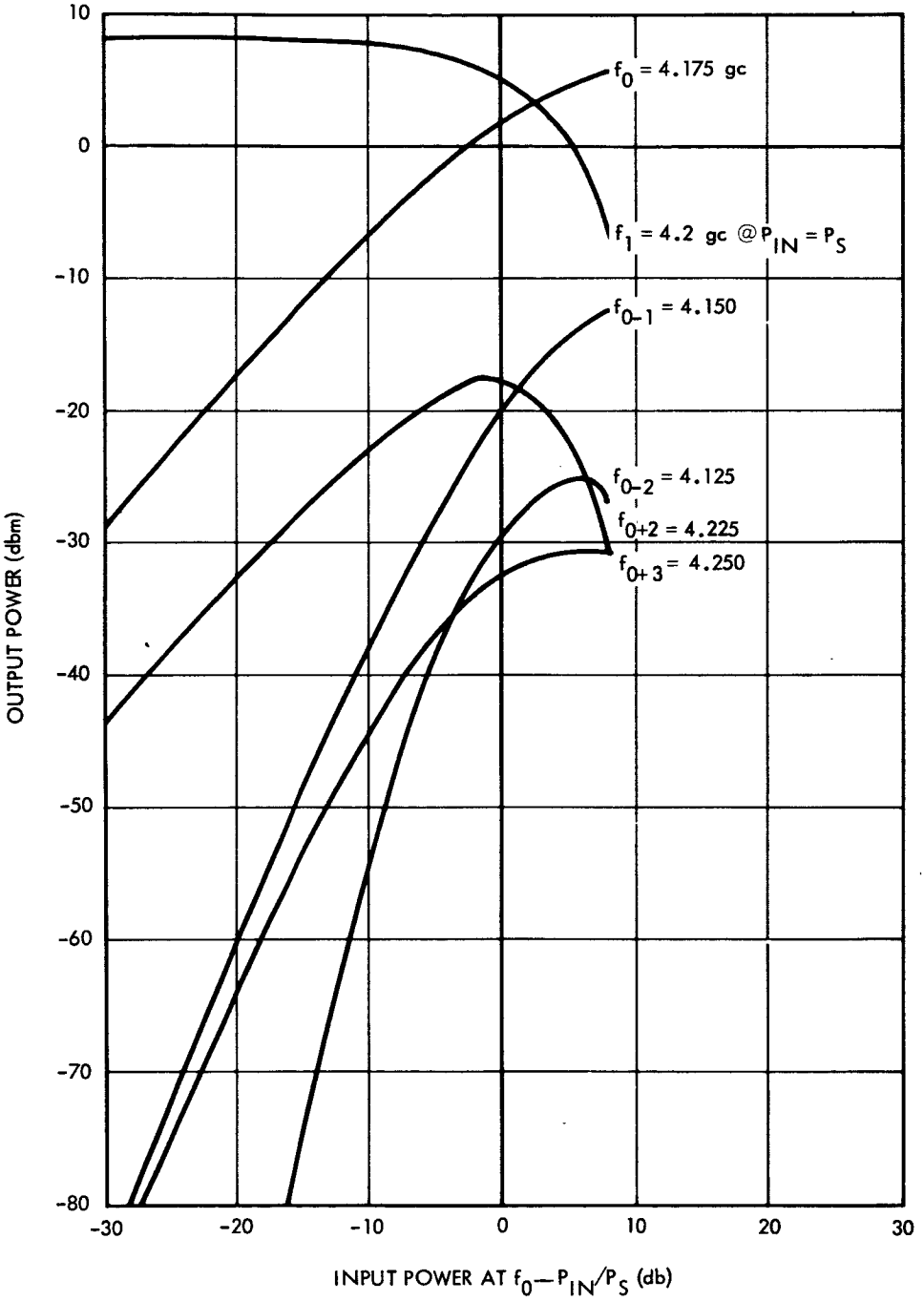

Figure 3-21. Intermodulation
TWT -- GE-3110, S/N 224

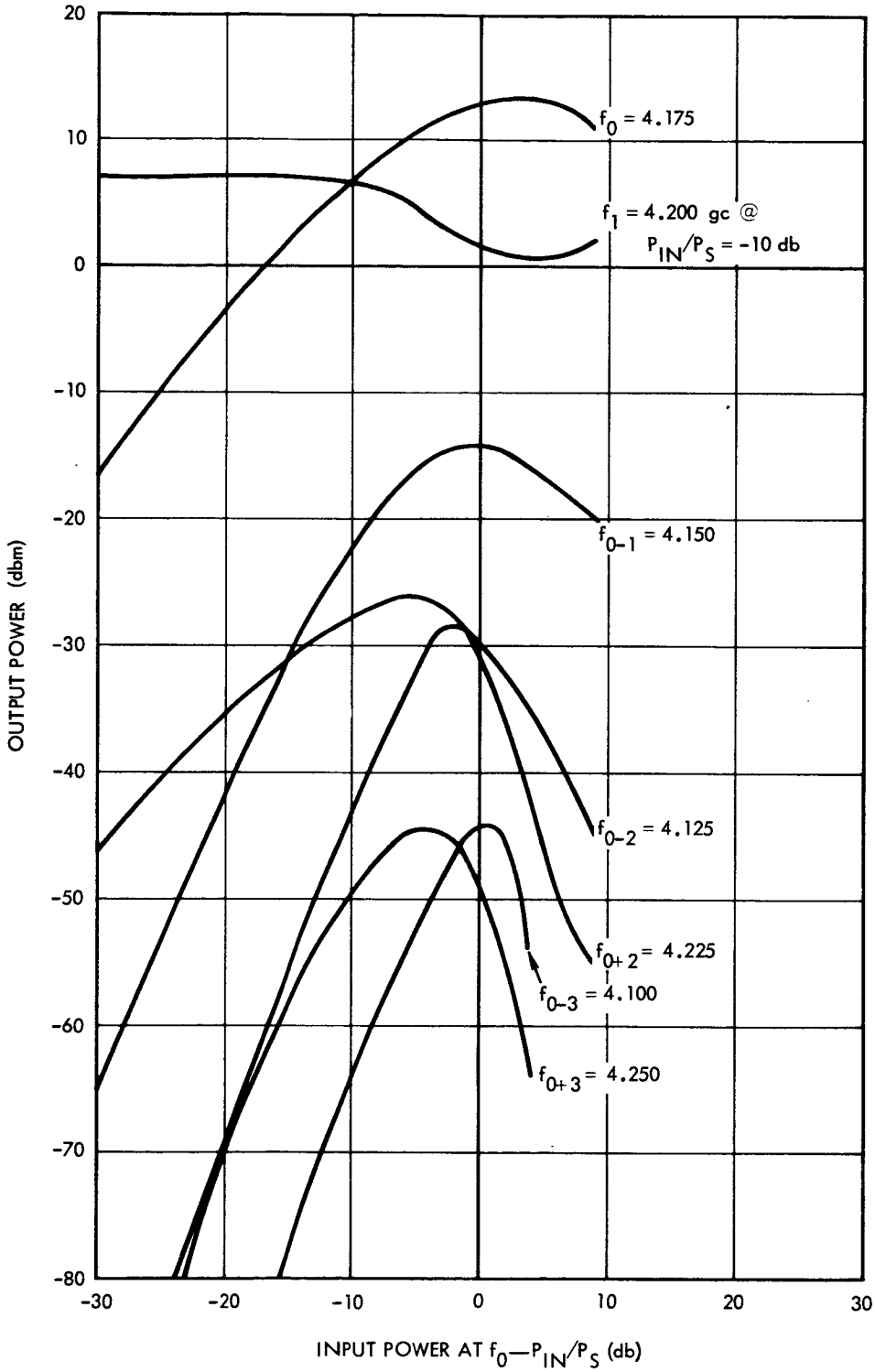

Figure 3-22. Intermodulation
TWT -- MEC M-5184, S/N 100

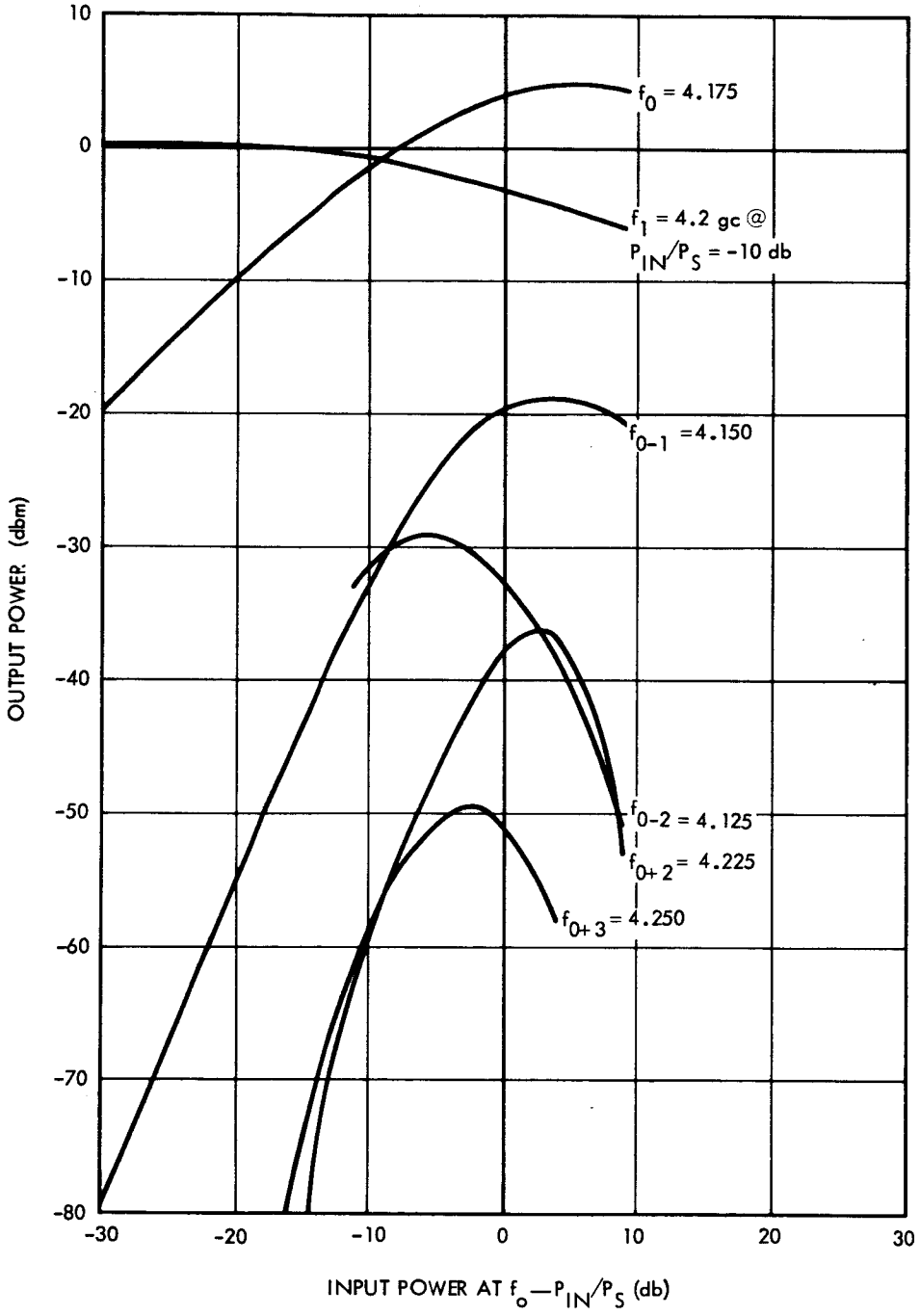

Figure 3-23. Intermodulation
TWT -- GE-3110, S/N 224

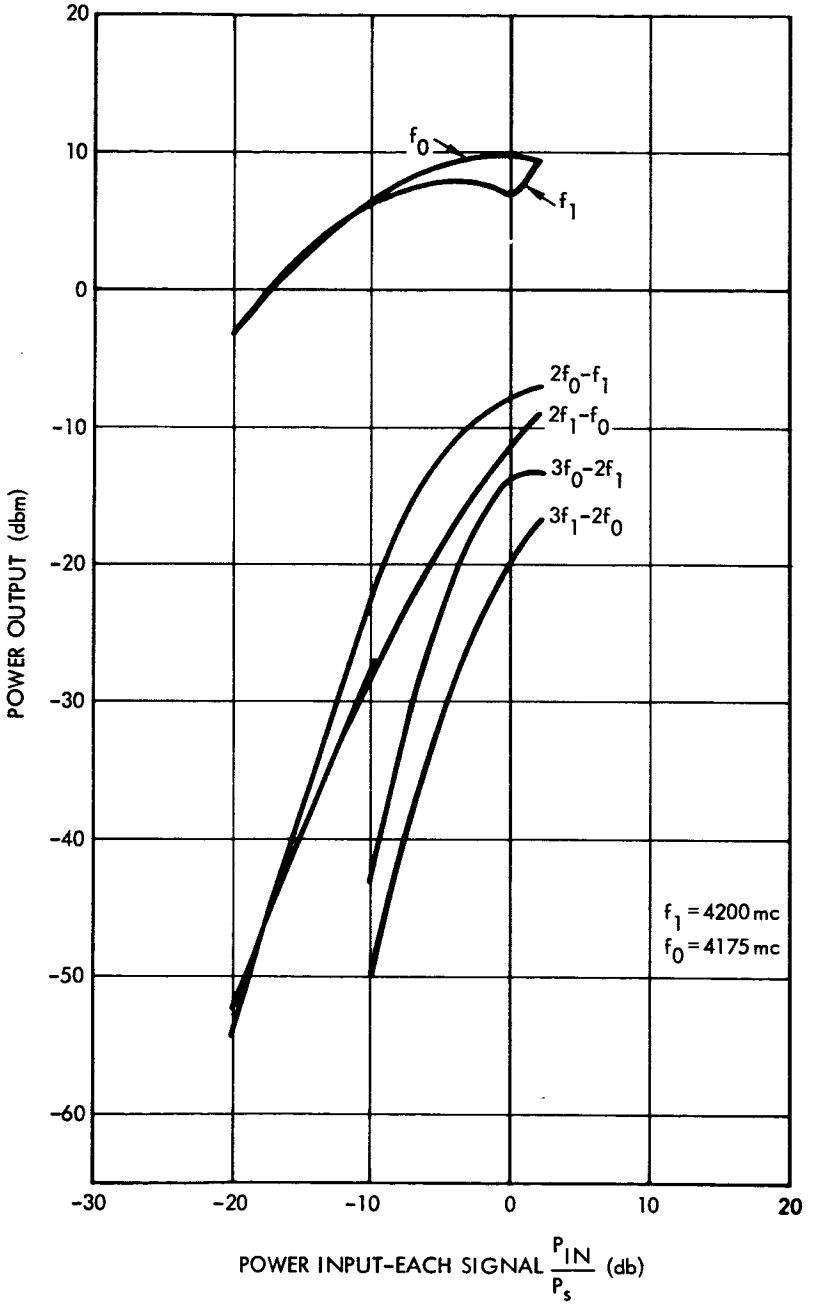

Figure 3-24. Intermodulation
TWT -- MEC M-5184, S/N 100

Test	Figures	"Best" TWT
Power-in/Power-out	3-6, 3-7	Indifferent
Gain-frequency	3-8, 3-9	MEC M-5184
Noise figure	3-10, 3-11	MEC M-5184
Gain and phase vs helix voltage	3-12, 3-13	MEC M-5184
Phase shift vs input power	3-14, 3-15	GE ZM-3110
Envelope delay vs frequency	3-16, 3-17	MEC M-5184
Small signal gain suppression	3-18, 3-19	GE ZM-3110
Intermodulation	3-20 to 3-23	GE ZM-3110

These results indicate that the MEC M-5184 is perhaps slightly better for a re-entrant loop application. However, the differences between the two tubes is, in most cases, very slight and no clear choice is evident. In addition, some characteristics are more important for this application, and it is necessary to assign weights to the test results in order to determine the best choice. Thorough evaluation of both tubes in loop operation is necessary to aid in assigning the relative weight that should be placed on each characteristic.

3.3 DOWN CONVERTER

The down converter for the re-entrant loop converts signals in the input band (5.925 gc - 6.425 gc) to the output band (3.7 gc - 4.2 gc) by means of a local oscillator at 10.125 gc. While conversion gain or slight conversion loss may be desirable, a conversion loss of about 10 db is acceptable with the excess gain available from the loop TWT. However, if the down converter is not to degrade the performance of the transponder, it is necessary that the conversion loss be reasonably flat across the band of interest. An objective for the variation in conversion loss was set at $\pm$ 0.2 db over any 50 mc interval to be consistent with the gain variation specified for the MEC M-5184 TWT. A desirable feature for the diplexer interface is for the converter to have the input and output signals available to a common port.

To achieve conversion gain or slight conversion loss, a variable capacitance diode is needed. A breadboard varactor down converter was developed in an attempt to minimize the conversion loss. Figures 3-25 and 3-26 show the block diagram and breadboard model of this down converter, respectively. A gain of over 30 db has been attained with less than 2 milliwatts of pump power at 10.125 gc; however, the gain was sensitive to mechanical vibrations and the bandwidth characteristics were poor. A completely stable varactor down converter yielded a bandwidth of 30 mc and conversion loss of 12 db.

The down converter is basically a parametric amplifier with the output at the idler frequency. Hence, it is very sensitive to impedance mismatch between the converter's resonant circuits and the diplexer junction, which can produce large losses and narrowband performance. Figure 3-27 shows the gain versus pump power for the breadboard converter. The sensitivity of the gain with pump power was magnified as a result of the large initial insertion loss caused by the impedance interactions. Attempts to increase the bandwidth were unsuccessful.

To overcome the bandwidth problems of a direct coupled varactor converter, a tunnel diode converter was investigated. Two tunnel diodes were purchased from Micro State Electronics Corporation.

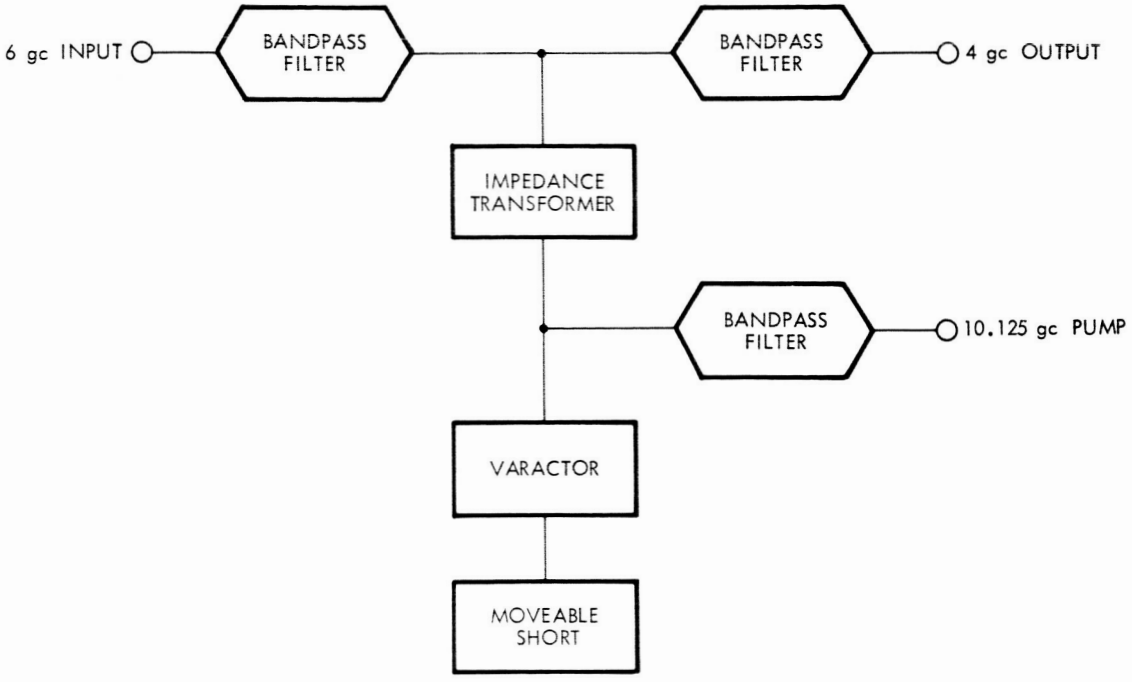

Figure 3-25. Varactor Lower Sideband Down Converter

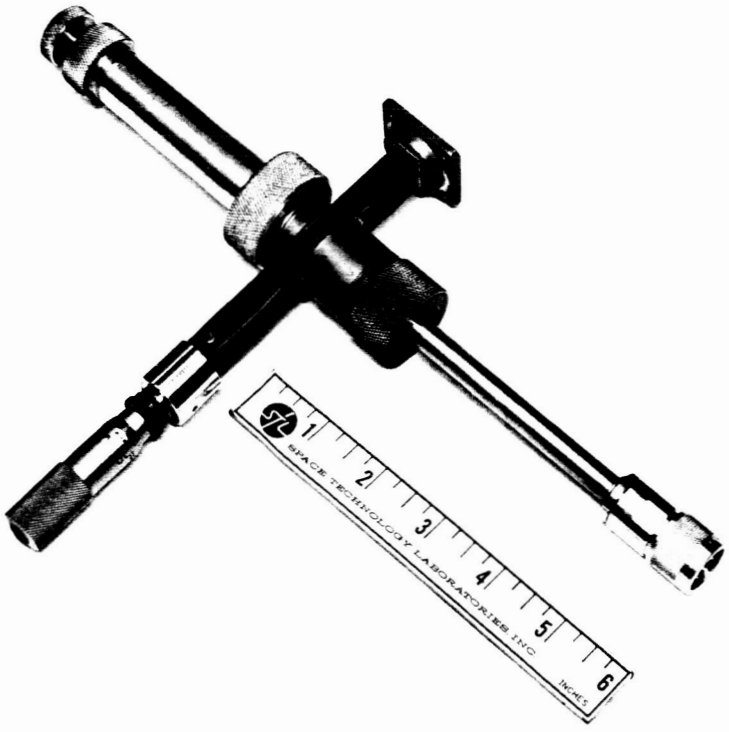

Figure 3-26. Coaxial Down Converter - 6 to 4 gc

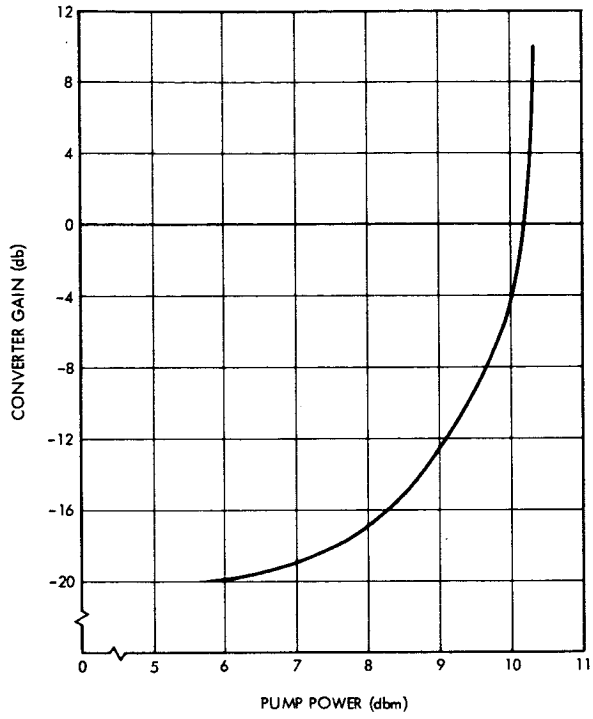

Figure 3-27. Pump Power vs Varactor Converter Gain

The stability of the tunnel diode down converter is a major problem due to the high frequencies involved and the requirement of a broadband impedance match much in excess of the two frequency bands of interest. The high cutoff frequency diodes are very susceptible to low power burnout. Thus, any unwanted oscillations are sufficient to destroy the diode before the frequency of oscillation is determined and the circuit changed. This happened to both the purchased units in the converter and the tunnel diode test circuit. Further investigation indicated that this frequently happened with the high cutoff diodes. Thus, it was felt that the tunnel diode down converter is sufficiently difficult to stabilize such that a considerable study program would be required to achieve it. This was beyond the scope of the program.

Because of the wideband requirement of the re-entrant loop along with the sensitive matching problems presented by varactors and instabilities of tunnel diodes associated with wideband matching mentioned above, it was decided to concentrate on the development of a down

converter based on the nonlinear resistance (rather than the nonlinear capacitance) of a diode. The following discussion presents some semi-quantitative computations which suggest the design approaches that were taken. An equivalent circuit for a mixer diode, together with typical element values, is shown in Figure 3-28.

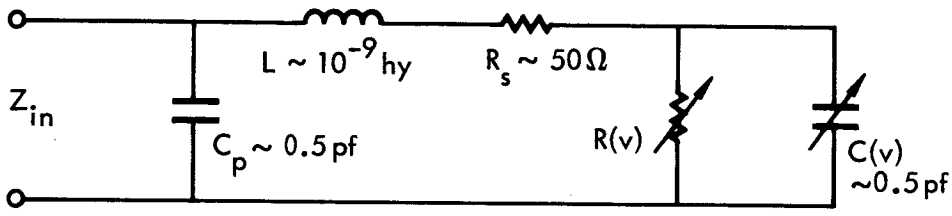

Figure 3-28. Mixer Diode Equivalent Circuit

Because of the nonlinear behavior of the diode, an exact solution for Z_{in} is quite involved and depends upon the drive level of the local oscillator, nonlinearity of R(v), etc. However it is felt that a useful approximation can be achieved by:

1) Assuming C(v) to have a constant value close to its average value

2) Assuming R(v) to be either an open circuit (diode back biased and nonconducting) or a short circuit (diode forward biased and conducting)

3) Computing $Z_{in}(\infty)$ for $R(v) = \infty$ and $Z_{in}(0)$ for $R(v) = 0$ and then assuming $Z_{in} \simeq Z_{in}(\infty)/2 + Z_{in}(0)/2$

The diode Z_{in}, computed as indicated above, is plotted in Figure 3-29. The resistive component is approximately 36 ohms in the 4 to 6 gc range and the reactive component is capacitive and in the order of 25 to 35 ohms over the same frequency range.

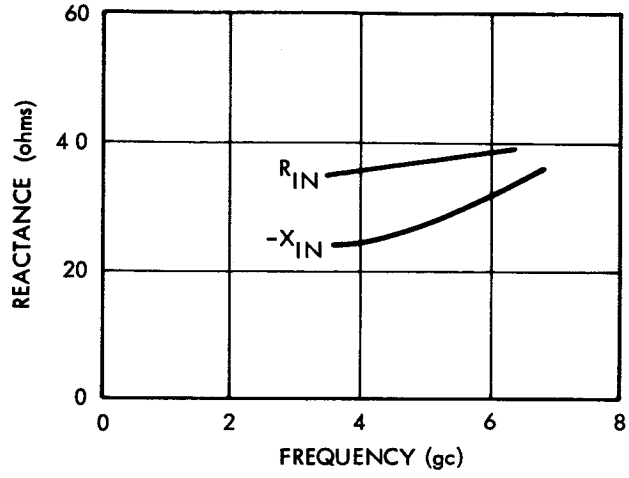

Figure 3-29. Pumped Diode Impedance Components

The capacitive reactance can be tuned out with a shorted transmission line, less than $\lambda/4$ in length, in series with the diode and the input-output port. This is the most direct approach and, as indicated by Figure 3-30, it appears feasible for a single series line to give an acceptable match over the entire interval of 3.7 to 6.425 gc.

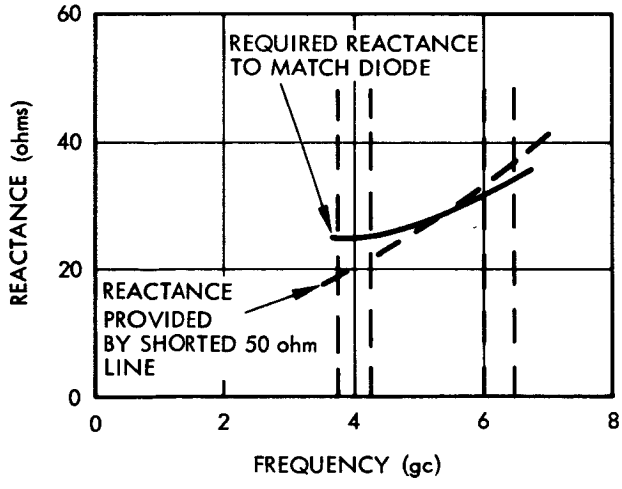

Figure 3-30. Match Attained with Shorted 50-ohm Line in Series with Diode

Another more involved approach is to attempt to match only the frequency intervals of interest (i.e., 3.7 - 4.2 gc and 5.925 - 6.425 gc) without regard for mismatch outside these intervals. This case arises when a coaxial high-pass filter is employed to isolate the input-output signals from the local oscillator source. The impedance presented by this filter at the diode can exhibit an anti-resonance at a frequency between the range of interest (say at 5 gc), when a match is established at the input-output frequency bands with the aid of an auxiliary shorted transmission line in series with the diode. The reactance curves and block diagram for this approach are shown in Figure 3-31.

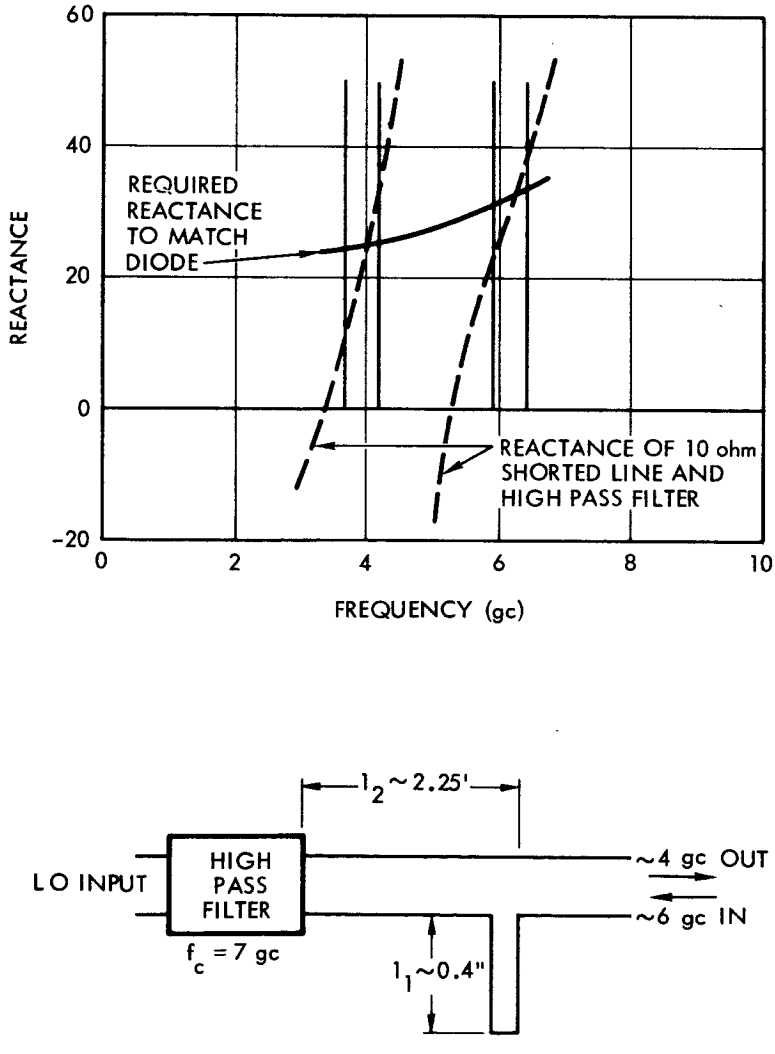

Figure 3-31. Coaxial Converter Reactance Curves

Breadboard models of the down converters suggested by Figures 3-30 and 3-31 were constructed. One breadboard converter, shown in Figure 3-32, consisted of a junction between 50-ohm coaxial line and X-band waveguide. A sliding waveguide short opposite the local oscillator signal and a coaxial sliding short opposite the input-output port was used to match the diode to the input-output circuit. Unfortunately, the wideband match to the input-output signals predicted by Figure 3-30 was not observed. This was possibly due to effects of the coax-waveguide junction and the prevention by the diode package itself of placing the coaxial short as close as necessary to the semiconductor element of the diode. With more work, this approach might give a broadband match. However, efforts were concentrated on realization of the second approach, indicated in Figure 3-31, since it initially exhibited more promise.

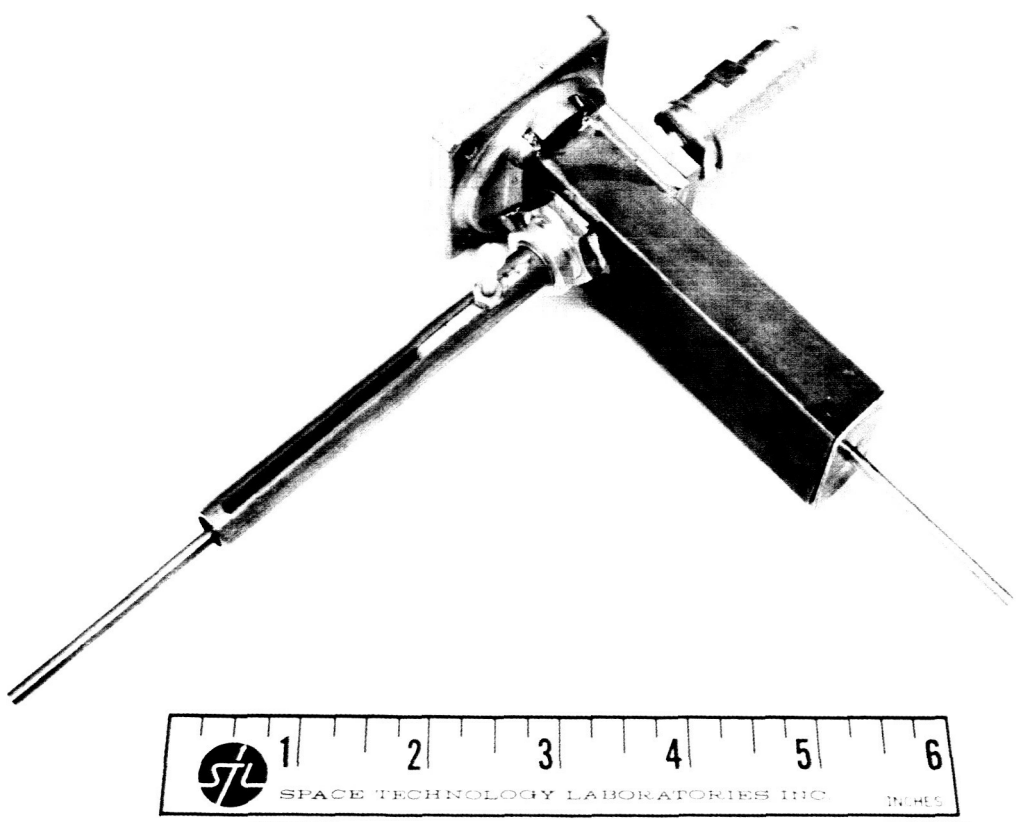

Figure 3-32. Waveguide-Coax Down Converter

The configuration suggested by Figure 3-31 consists of a mixer diode coaxially mounted in the center conductor, a low impedance series tuning line concentric with the outer conductor, and a capacitively coupled 8-pole high-pass filter.

Figure 3-33 shows a picture of the final down converter used in the transponder and an engineering drawing is shown in Figure 3-34. The MA-415E diode is mounted in a coaxial circuit with a 6.0 and 4.0 gc band reject filter behind the diode to optimize the 6.0 gc signal into the diode and the 4.0 gc signal out of the converter. The 10.125 gc pump

Figure 3-33. Coaxial Down Converter

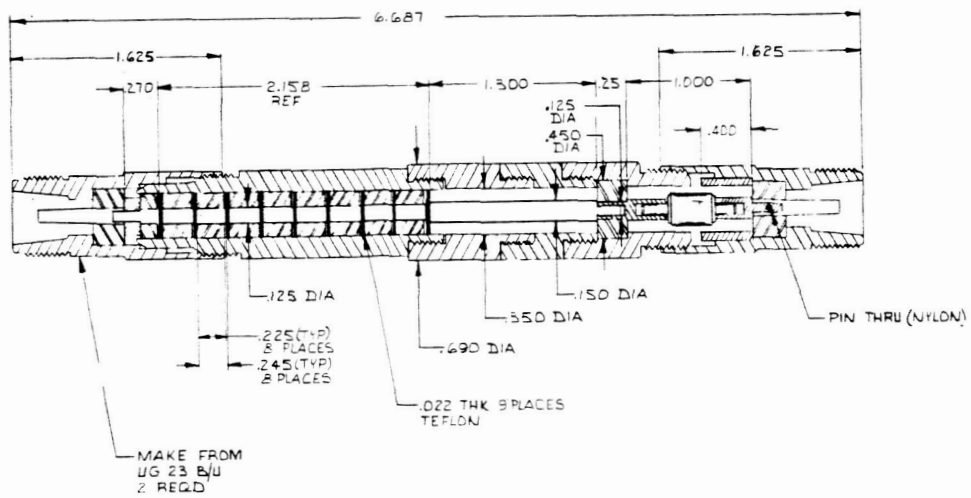

Figure 3-34. Coaxial Down Converter Engineering Drawing

passes through the 6.0-4.0 gc band reject filter and is terminated behind the diode by an open circuit in series with the outer conductor of the coaxial converter and appropriately spaced to optimize the 10.125 gc pump interaction with the diode.

Figure 3-35 plots the conversion loss of the resistive converter as a function of the local oscillator power and indicates an optimum LO power of 2 to 10 dbm. Conversion loss versus frequency at an LO power of 8 dbm is shown in Figures 3-36 and 3-37. A swept source was used in plotting Figure 3-36. Figure 3-37 shows the same information taken on a spot frequency measurement basis for comparison. Except for the fine structure evident in the swept measurements, the results of the two methods agree to within about 1 db over the 5.925 gc to 6.425 gc band. Figures 3-38 and 3-39 show block diagrams of the test setups used for the swept and spot frequency measurements respectively. Note that the diplexer was used in making the measurements; hence, the effects of diplexer insertion loss between ports 3 and 5 and between ports 5 and 4 are included in the curves of Figures 3-36 and 3-37.

The initial objective of $\pm$ 0.2 db variation in conversion loss over any 50 mc band is not met but the down converter is satisfactory otherwise.

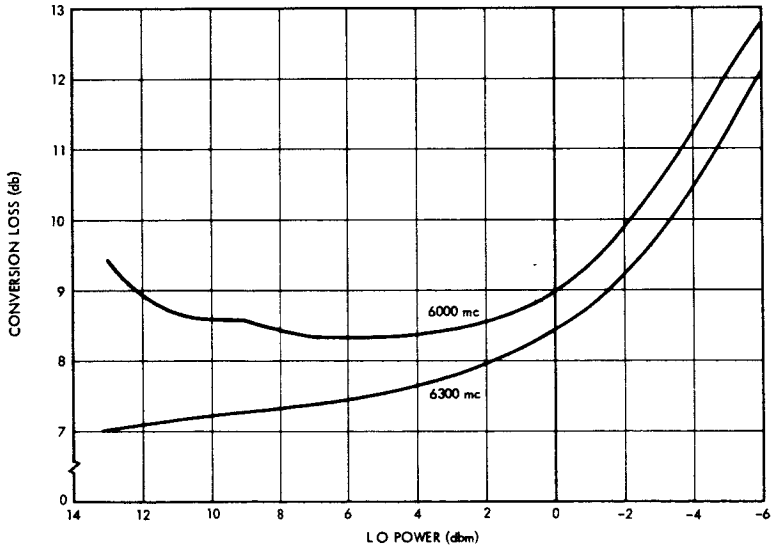

Figure 3-35. Resistive Converter Conversion Loss vs Local Oscillator Power

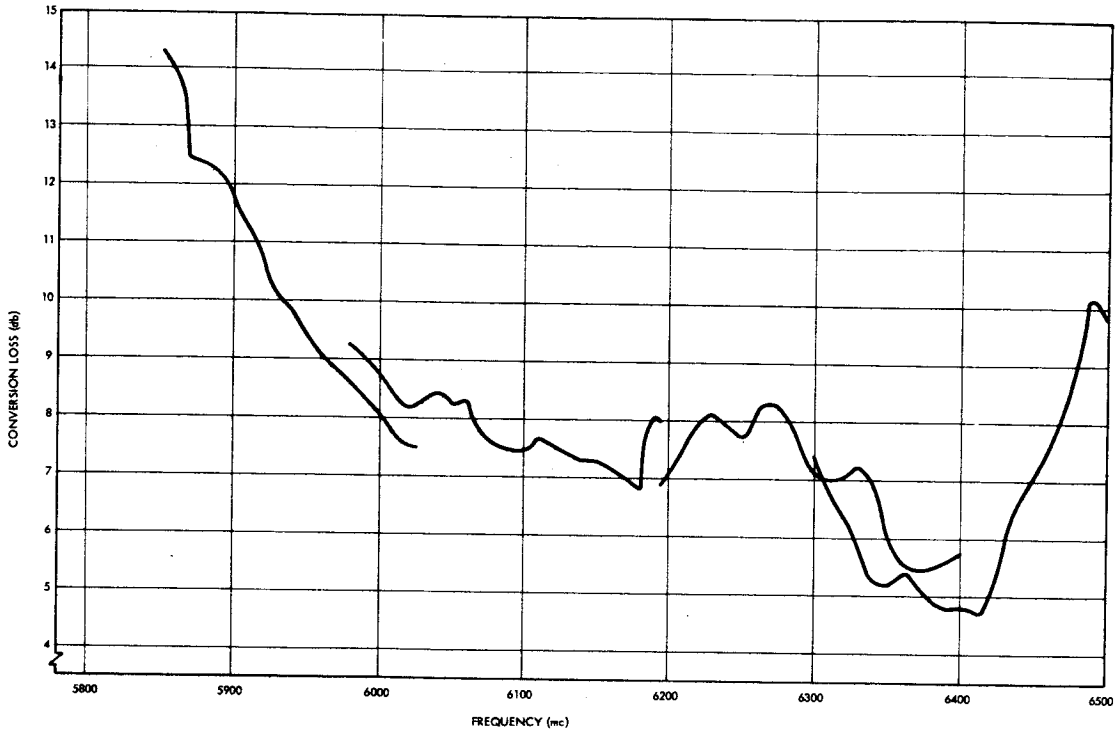

Figure 3-36. Conversion Loss vs Frequency Data from Swept Measurements

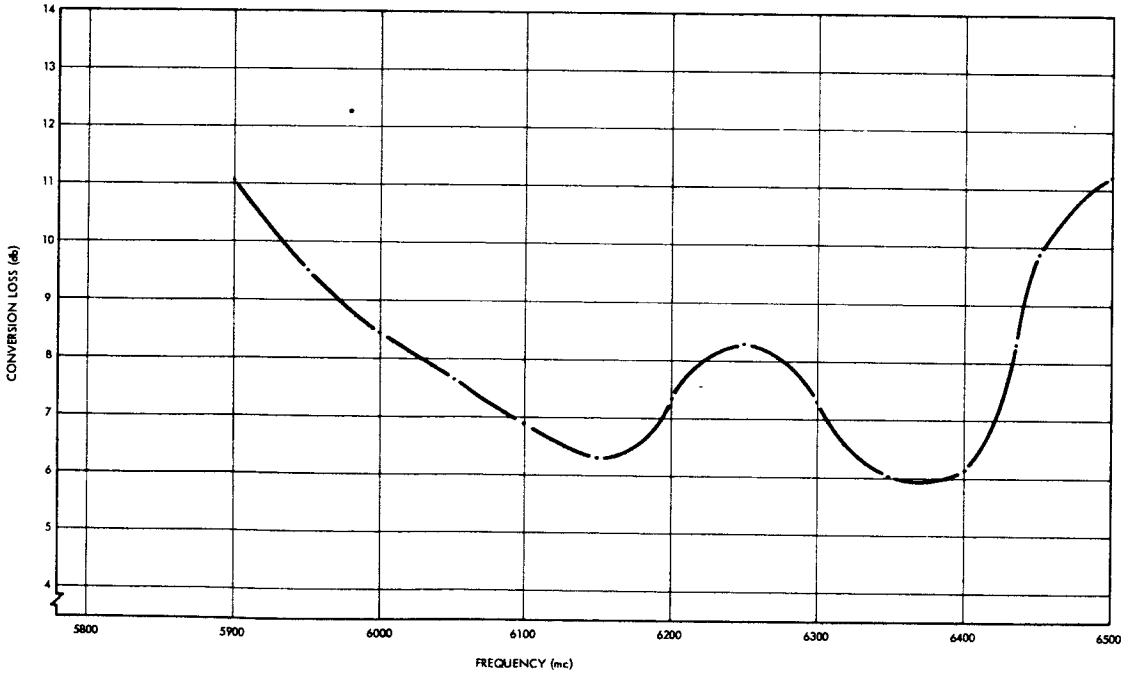

Figure 3-37. Conversion Loss vs Frequency Spot Measurements at 50 mc Intervals

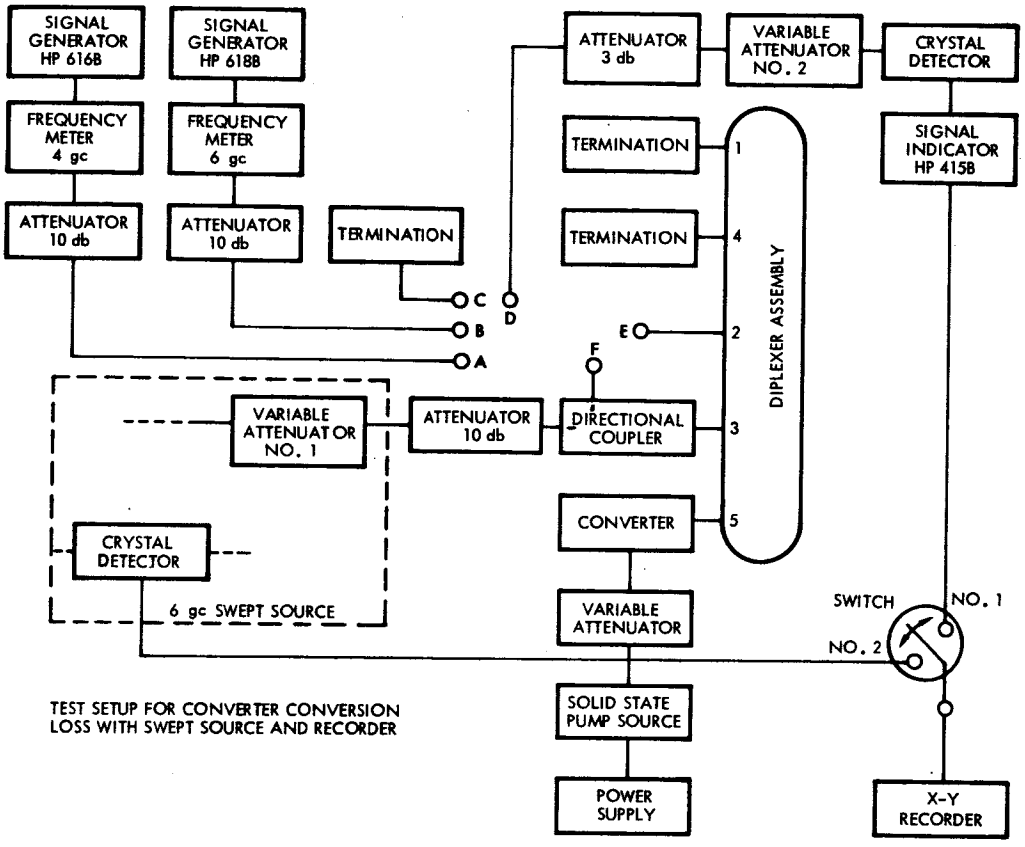

TEST SETUP FOR CONVERTER CONVERSION LOSS WITH SWEPT SOURCE AND RECORDER

Figure 3-38. Test Setup for Converter Conversion Loss with Swept Source and Recorder

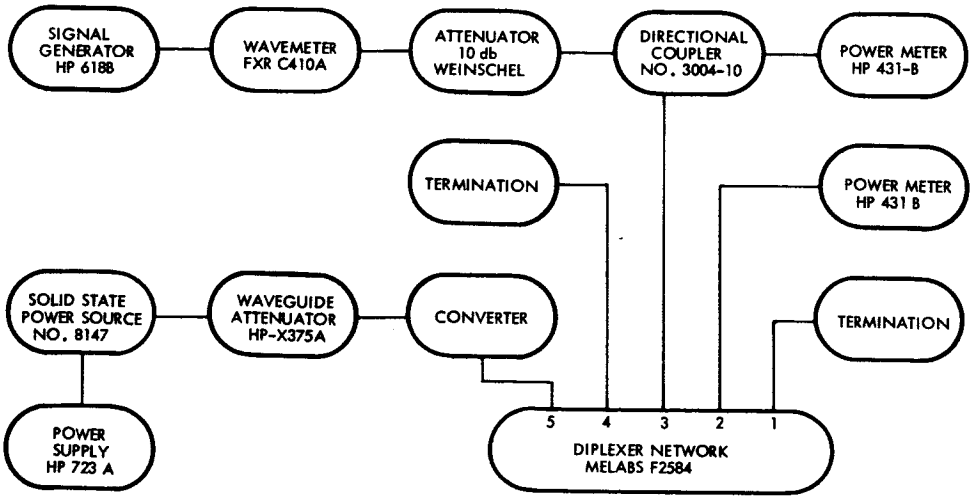

Figure 3-39. Converter Conversion Loss Measurement Circuit

3.4 TRANSPONDER COMPONENTS

A 10.125 gc solid state power source is used for the LO in the re-entrant loop. The choice of this frequency permits input signals to the transponder at any frequency within the 5.925 gc to 6.425 gc communication band to be retransmitted at an output frequency contained within the 3.7 gc to 4.2 gc communication band. The alternate frequency choice of 2.225 gc requires that the harmonics of the LO be suppressed which makes the diplexer filtering requirements more difficult to achieve.

The LO consists of an oven-stabilized crystal oscillator at approximately 106 mc followed by a four stage varactor X96 multiplier chain. Figure 3-40 shows the output power of the LO as a function of the dc input voltage. At a nominal voltage of 28 vdc the LO output power is about 26 dbm. Since the down converter requires a local oscillator power of 2 to 10 dbm for minimum conversion loss, it is necessary to use a pad between the LO and down converter. In the transponder, a 6 db pad is used to limit the LO power to the down converter to 8 dbm.

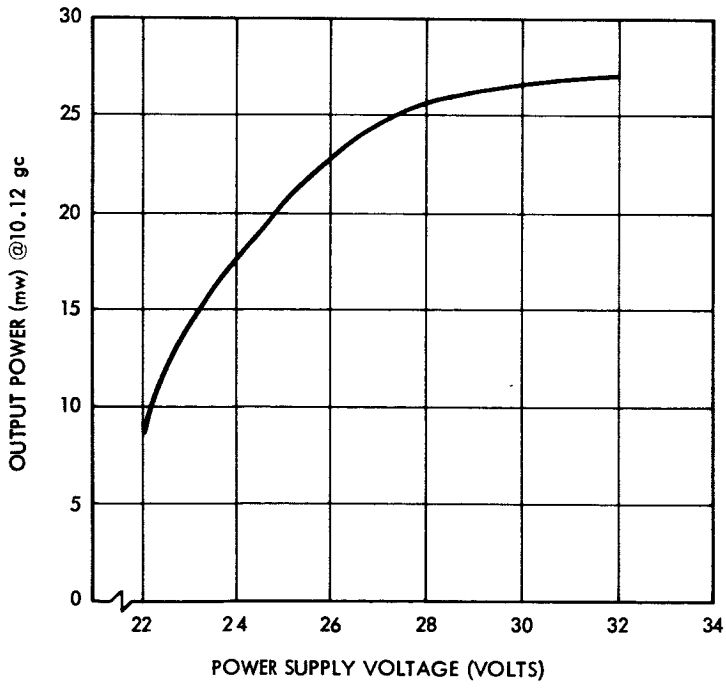

Figure 3-40. Output Power vs Input Voltage

A block diagram of the dual diplexer used to separate the signals in the 6 gc and 4 gc bands is shown in Figure 3-41. In-band insertion loss versus frequency characteristics of the diplexer are shown in Figures 3-42 to 3-45. The isolation between channels is greater than 65 db at all ports which is sufficient to inhibit loop oscillation.

The tunnel diode preamplifier is a coaxial type purchased from International Microwave Corporation. Figure 3-46 shows the gain-frequency characteristic of the TDA with the bias set as received from the manufacturer. This bias setting is for best noise figure but it may be adjusted for better gain. However, this was not done and the amplifier was used with the characteristics as shown.

The measured noise figure of the TDA is 7 db, which is 2 db higher than specified. Several attempts to achieve the 5 db noise figure specified were unsuccessful and measurements on the overall transponder also verify the 7 db value.

A government furnished Hughes 384-H TWT was used as the transponder power amplifier. The power-in/power-out and saturated gain versus frequency characteristics of this tube are shown in Figures 3-47 and 3-48 respectively.

It is well to note that the input power required for saturation is considerably below the output power obtainable from the loop tube. With the present PA and power supply a pad is necessary between the loop TWT and PA to prevent over driving the PA. However, the transponder could yield an output power in the range of 40 watts with a power amplifier of the same gain as the 384-H.

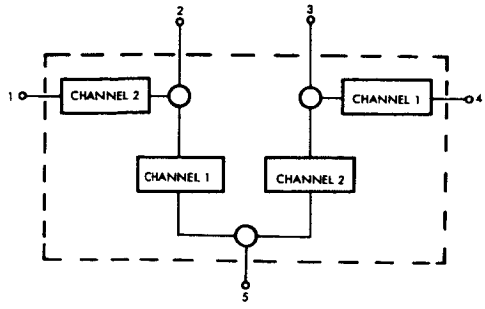

Figure 3-41. Dual Diplexer Block Diagram

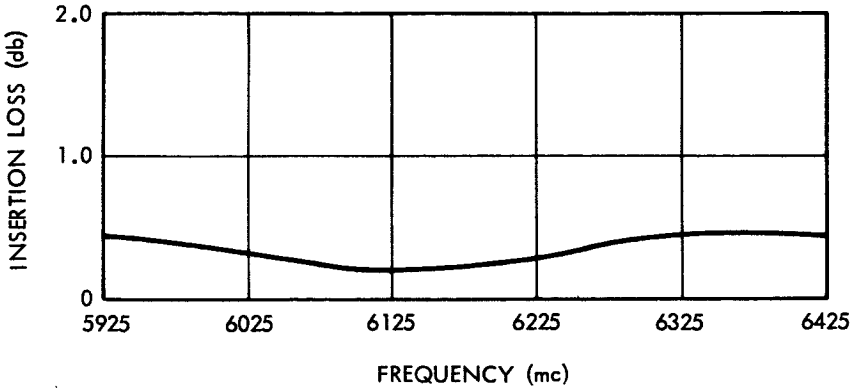

Figure 3-42. Dual Diplexer Insertion Loss Ports 1 to 2

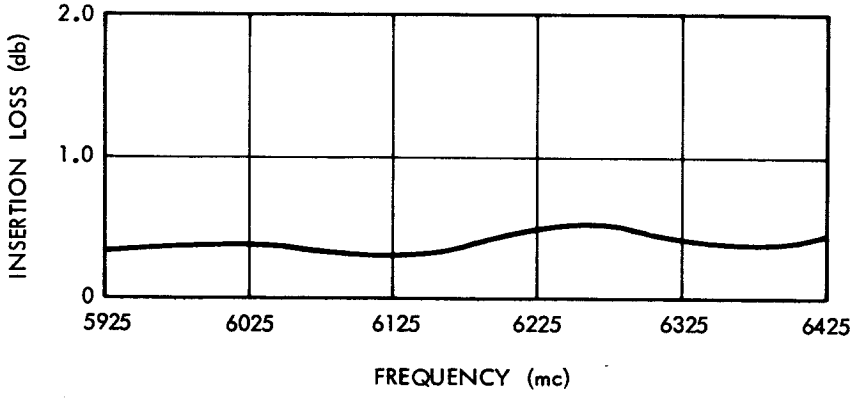

Figure 3-43. Dual Diplexer Insertion Loss Ports 3 to 5

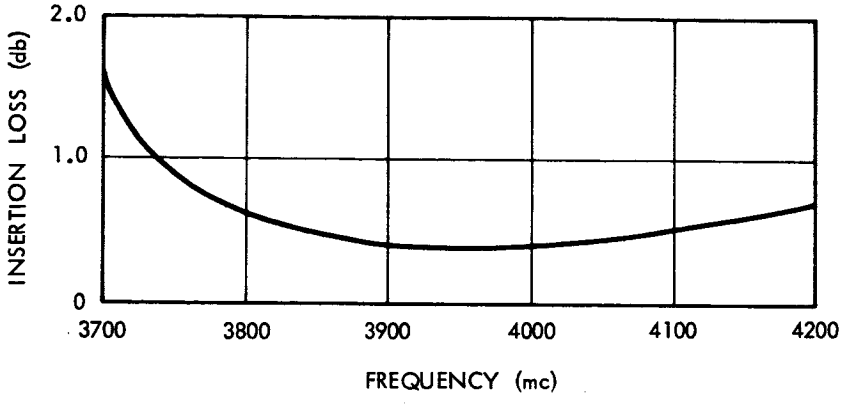

Figure 3-44. Dual Diplexer Insertion Loss Ports 5 to 2

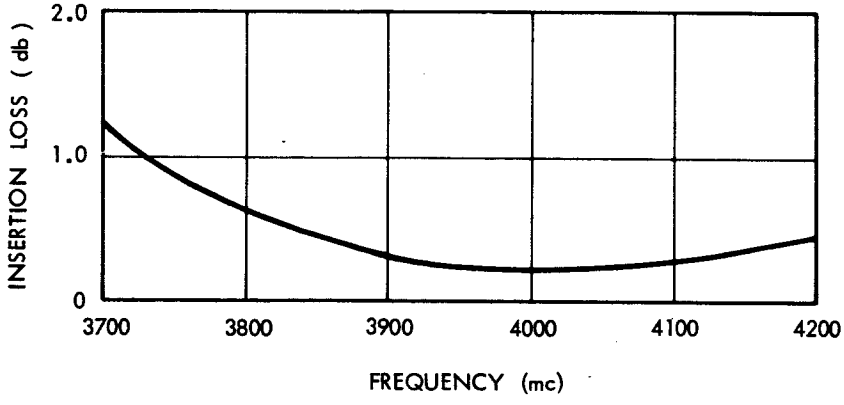

Figure 3-45. Dual Diplexer Insertion Loss Ports 3 to 4

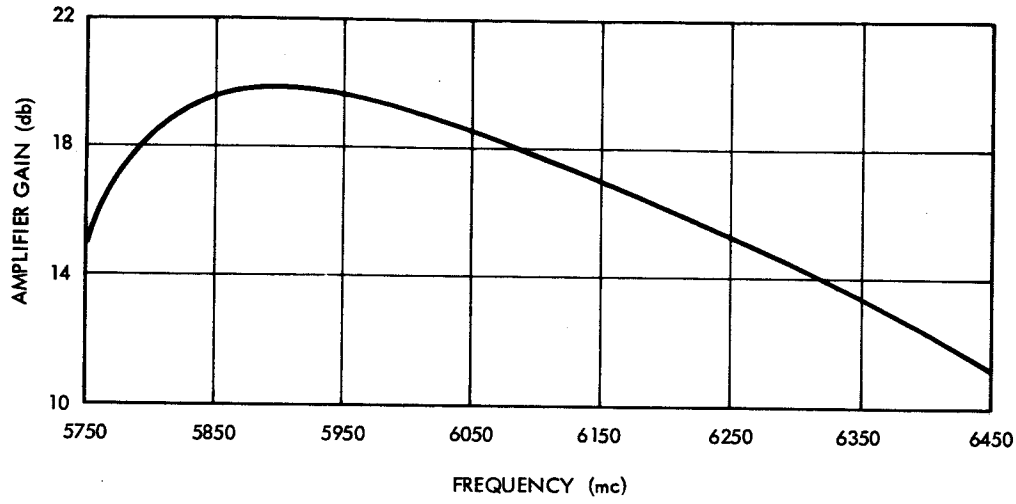

Figure 3-46. Gain vs Frequency Tunnel Diode Amplifier
International Microwave Corp.
Model ACR-5950-17

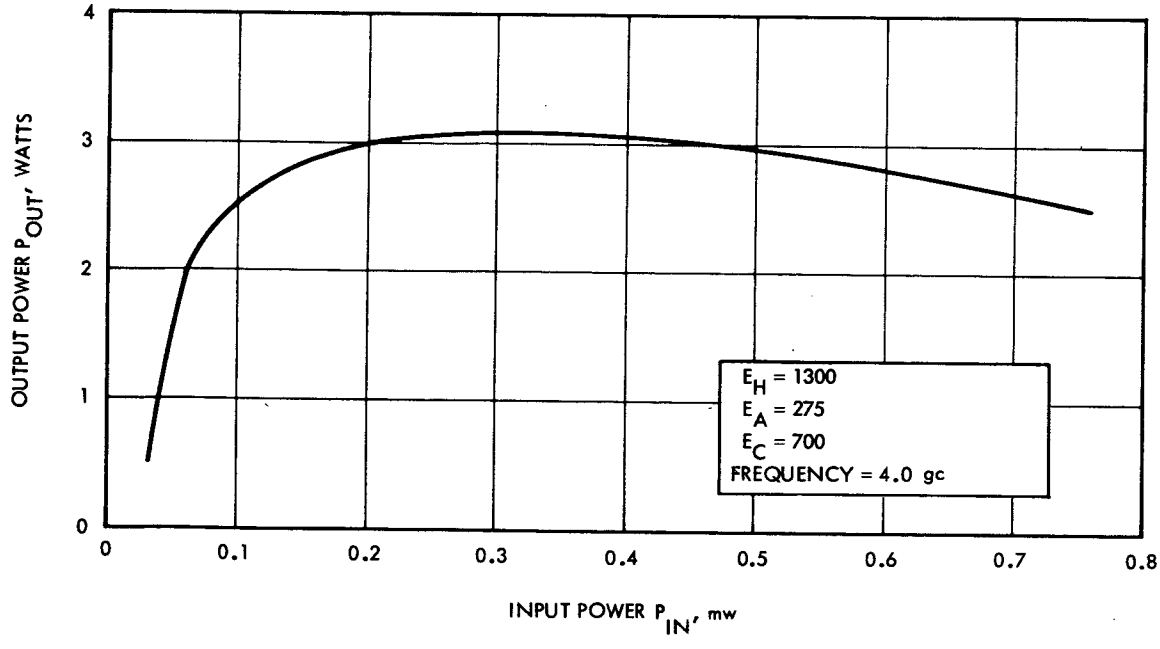

Figure 3-47. Power Out vs Power in
Hughes Model 384, S/N 75

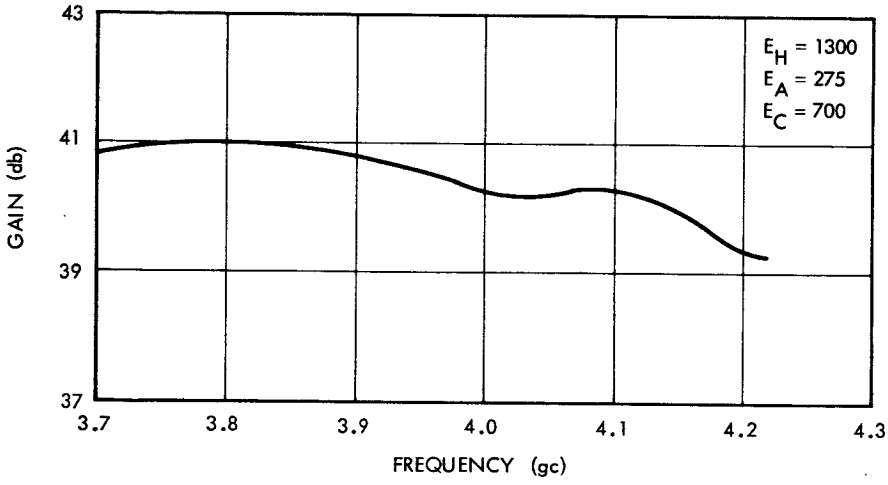

Figure 3-48. Saturation Gain vs Frequency
Hughes Model 384, S/N 75

4.0 TRANSPONDER TEST RESULTS

Measurements were made to evaluate the re-entrant loop amplifier and the total transponder. All measurements were taken using the MEC TWT as the loop tube since time did not permit evaluation of the GE TWT in the re-entrant loop. However, it is recognized that the GE tube has some characteristics which may make it the more desirable choice in some cases. Emphasis has been placed on the re-entrant loop as this is considered the major area of investigation.

The closed loop was examined for stability and spurs and no indications of oscillation were observed. Some spurs were noted and found to be due to the local oscillator-converter combination. The largest spurs appear approximately 100 mc either side of the desired signal in the 4 gc band and they are about 30 db down from the signal. The spurs are apparently due to leakage from the local oscillator, which has a basic crystal oscillator frequency of 106 mc, mixing with the 6 gc signal in the converter and producing sidebands either side of the desired 4 gc output.

Figure 4-1 shows the power-in/power-out characteristics of the loop. Gain-frequency characteristics are shown in Figure 4-2 for small signal and loop saturation. The variations in gain with frequency are principally due to the variations in conversion loss of the down-converter, although the low gain in the 3.7 to 3.8 gc range is not fully understood. Two phenomena of interest can be noted in Figure 4-1: the saturated output power is less than that of the tube alone (Figure 3-6), and the slope of the linear or small signal portion of the curves is not unity in contrast to what one would expect. The first phenomenon, lower saturated power, is due to suppression of the 6 gc signal by the 4 gc signal as the 4 gc input power to the tube approaches P_S, thus limiting the output power before the saturated power level of the tube is reached. This results in a saturated output power of the loop some 4 or 5 db lower than that of the tube itself. Actually, the total output power can be increased beyond that indicated by the curves, but the additional power is due to distortion products and not increased signal power.

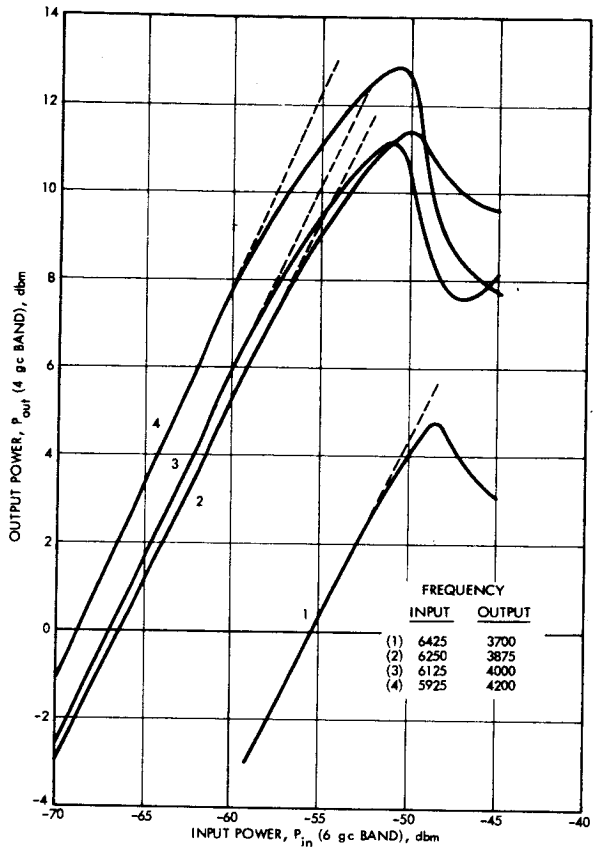

Figure 4-1. Power Output vs Power Input, Re-entrant Loop

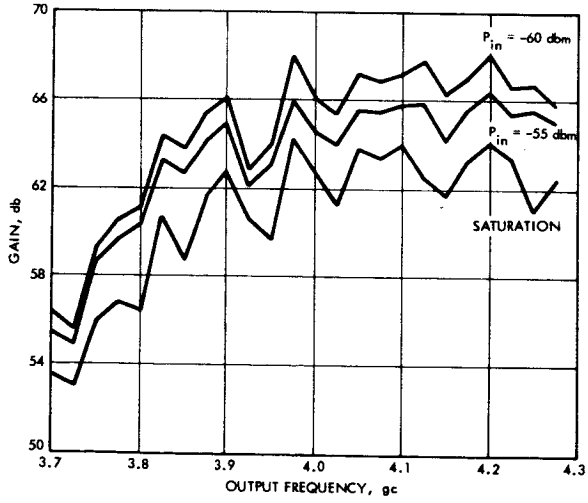

Figure 4-2. Gain vs Frequency, Re-entrant Loop

Suppression also causes the depression in the slopes. This, the second phenomenon, is discussed more fully in Section 6. The slopes are seen to vary from about 0.8 to 0.9 depending on frequency, the result being that the loop gain is dependent on input power even when operated well below loop saturation. This effect is also noted in Figure 4-2 where two different small signal levels are plotted.

Intermodulation curves for the loop are shown in Figure 4-3. In plotting this set of curves the input powers of the two signals, f_1 and f_2, in the 6 gc band were adjusted to equal levels and the output signals and intermodulation products present in the 4 gc band plotted versus the input level of a single signal. The total input power to the TWT is 3 db higher. To compare the intermodulation curves of the loop to those of

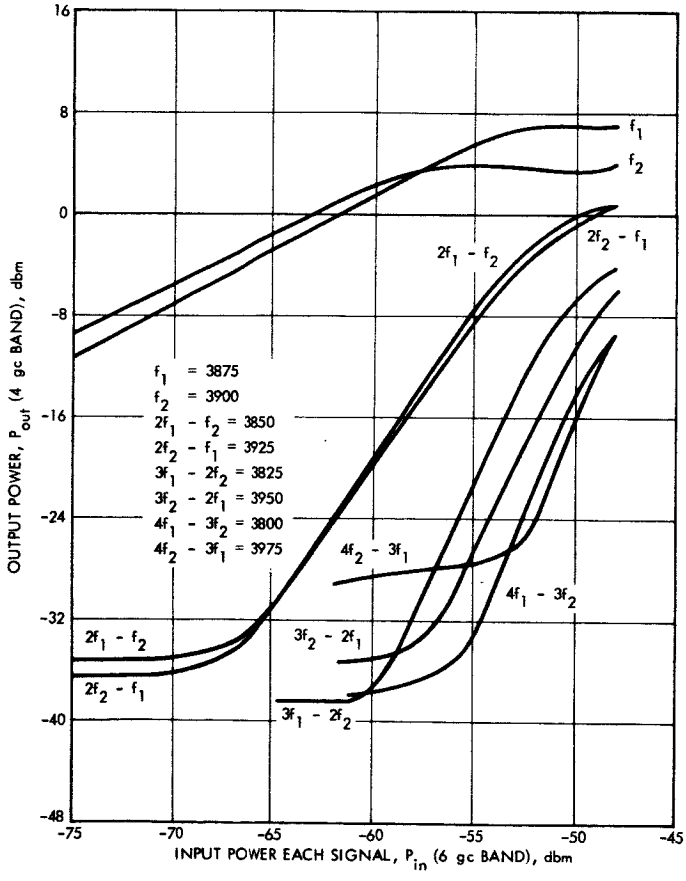

Figure 4-3. Re-entrant Loop Intermodulation

the TWT alone, the compression curves of Figure 4-1 may be normalized to a quantity P_{SL} for the loop in the same manner that P_S was determined for the TWT measurements. Performing this normalization, P_{SL} for curve 3 (Figure 4-1) is found to be -53 dbm. Then, from Figure 4-3, the third order products for input signal levels of $(P_{SL} - 10)$ or -63 dbm are about 26 db below the desired carriers. This compares very favorably with Figures 3-22 and 3-24 which show the third order products to be about 28 db below the desired signals for input levels of $(P_S - 10)$ with the TWT alone. However, the output power of the loop is some 6 db below that of the TWT and essentially the higher gain of the loop has been traded for a lower output power while maintaining the same intermodulation.

Figures 4-4 and 4-5 show the power-in/power-out and gain-frequency characteristics, respectively, of the entire transponder. The nonunity slope and gain-frequency variations may also be noted in these curves. The power amplifier tube was rather poorly matched to the re-entrant loop tube which made it necessary to use a pad between the output of the loop (port 4 of the diplexer) and the PA. A 12 db pad was selected as a compromise such that the loop could be operated over the range of interest without driving the PA too far into saturation. This is possible since the Hughes 384-H TWT used for a PA has a broad saturation range; however, the gain-frequency characteristic shown in Figure 4-5 is somewhat smoothed out due to the relative insensitivity to input power of the PA near saturation.

In making the measurements for Figures 4-4 and 4-5, it is also necessary to have a pad between the tunnel diode amplifier and the input to the loop (port 1 of the diplexer). Without a pad the gain of the TDA and re-entrant loop is sufficient to raise the noise at the input of the TDA to a high enough level to saturate the PA. The following calculation illustrates this:

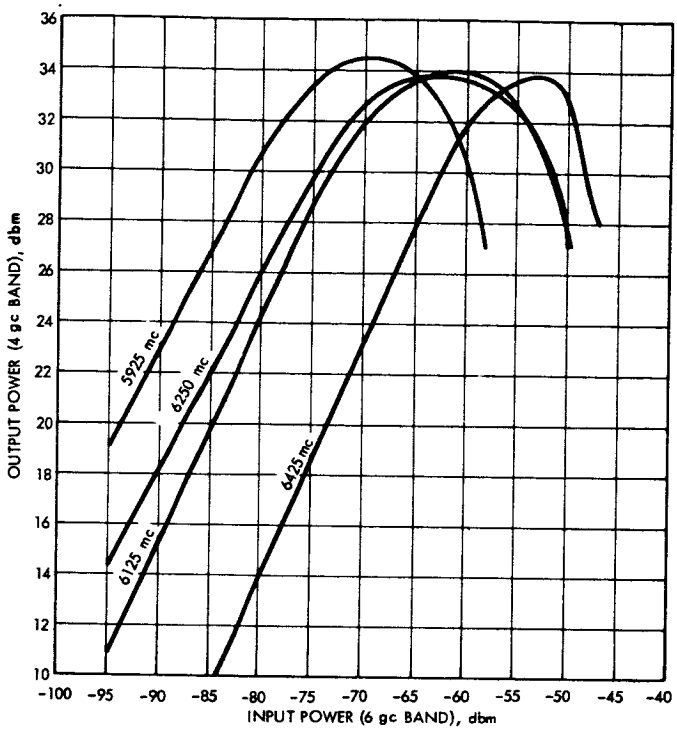

Figure 4-4. Output Power vs Input Power, Transponder

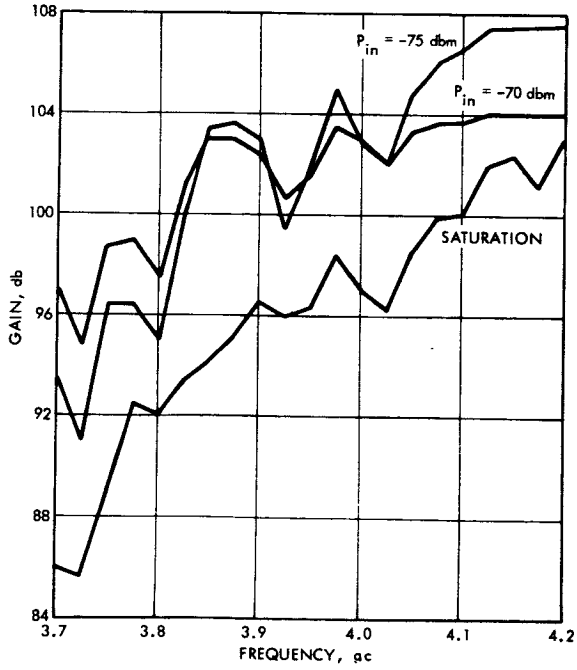

Figure 4-5. Gain vs Frequency, Transponder

Noise level	
-114 dbm/mc	kT
+7 db	noise figure TDA at 6 gc
+19 db	gain of TDA at 6 gc
+27 db	500 mc bandwidth
-61 dbm	input noise power to re-entrant loop
+68 db	gain of loop at P_{in} -61 dbm
-12 db	pad
-5 dbm	input noise power to PA

The -5 dbm noise level being higher than that required to saturate the PA (about -6 dbm), the system will operate saturated on noise unless some further gain limitation is imposed. For purposes of making the measurements on the entire transponder, a 10 db pad was used between the TDA and loop. This is enough attenuation to prevent saturation on noise and to permit measurements, provided a narrow filter centered on the desired signal is used at the output to limit the noise applied to the test equipment. Figures 4-4 and 4-5 include the effect of the 10 db pad.

When the re-entrant loop and power amplifier were first operated together, there was a strong oscillation in the 4 gc band. The oscillation was found to be taking place between the 4 gc input of the re-entrant TWT and the output of the PA and was traced to RF leakage on the power leads of the PA coupling into the leads of the MEC tube. The high gain between the two TWT's (about 70 db with the 12 db pad) and their proximity in the package was sufficient to sustain oscillation. The additional isolation necessary for stability under all conditions was provided by ferrite RF suppressor beads on the power leads and shielding both with braid and silver loaded epoxy.

A 12 db noise figure for the loop was measured. This agrees with the measured noise figure of the MEC TWT and shows no degradation due to loop operation. The noise figure of the entire transponder with the 10 db pad is 9.5 db, which is in agreement with the 7 db noise figure

measured for the tunnel diode amplifier. Without the 10 db pad, a noise figure of 8.5 db is measured. However, this is misleading since the noise power of the argon noise source, when amplified by the full gain of the TDA, is high enough to drive the loop into the compression range. This results in the 8.5 db figure measured rather than a lower value (7.1 to 7.9 db) as expected.

A TV demonstration test was set up using a split screen monitor to determine the effect of the re-entrant loop on television signals. Figure 4-6 shows the block diagram of the test setup used. The 20 mc video carrier is upconverted by the first mixer and the triple-stub tuner serves as a narrowband filter which allows only one sideband to pass. The FM carrier is then amplified by the re-entrant loop

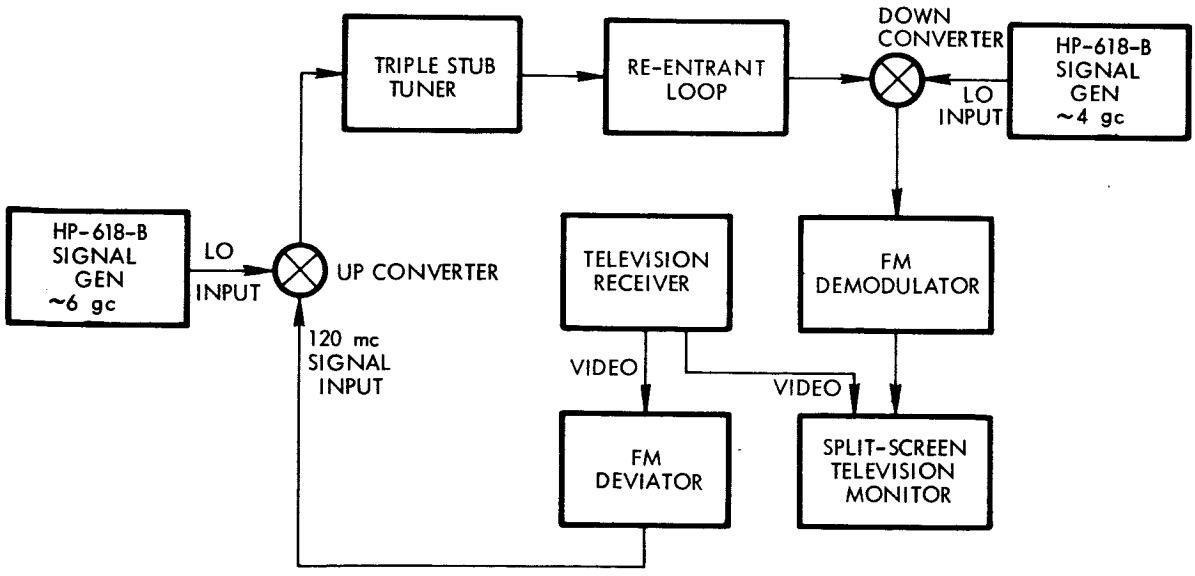

Figure 4-6. Simplified TV Test Block Diagram

(or entire transponder) and the 4 gc output signal is downconverted to 120 mc and fed to the FM demodulator. It is important that the 6 gc LO input to the first mixer be completely tuned out by the triple-stub tuner; otherwise, it will appear at the output of the loop at 4 gc and act as an LO signal into the second mixer. This results in a picture, although distorted, even with no 4 gc LO drive to the second mixer.

Figures 4-7 and 4-8 show pictures of the split screen monitor presentation where the video signal displayed on the left side of the screen has been passed through the entire transponder. Figure 4-7 is with the 10 db pad between the TDA and re-entrant loop and the input signal level adjusted to saturate the PA. The 10 db pad is removed in Figure 4-8 and the input signal adjusted for best obtainable picture without regard to level. The poor picture quality apparent in Figure 4-8 is due to the fact that the transponder saturates on noise when the 10 db pad is not used, limiting the S/N ratio that can be achieved at the output to a lower value. Figures 4-9 through 4-11 were taken with the signal output from the re-entrant loop (PA removed) and no pad between the TDA and loop. The input signal level to the TDA is indicated on the figures and an estimate of the S/N ratio at the output of the loop given. These S/N ratios are the output video modulated signal power to the noise power in the 500 mc bandwidth of the loop and not the S/N ratio displayed by the monitor. Figures 4-12 through 4-15 show the results when the 10 db pad is used. The higher S/N ratios achievable, using the pad, are apparent from the pictures. Results of passing the signal through the loop amplifier only (port 1 to port 4 of the diplexer) are shown in Figures 4-16 through 4-20. Figure 4-21 is a reference picture showing the effect of the test equipment on the picture quality. For this picture, the output signal of the FM deviator is applied directly to the demodulator, bypassing the re-entrant loop.

Re-entrant Picture Original Picture

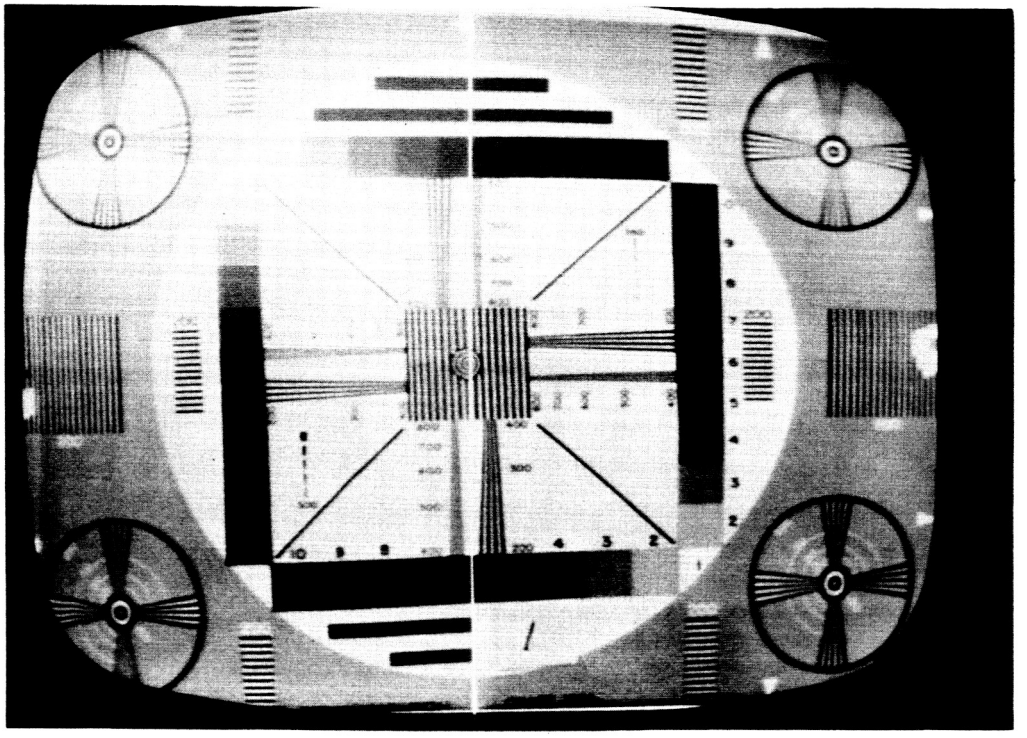

Figure 4-7. Transponder with 10 db Pad Between TDA and Loop, Saturated Output - Hughes TWT

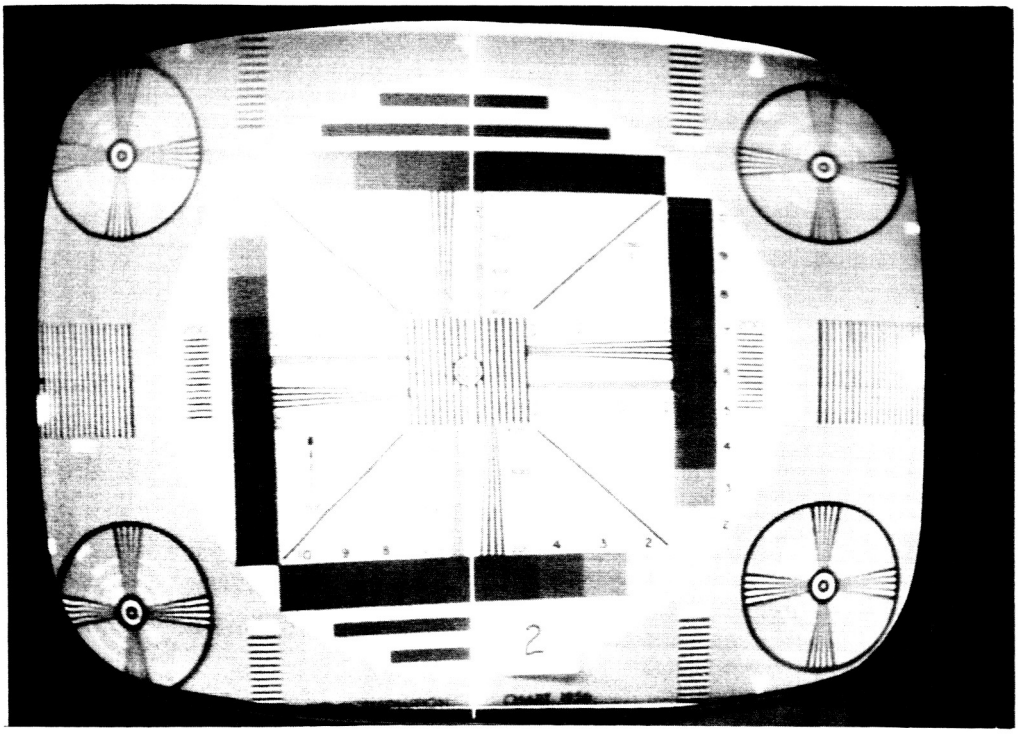

Figure 4-8. Transponder - No Pad (Saturates on Noise Input) Signal Adjusted for Best Picture

Re-entrant Picture Original Picture

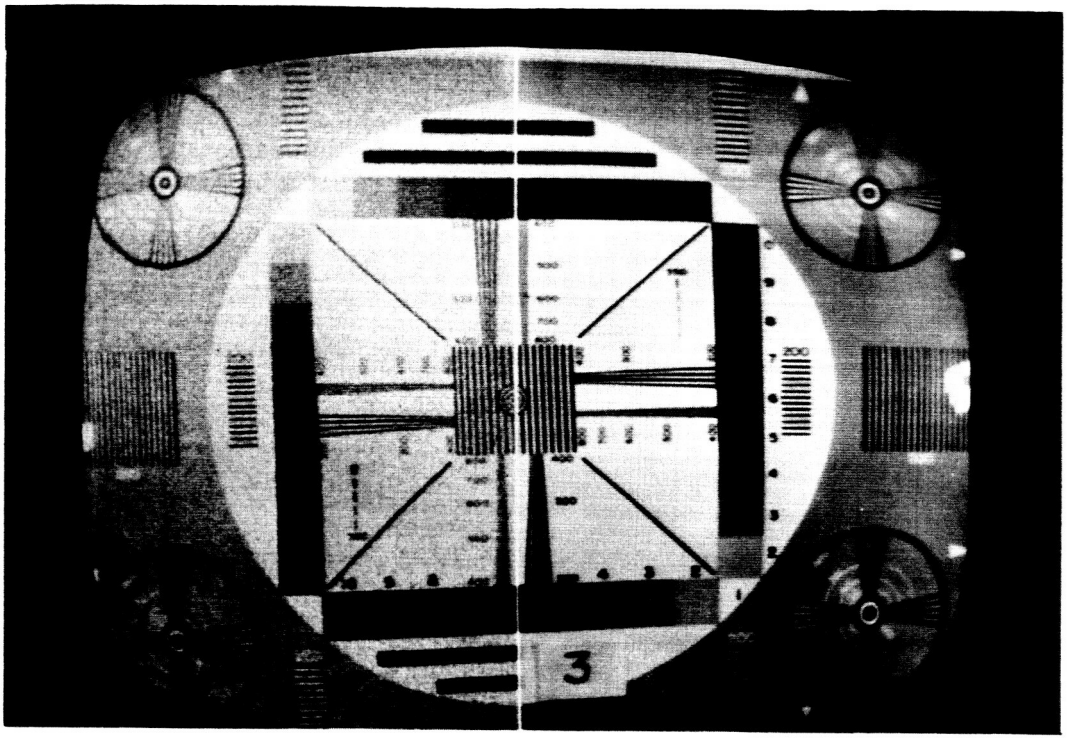

Figure 4-9. Re-entrant Loop and TDA - No Pad
Input Signal = -80.5 dbm, $(S/N)_o \simeq 0.5$ db

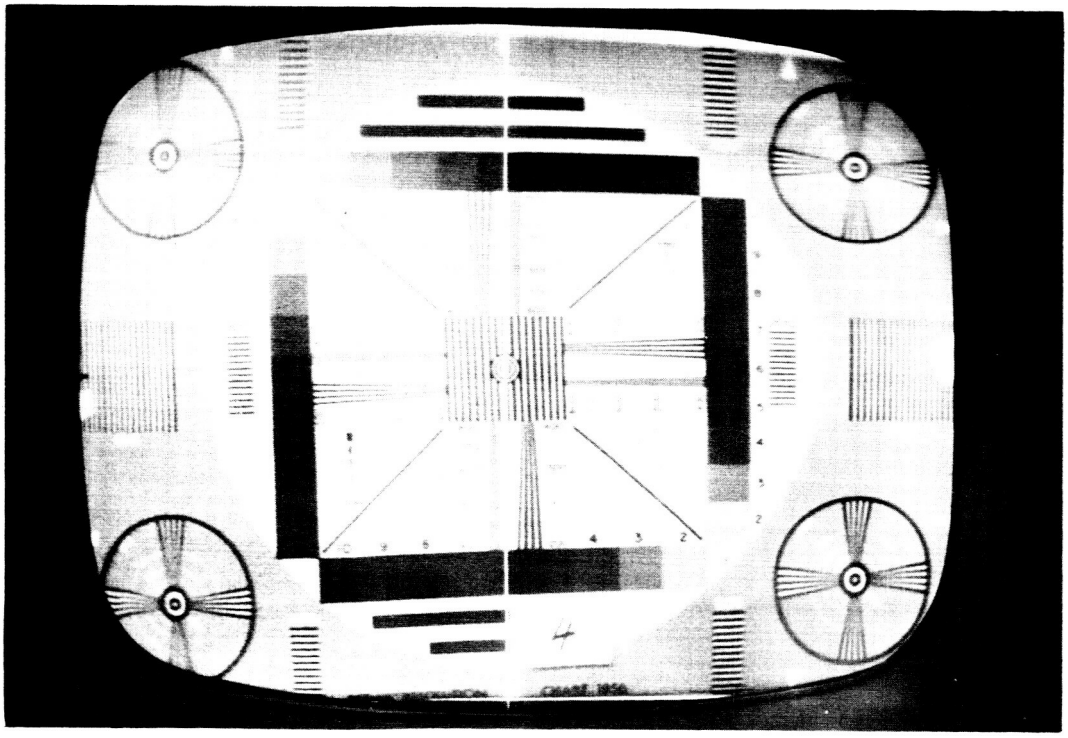

Figure 4-10. Re-entrant Loop and TDA - No Pad
Input Signal = -74 dbm $(S/N)_o \simeq 4.5$ db

Re-entrant Picture Original Picture

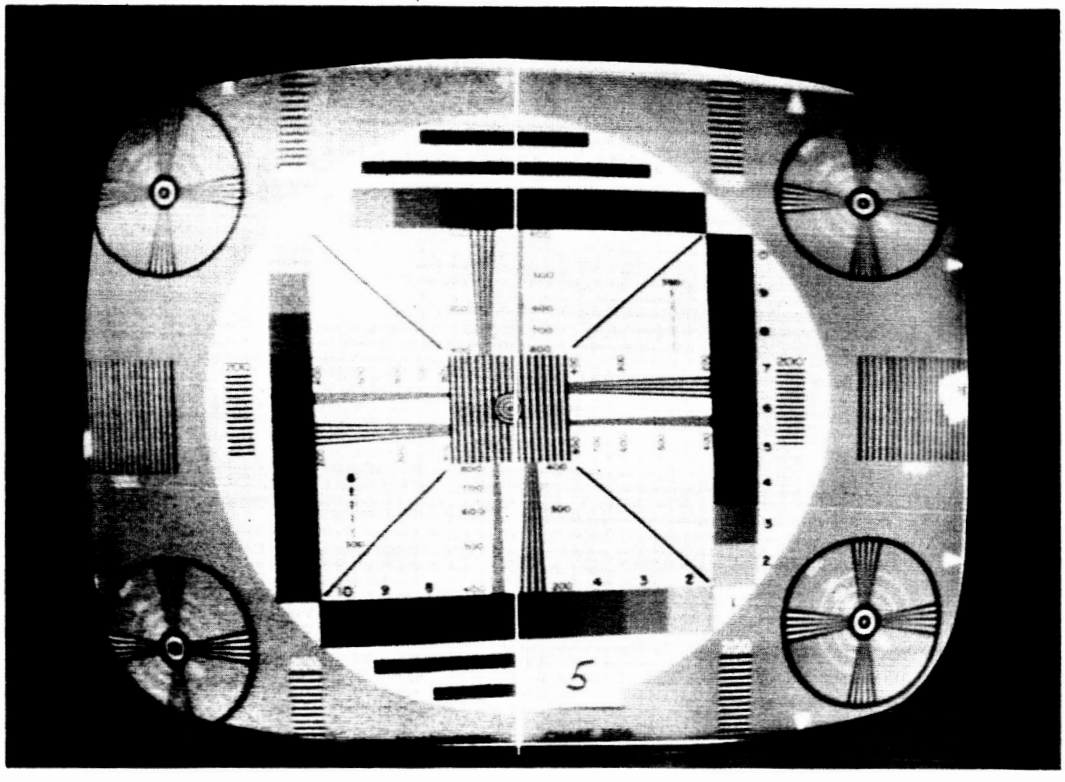

Figure 4-11. Re-entrant Loop and TDA - No Pad
Input Signal = -72.5 dbm $(S/N)_o \simeq 5.5$ db;
(Loop Saturated)

Re-entrant Picture Original Picture

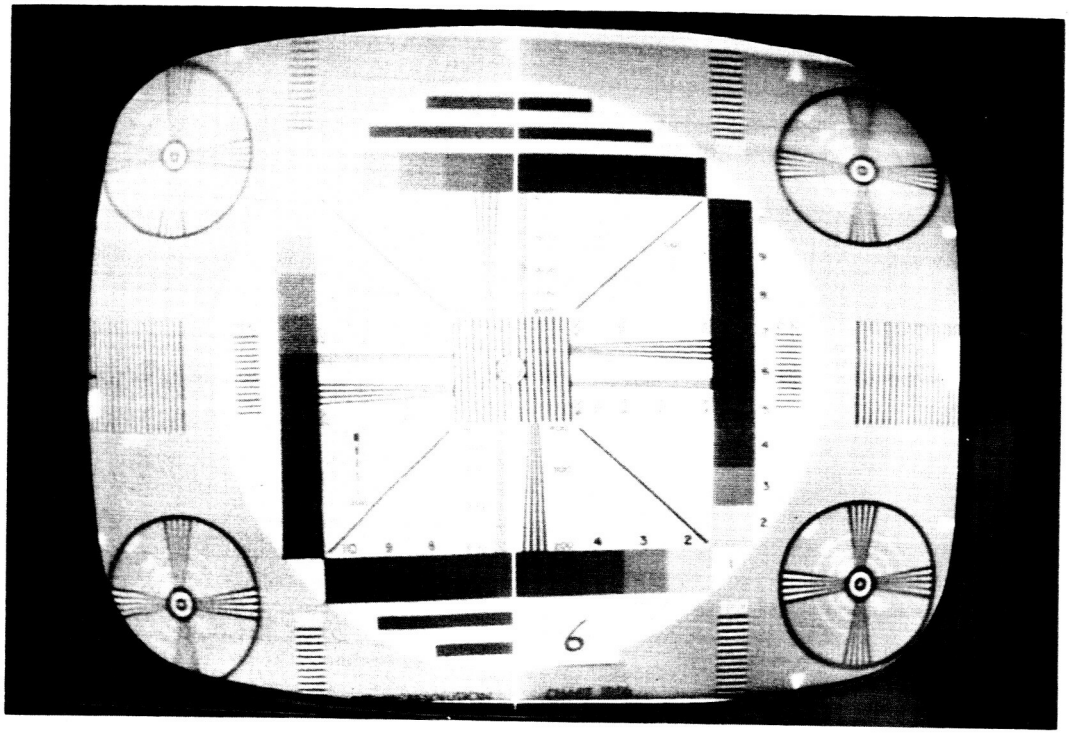

Figure 4-12. Re-entrant Loop and TDA - 10 db Pad
Input Signal = -75 dbm $(S/N)_o \simeq 3.5$ db

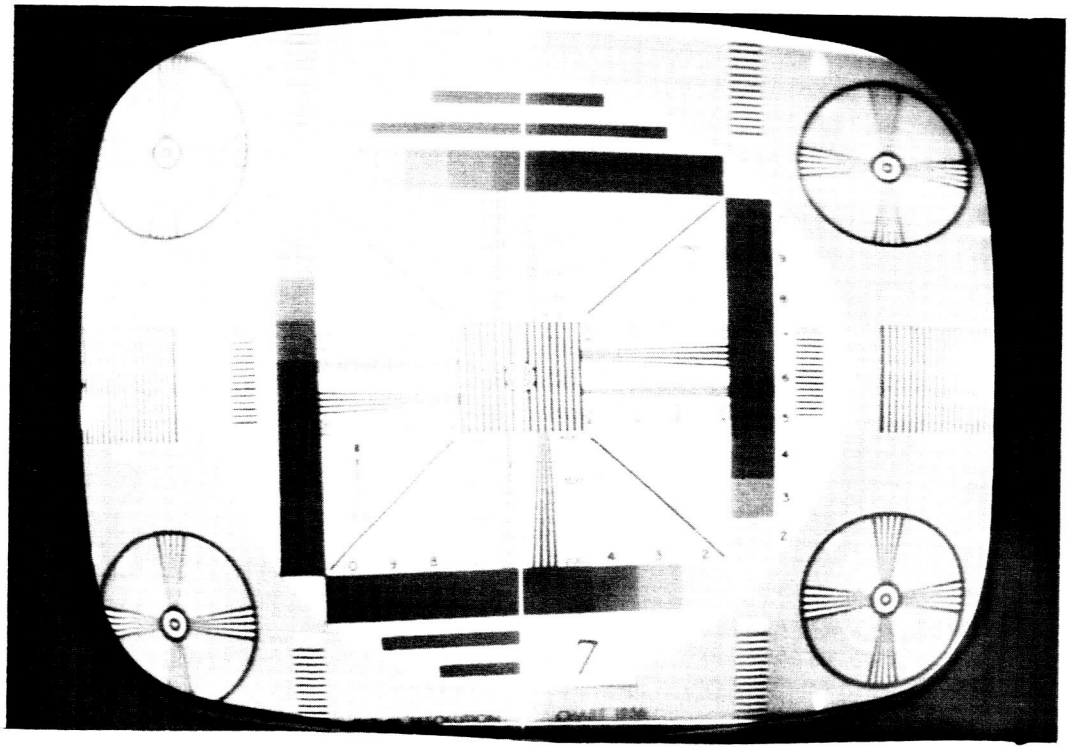

Figure 4-13. Re-entrant Loop and TDA - 10 db Pad
Input Signal = -67.5 dbm $(S/N)_o \simeq 10.0$ db

Re-entrant Picture Original Picture

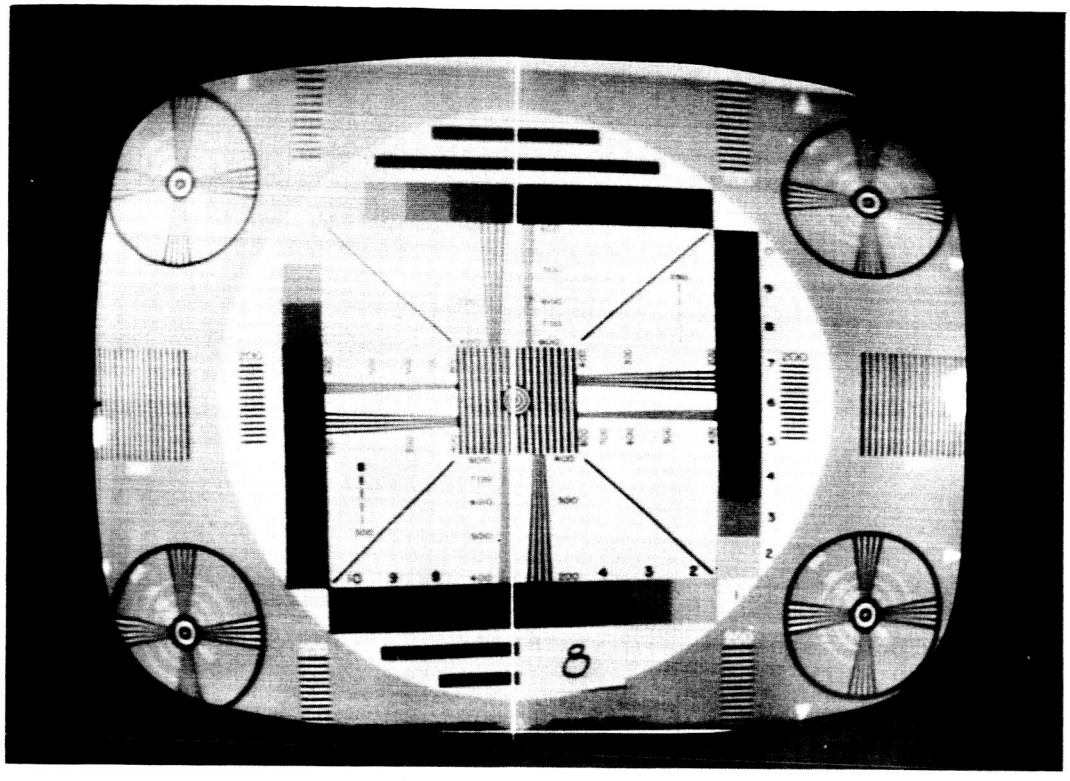

Figure 4-14. Re-entrant Loop and TDA - 10 db Pad
Input Signal = -61.5 dbm $(S/N)_o \simeq 11.5$ db

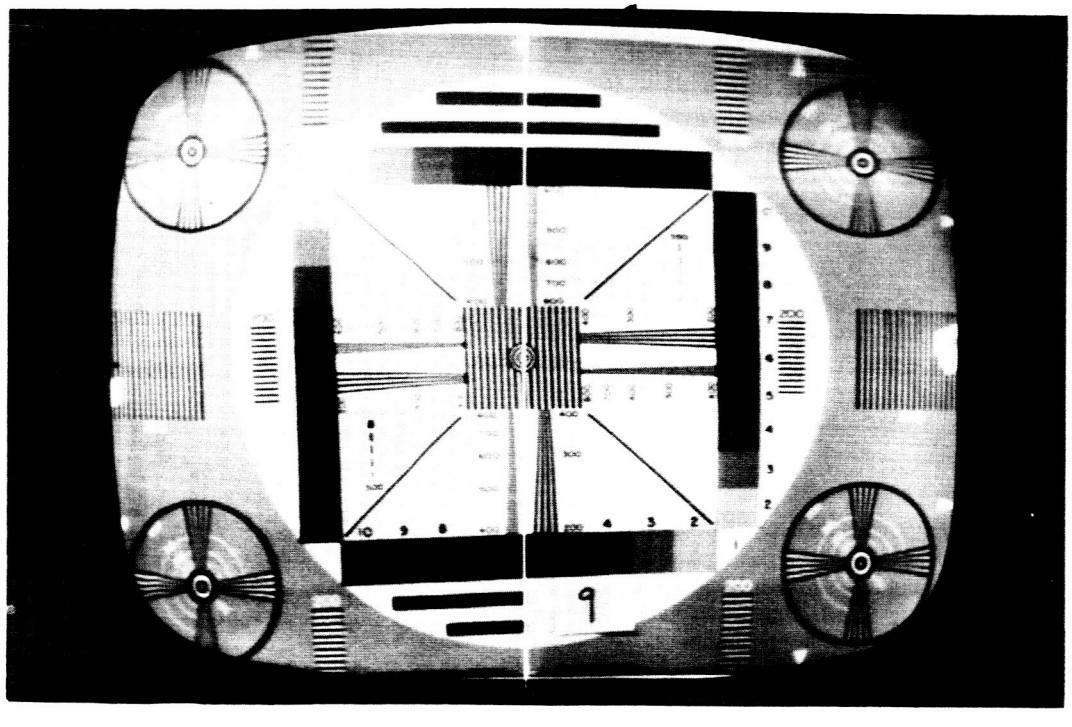

Figure 4-15. Re-entrant Loop and TDA - 10 db Pad
Input Signal = -60.0 dbm $(S/N)_o \simeq 13.0$ db
Loop Saturated

Re-entrant Picture Original Picture

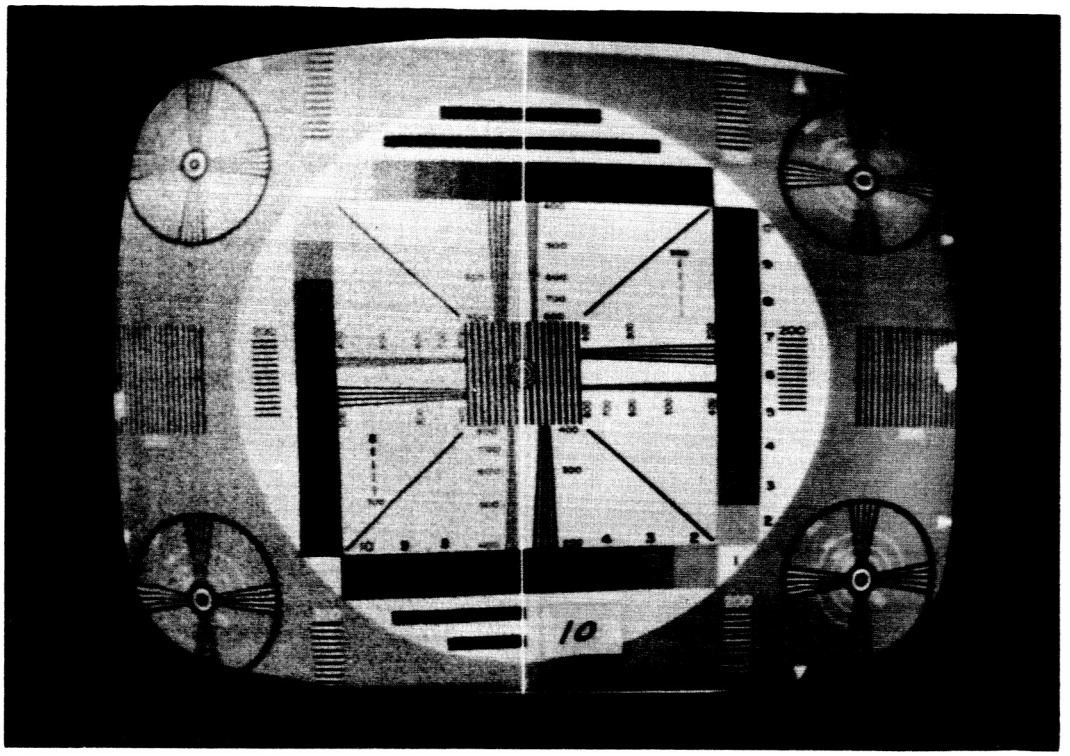

Figure 4-16. Re-entrant Loop Only
Input Signal = -71.2 dbm $(S/N)_o \simeq 2$ db

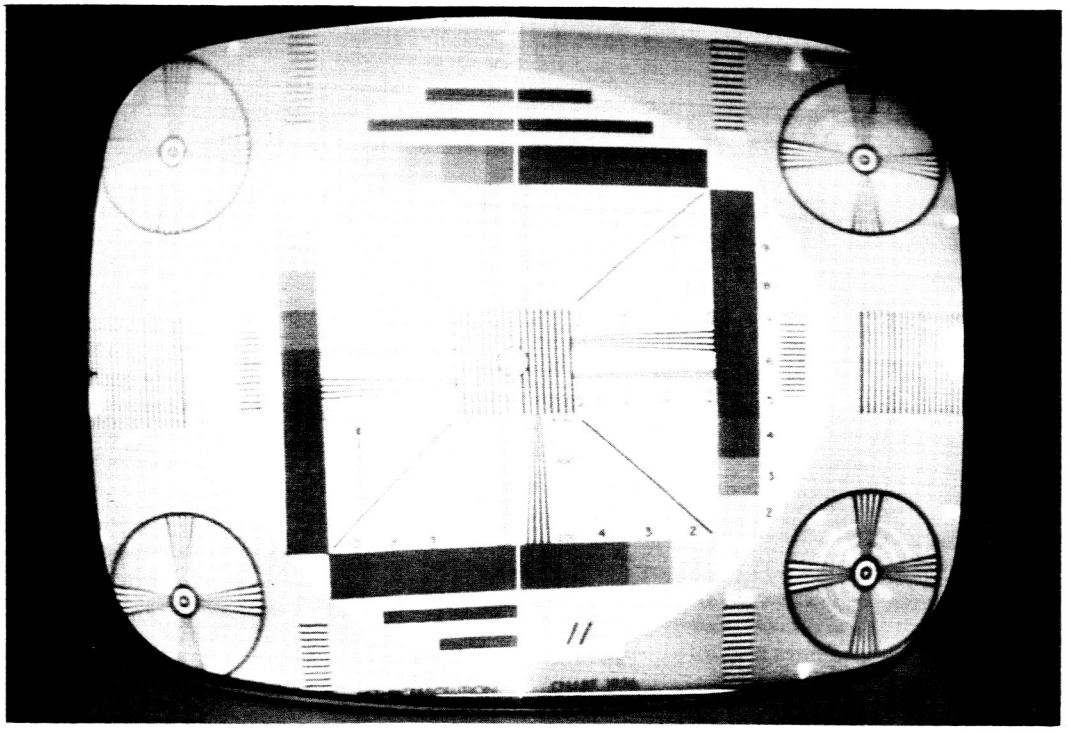

Figure 4-17. Re-entrant Loop Only
Input Signal = -64.2 dbm $(S/N)_o \simeq 6.5$ db

Re-entrant Picture Original Picture

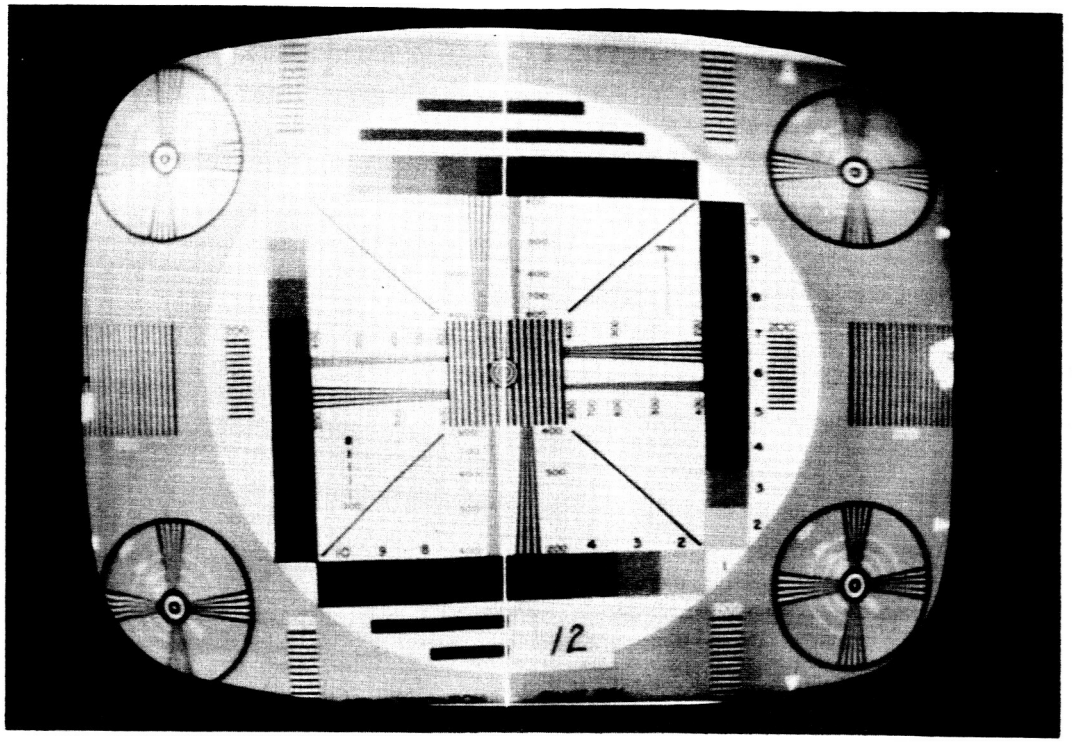

Figure 4-18. Re-entrant Loop Only
Input Signal = -57.6 dbm $(S/N)_o \simeq 9.0$ db

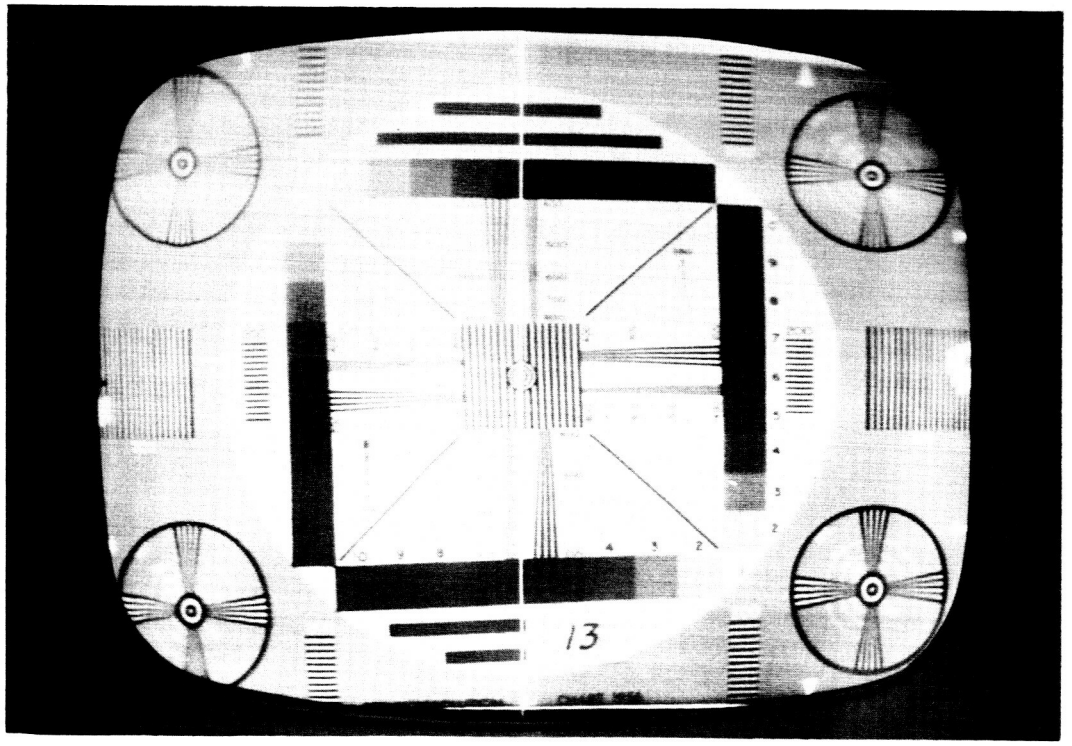

Figure 4-19. Re-entrant Loop Only
Input Signal = -51.8 dbm $(S/N)_o \simeq 13.5$ db

Re-entrant Picture Original Picture

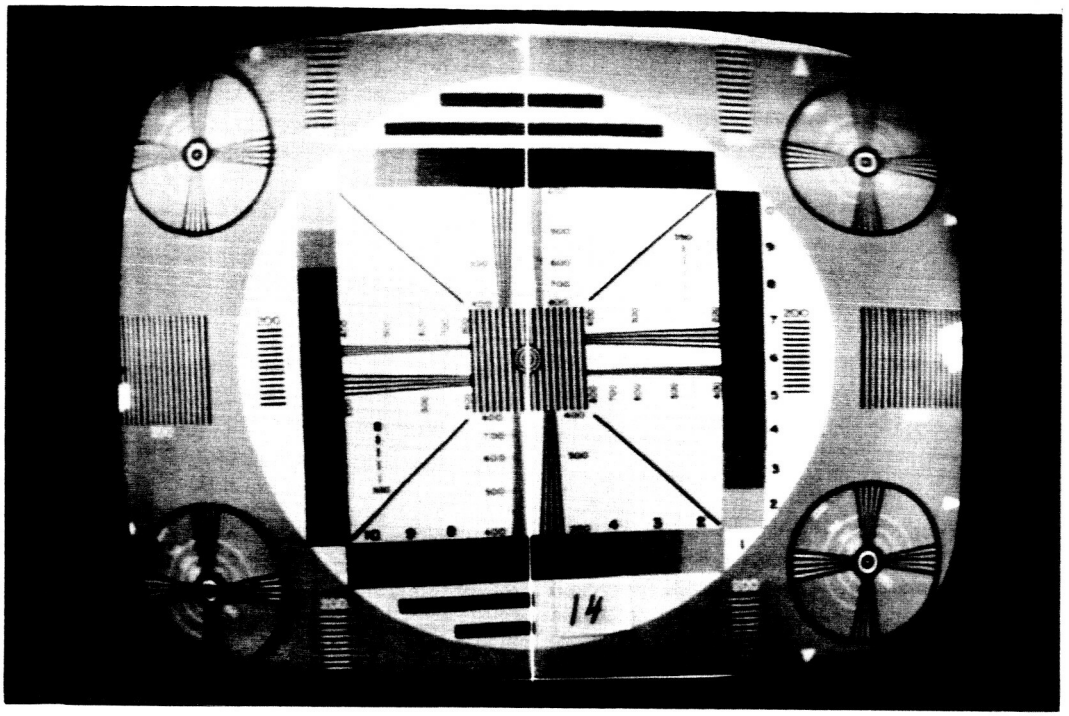

Figure 4-20. Re-entrant Loop Only
Input Signal = -50.5 dbm $(S/N)_o \simeq 14.5$ db
Loop Saturated

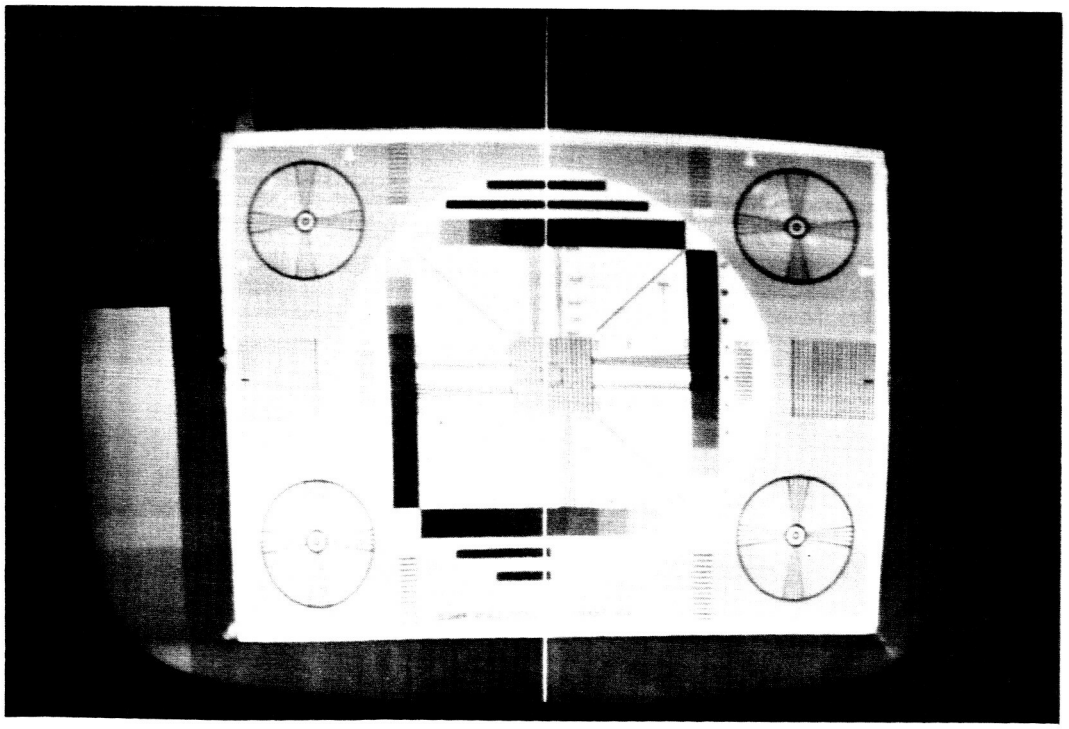

Figure 4-21. Reference Calibration Loop Bypassed

5.0 INTERMODULATION DISTORTION

In this section we treat the effect on the received baseband of intermodulation distortion resulting from nonlinear amplification by the loop. The intermodulation noise, as seen at baseband, is of principal concern in any design and in the case of the re-entrant TWT offers a means of establishing an operating point for the loop. Also, for a multiple access system, intermodulation will most likely be the limiting factor in determining how many individual carriers can be amplified simultaneously.

The input signal to the re-entrant loop is assumed to consist of equal level angle-modulated carriers. Each of the carriers in turn is taken to be modulated by a multichannel telephone signal in frequency division multiplex (FDM). In addition, each of the carriers is assumed to have identical modulation parameters; i.e., equal number of channels, equal deviations, etc. This model can be readily extended to include unequal carrier levels and different loading for each carrier, but the model is convenient analytically and is considered to be realistic. Two different frequency assignment schemes are analyzed. The first is a 20-carrier system with each carrier modulated by a 300-channel FDM telephone signal. The second system has six carriers with 1200 telephone channels each. Figures 5-1 and 5-2 show the specific frequency assignments of the carriers assumed for each system.

A standard method of evaluating the effect of intermodulation distortion is to determine the equivalent intermodulation noise as seen at the received baseband. This effective noise is expressed as the amount of psophometrically weighted noise present in any telephone channel (usually the worst) due to intermodulation. Expressions for the amount of psophometrically weighted noise in any telephone channel due to each type of third order product are derived in Appendix D. These are:

For the (2A-B) type products

$$N_{pw} = \left[\frac{3.1 \times 10^{12} f^2 C_1^{\,2}/2}{10^{0.25}\, 4 \sqrt{3\pi}\, \sqrt{P_{eq}}\, I(f)\, f^3_{drms}} \right] \exp \left[- \frac{(f - \Delta f)^2}{12\, P_{eq}\, f^2_{drms}} \right] \qquad (5\text{-}1)$$

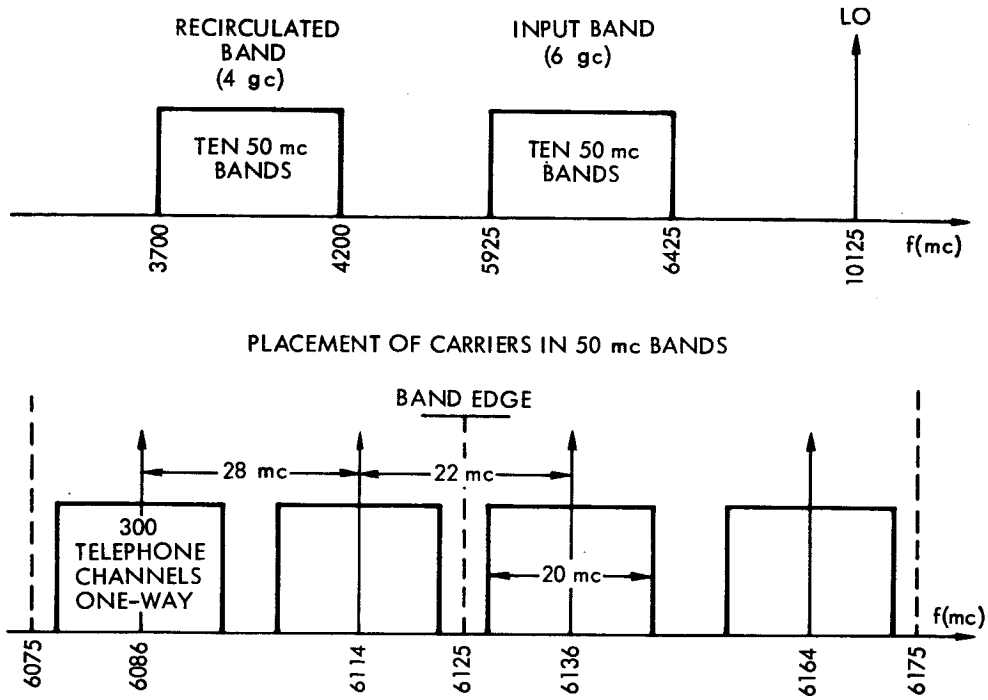

Figure 5-1. Assumed Frequency Assignments, 20-Carrier System

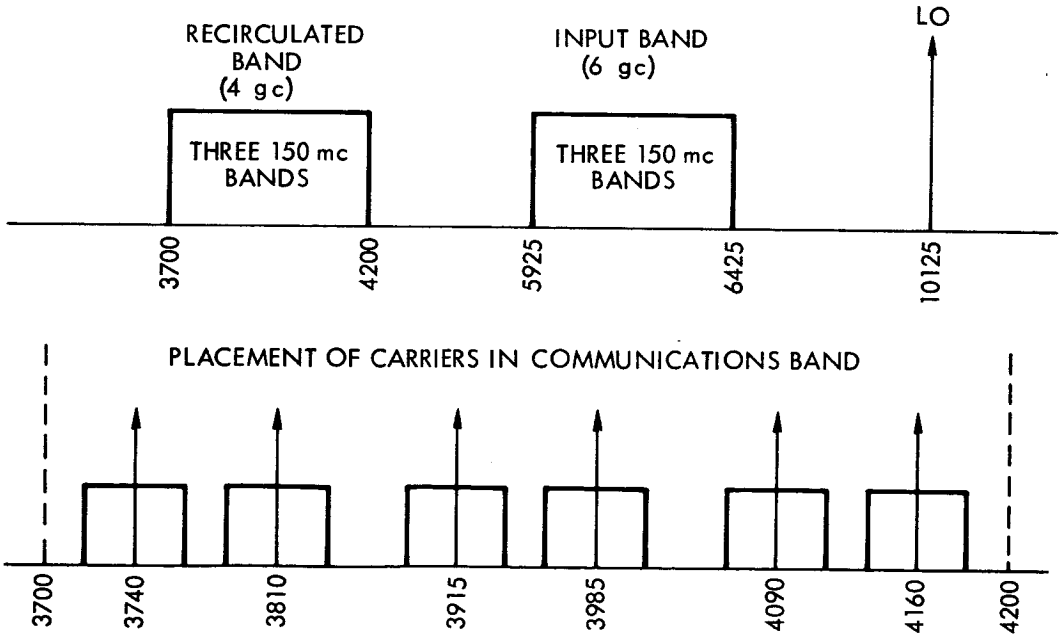

Figure 5-2. Assumed Frequency Assignments, 6-Carrier System

For (A + B - C) type products

$$N_{pw} = \left[\frac{3.1 \times 10^{12} f^2 C_2^2/2}{10^{0.25} 4 \sqrt{2\pi} \sqrt{P_{eq}} I(f) f^3_{drms}} \right] \left[\exp - \frac{(f - \Delta f)^2}{8 P_{eq} f^2_{drms}} \right] \quad (5\text{-}2)$$

where

N_{pw} = psophometrically weighted noise in the telephone channel located at frequency f

$C^2/2$ = power of third order product relative to the desired carrier

P_{eq} = equivalent noise power representing a multichannel FDM signal[4]

= $-15 + 10 \log_{10} (N_c)$, dbm 0; $N_c \geq 240$ channels

f_{drms} = frequency deviation of the carrier by an 800 cps test tone of 0 dbm0 power level

$I(f)$ = pre-emphasis improvement factor at frequency f

Δf = frequency separation of third order produce and desired carrier

In the case of 6 db per octave pre-emphasis, the quantity $f^2/I(f)$ is a constant, dependent only on the number of channels, and the worst channel is located where $(f - \Delta f)$ is smallest. Figures 5-3 through 5-6 plot the intermodulation noise (Equations (5-1) and (5-2)) in the worst channel for the case of 300 telephone channels and 6 db per octave pre-emphasis, with f_{drms} as a parameter. The worst channel for $\Delta f = 0$ is the bottom channel (f = 60 kc) and for $\Delta f = 25$ mc is the top channel (f = 1.3 mc). When CCIR pre-emphasis is used, the location of the worst channel is dependent on both the test tone deviation, f_{drms}, and the separation of the carrier and interfering product.

[4] International Radio Consultative Committee (CCIR), "Documents of the IXth Plenary Assembly, Los Angeles, 1959 (Second Impression 1960)," Vol. I, Recommendations, 1. 268.

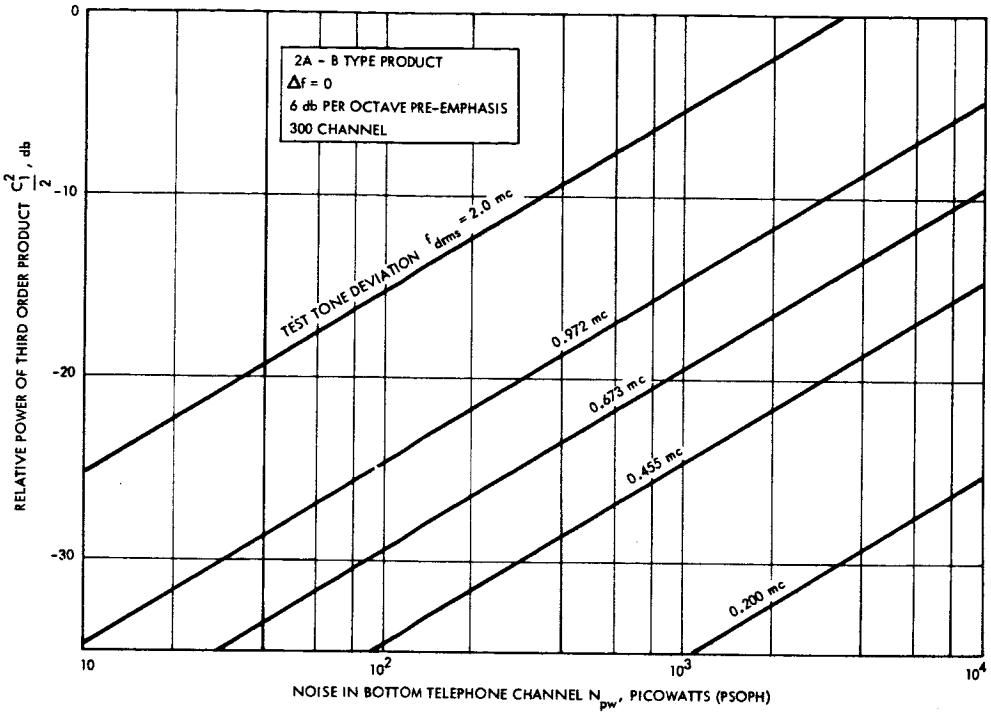

Figure 5-3. Noise Due to Interference Between Carrier and Third Order Product

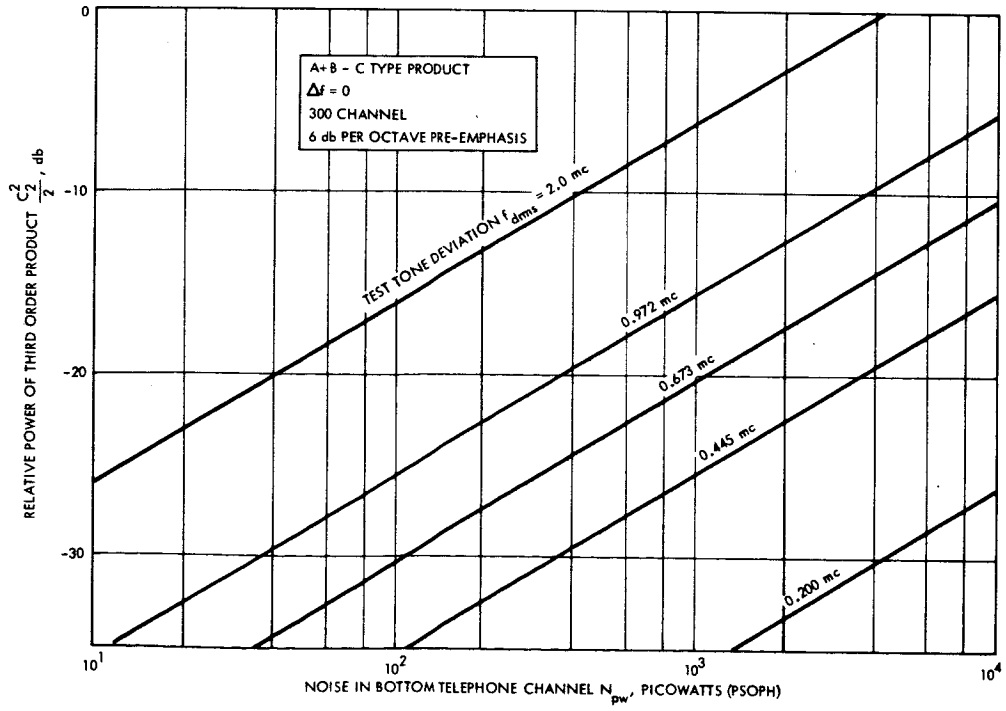

Figure 5-4. Noise Due to Interference Between Carrier and Third Order Product

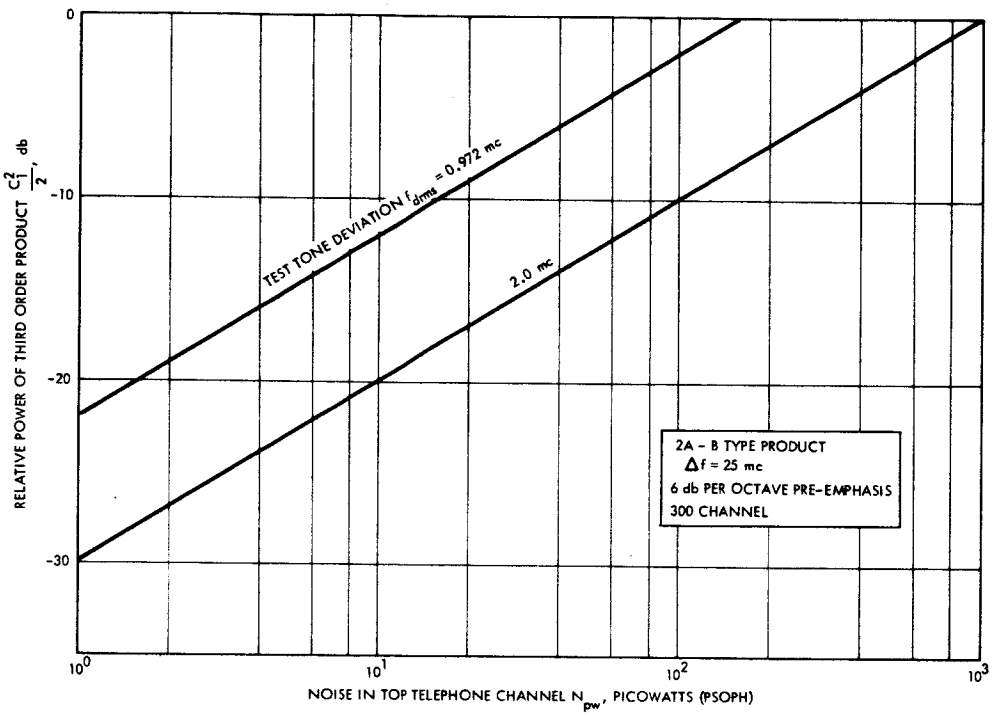

Figure 5-5. Noise Due to Interference Between Carrier and Third Order Product

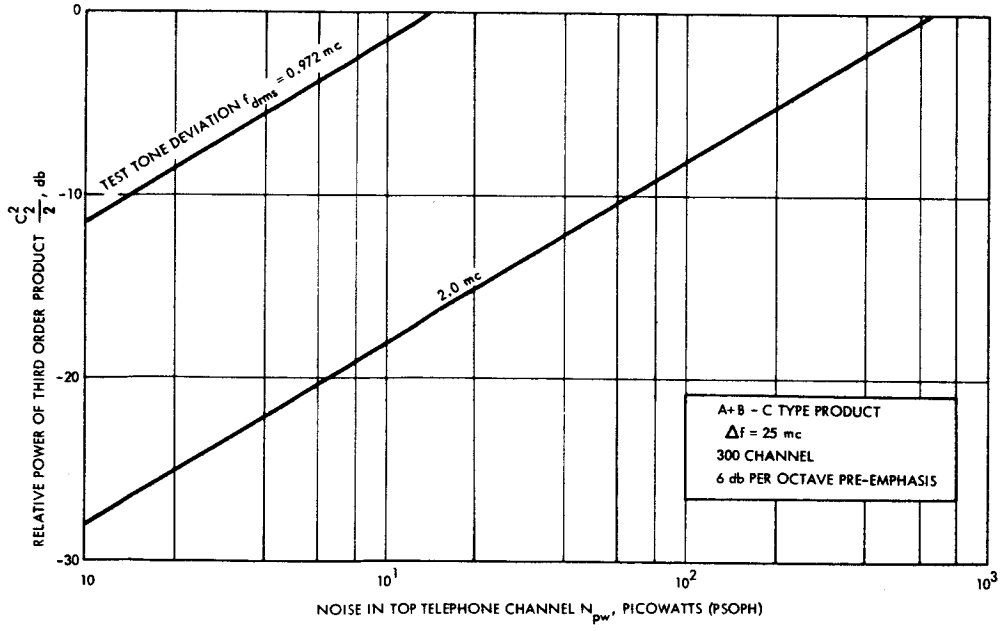

Figure 5-6. Noise Due to Interference Between Carrier and Third Order Product

A method of determining the location of the worst channel is derived in Appendix D (Equation (D-54)). Figure 5-7 shows the worst channel location for the (2A-B) type product as a function of f_{drms} for the 300-channel case and $\Delta f = 0$. For $\Delta f = 25$ mc, the worst channel is found to be the top channel for all deviations. Figures 5-8 and 5-9 plot the intermodulation noise in the worst telephone channel due to interference by the (2A-B) type product for $\Delta f = 0$ and $\Delta f = 25$ mc respectively, when CCIR pre-emphasis is used.

To compute the total noise due to intermodulation, it is necessary to know the location of all the products which fall within the band of interest. A computer program has been written and used to determine the location of the third order intermodulation products for a given frequency assignment. Figure 5-10 shows the distribution of third order products which fall within the 3.7 to 4.2 gc band for the 20-carrier system. It is seen that in a worst case there are 91 products of the (A + B - C) type and four of the (2A-B) type. It is interesting to note that the frequencies for these worst cases correspond to frequencies of desired carriers such that $\Delta f = 0$. The large number of IM products for the 20-carrier system make it impossible to find a reasonable operating point for the present re-entrant loop.

As a specific example, consider the 20-carrier system using 6 db per octave pre-emphasis and a test tone deviation $f_{drms} = 0.972$ mc. Assuming a relative third order product level $C_2^2/2 = -30$ db, Figure 5-4 shows that each product contributes 36 pw of noise to the bottom channel. Thus, in the worst case with 91 such products ($\Delta f = 0$), the total contribution is 3,276 pw, considerably more than could be tolerated. The total intermodulation noise is much higher when the contributions from all the products are included.

Fewer carriers greatly reduce the number of intermodulation products. This is indicated in Figure 5-11 which shows the distribution of third order products for the six-carrier system. The worst case for this system has five products of the (A + B - C) type with $\Delta f = 0$ and two products of each type at $\Delta f = 35$ mc. Products separated by more than 35 mc contribute a negligible amount of noise. Figures 5-12 through 5-15 plot the intermodulation noise in the worst channel due to

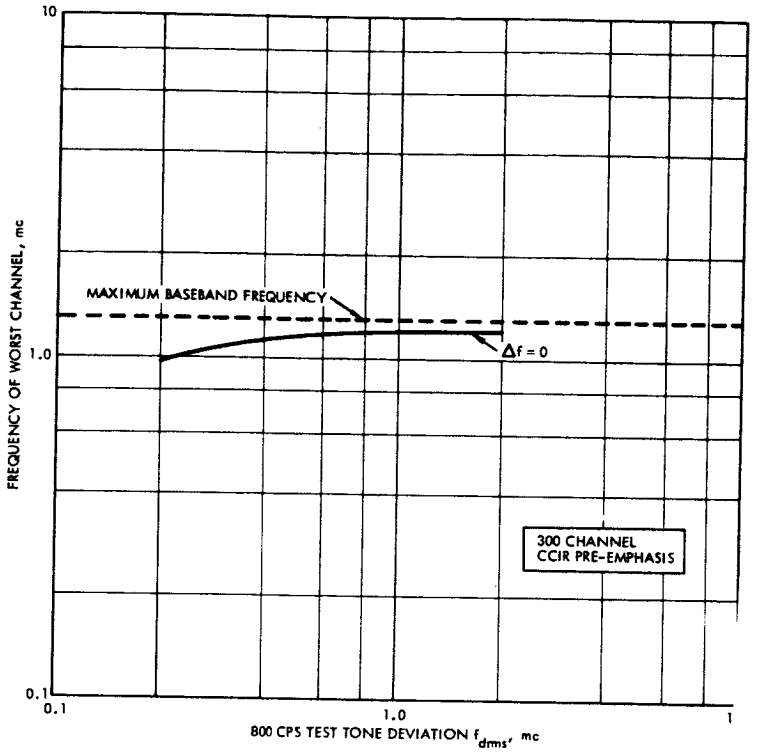

Figure 5-7. Location of Worst Channel for Intermodulation Noise Due to Third Order Product

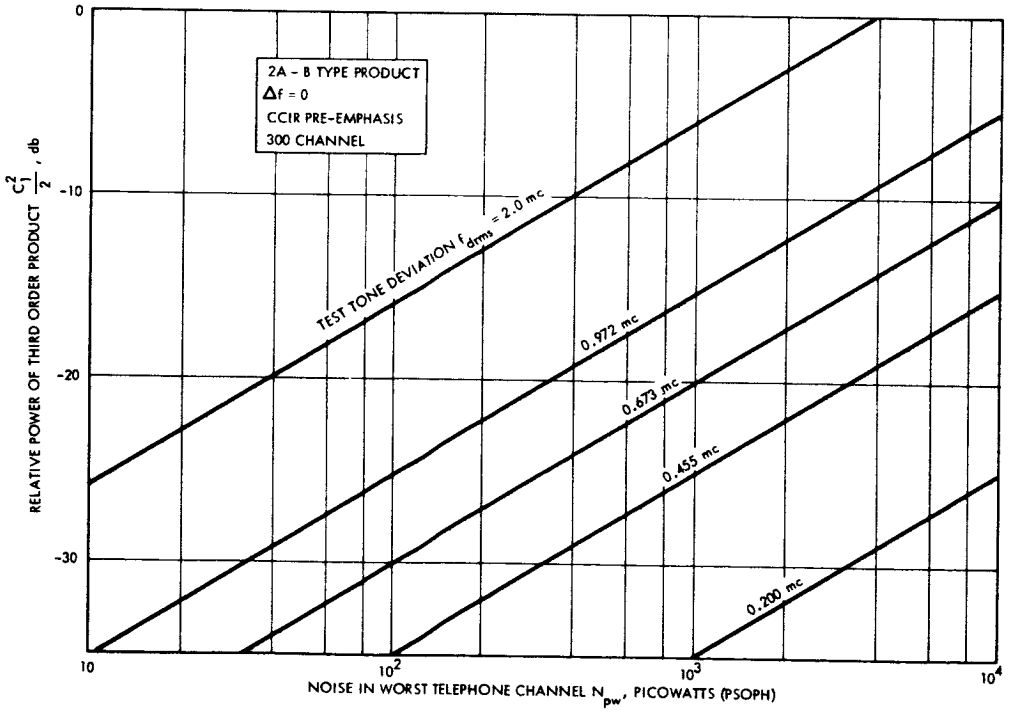

Figure 5-8. Noise Due to Interference Between Carrier and Third Order Product

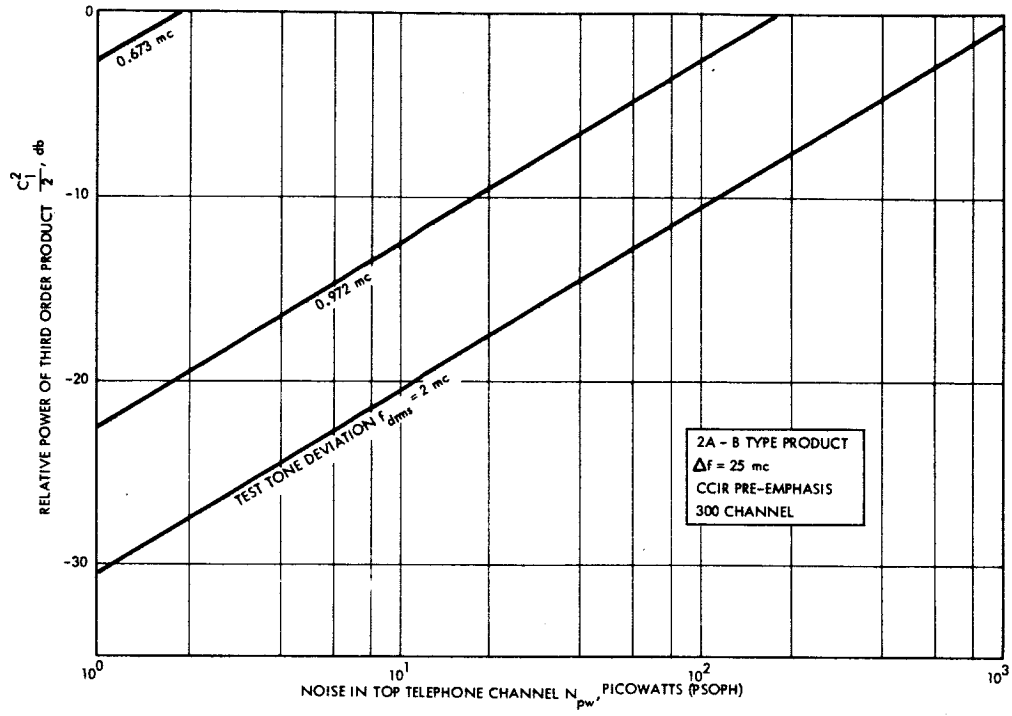

Figure 5-9. Noise Due to Interference Between Carrier and Third Order Product

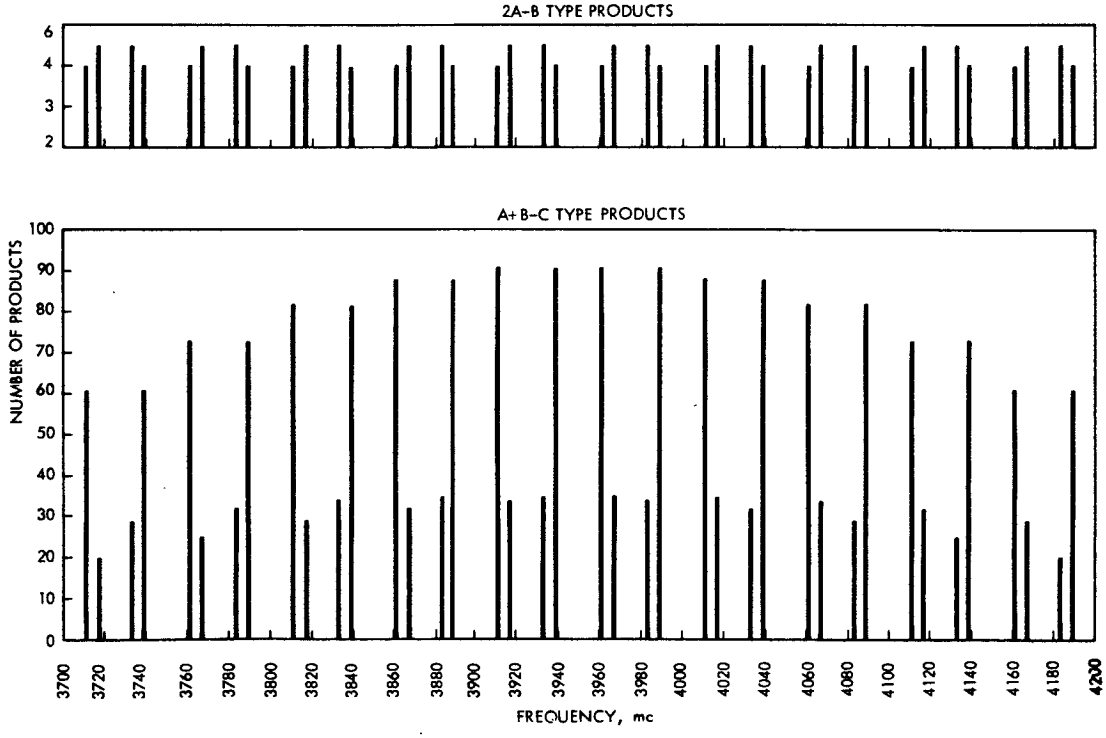

Figure 5-10. Distribution of Third Order Intermodulation Products for 20 Carriers

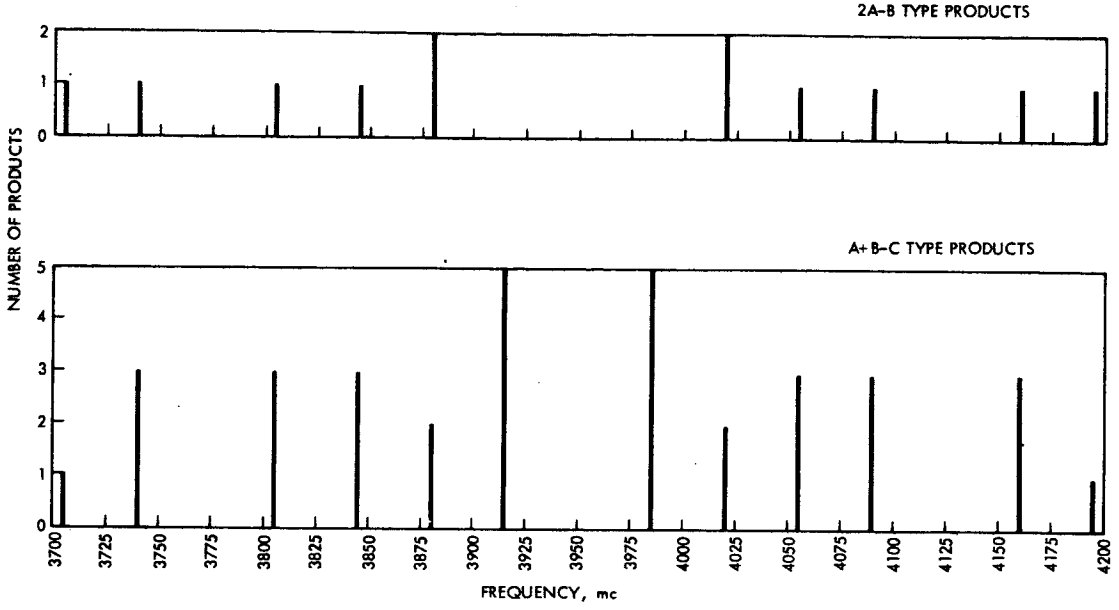

Figure 5-11. Distribution of Third Order Intermodulation Products for Six Carriers

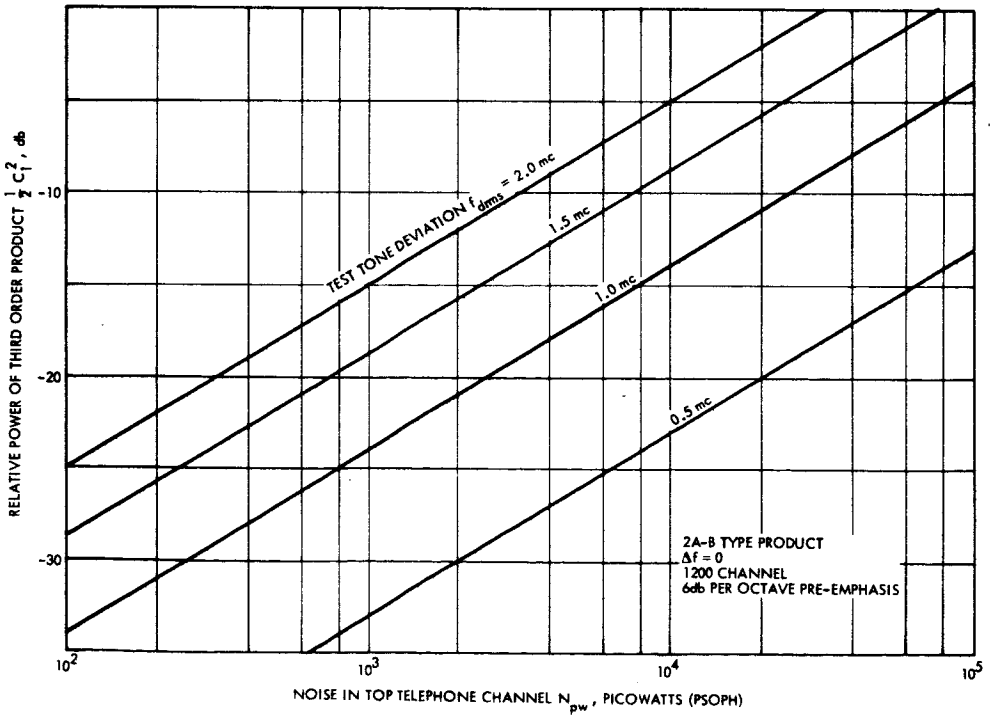

Figure 5-12. Noise Due to Interference Between Carrier and Third Order Product

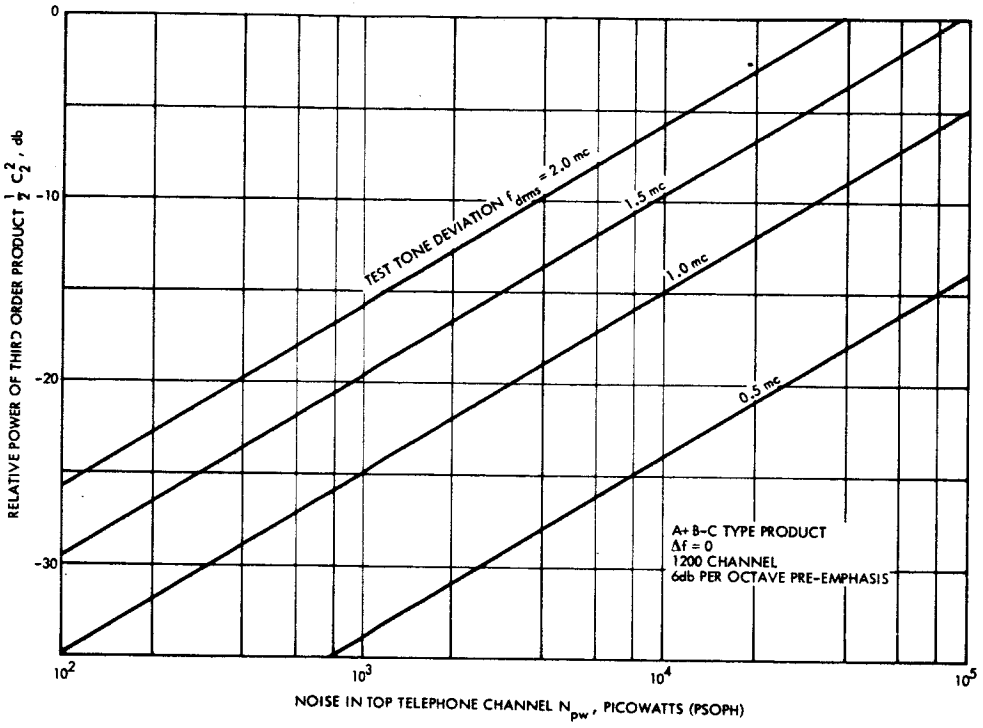

Figure 5-13. Noise Due to Interference Between Carrier and Third Order Product

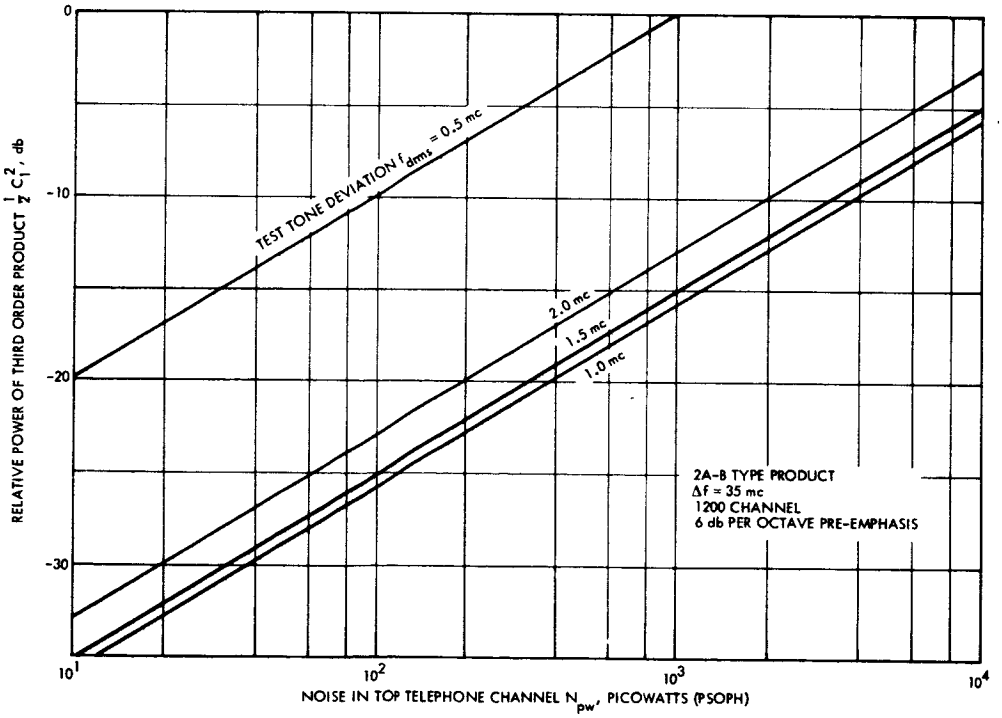

Figure 5-14. Noise Due to Interference Between Carrier and Third Order Product

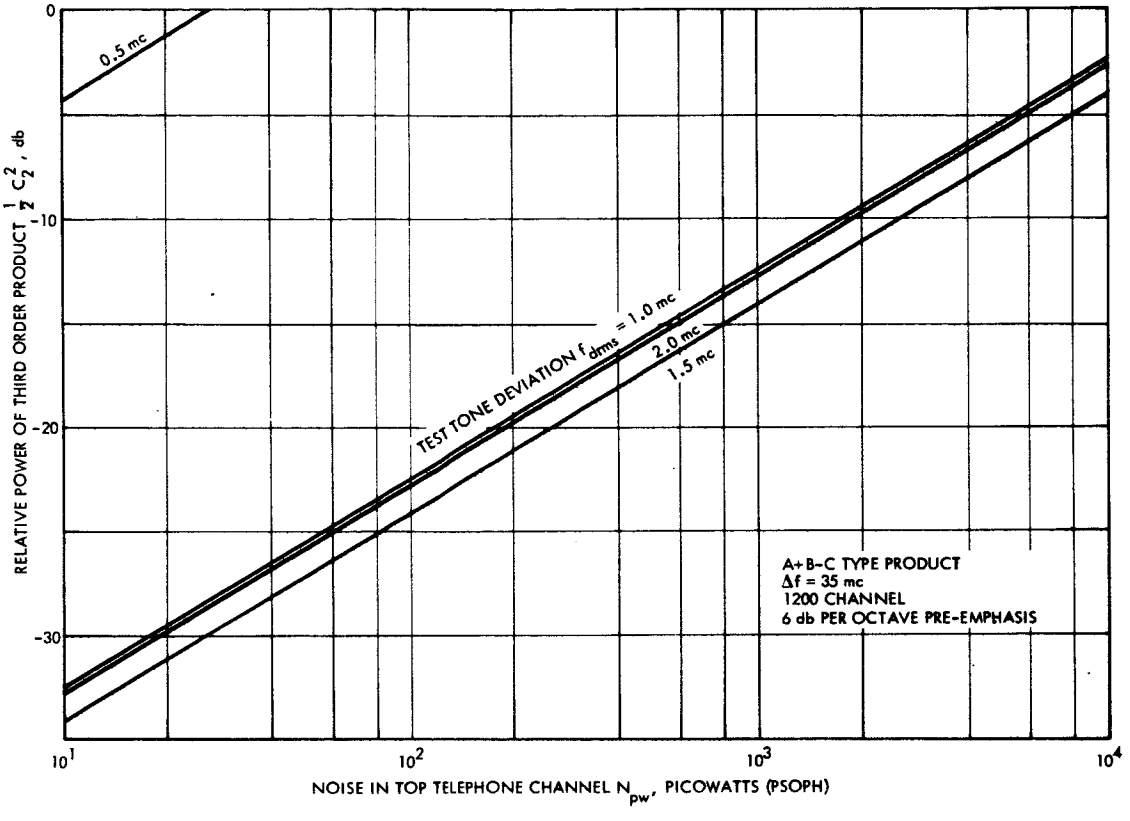

Figure 5-15. Noise Due to Interference Between Carrier and Third Order Product

interference between the carrier and a third order product for 1200 telephone channels with 6 db per octave pre-emphasis. Carrier and product frequency separations of 0 and 35 mc are represented which correspond to the nearest or worst products from Figure 5-11. As was the case for 300 channels, the location of the worst channel with CCIR pre-emphasis is not necessarily the top or bottom channel. Figure 5-16 shows the location of the worst channel versus f_{drms} when CCIR pre-emphasis is used for $\Delta f = 0$ and both types of product. For $\Delta f = 35$ mc the top channel ($f = 5.56$ mc) is the worst. Figures 5-17 through 5-20 plot the intermodulation noise in the worst telephone channel when CCIR pre-emphasis is used for 1200 channels.

As an example of the total noise calculation, consider the six-carrier system with the same operating conditions as the previous example. That is, using 6 db per octave pre-emphasis, $f_{drms} = 1.0$ mc, and a relative third order product level $C_2^2/2 = -30$ db. Then from Figures 5-13, 5-14, and 5-15 we have

5 (A + B - C)	type with Δf = 0 mc	at 310 pw each	= 1,550 pw
2 (A + B - C)	type with Δf = 35 mc	at 17.5 pw each	= 35 pw
2 (2A - B)	type with Δf = 35 mc	at 9.5 pw each	= 19 pw
	Total intermodulation noise		= 1,604 pw

Note that the power level of the (2A - B) type product is 6 db lower than (A + B - C) type; i.e., $C_1^2/2 = -36$ db. Table 5-1 shows the total intermodulation noise for the other combinations of deviation and pre-emphasis and relative product levels of -30, -25, and -20 db.

The values given for CCIR pre-emphasis are somewhat high as the noise in the worst channel for each type product and separation were merely added to find the total. Actually, the worst channel occurs at different frequencies and the worst channel contributions should not be added directly. This error is quite small, however, since the principal contribution is due to the (A + B - C) type product located where $\Delta f = 0$.

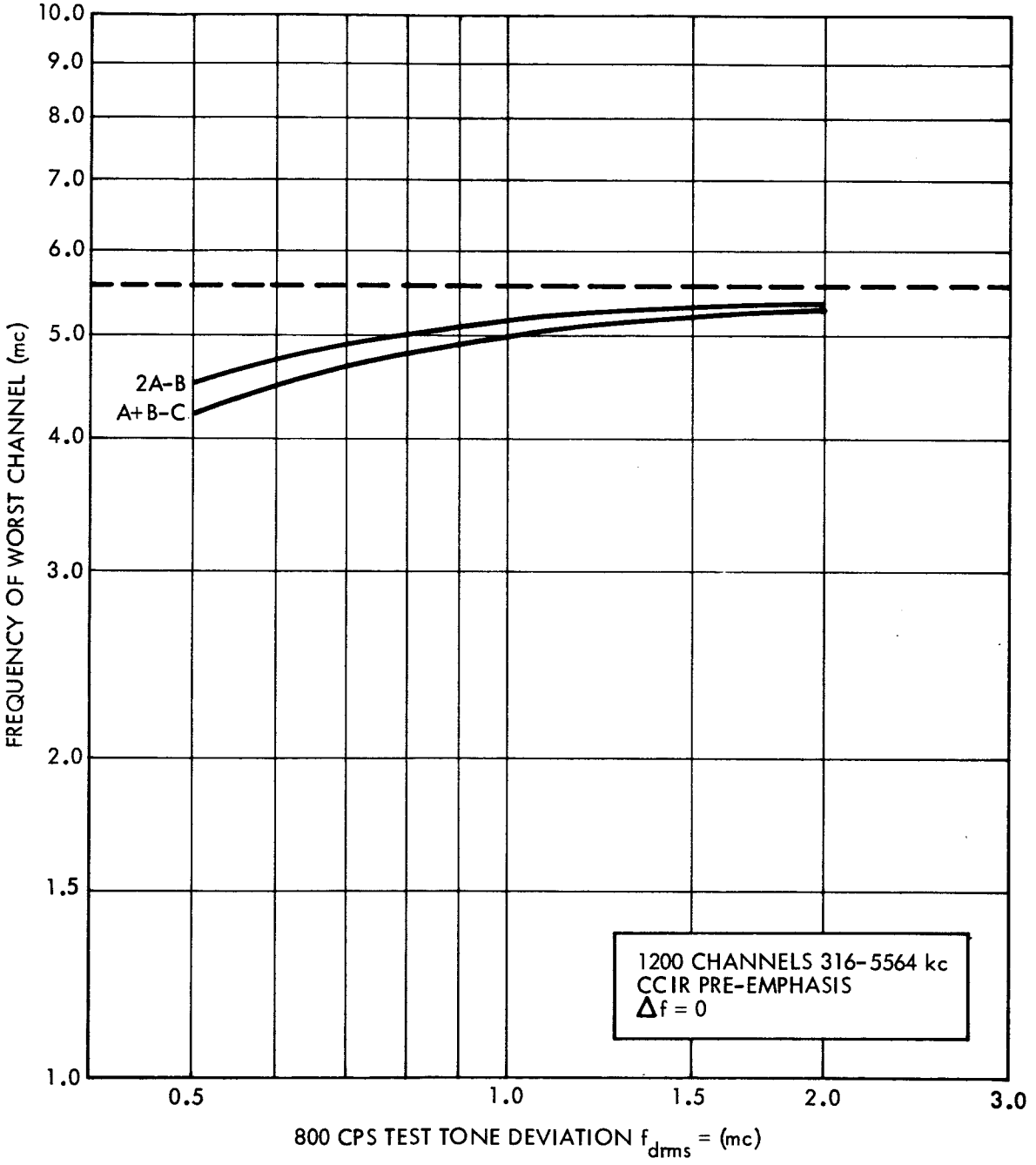

Figure 5-16. Location of Worst Telephone Channel for Intermodulation Noise

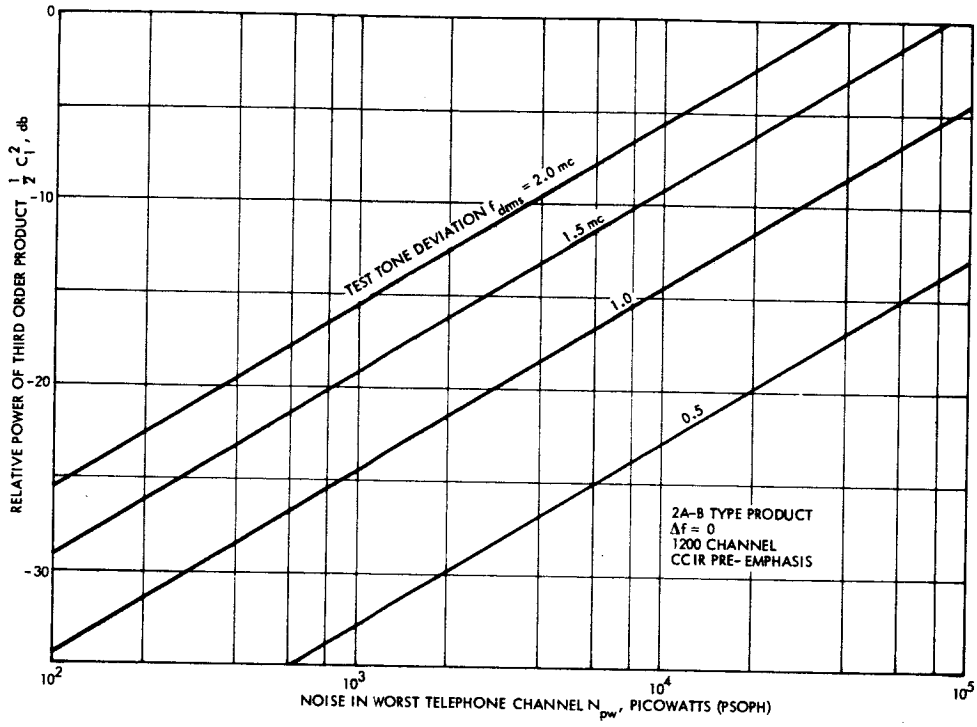

Figure 5-17. Noise Due to Interference Between Carrier and Third Order Product

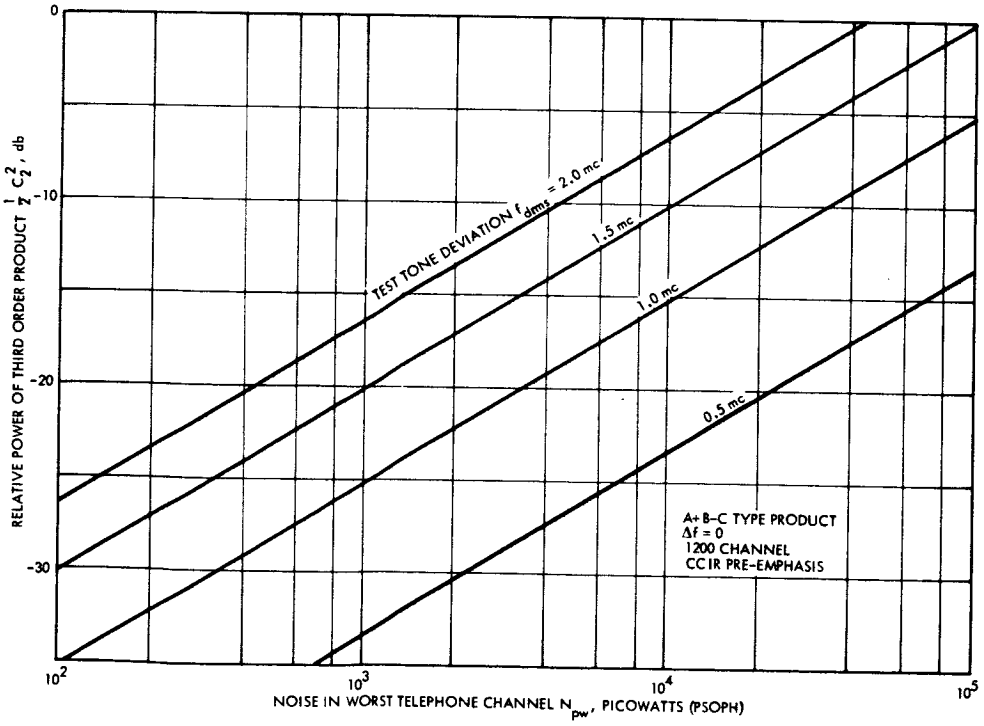

Figure 5-18. Noise Due to Interference Between Carrier and Third Order Product

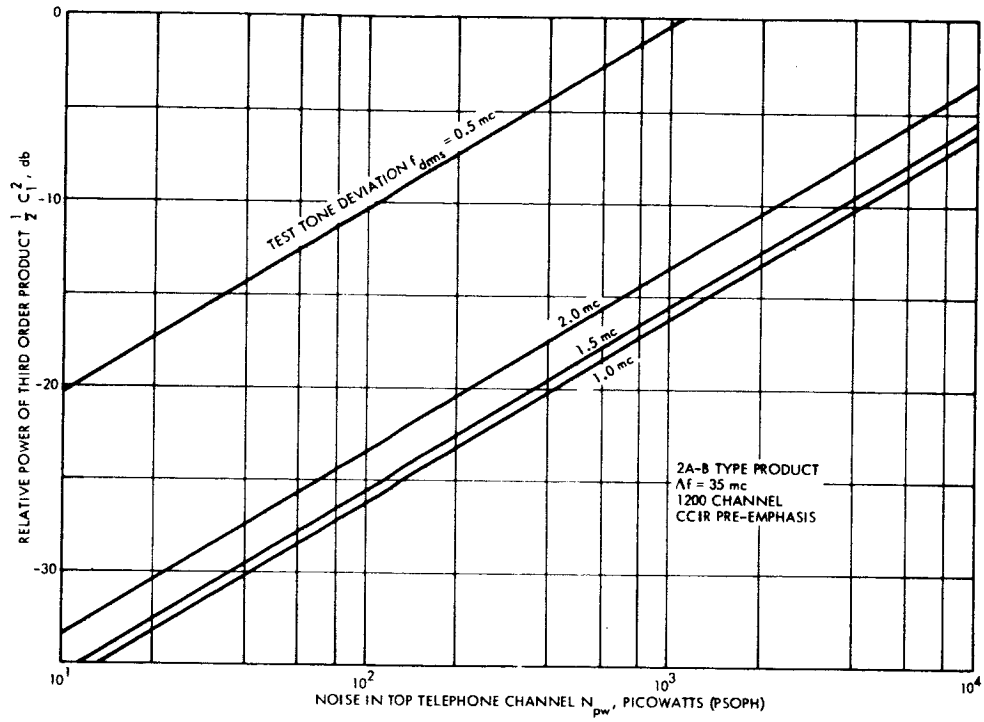

Figure 5-19. Noise Due to Interference Between Carrier and Third Order Product

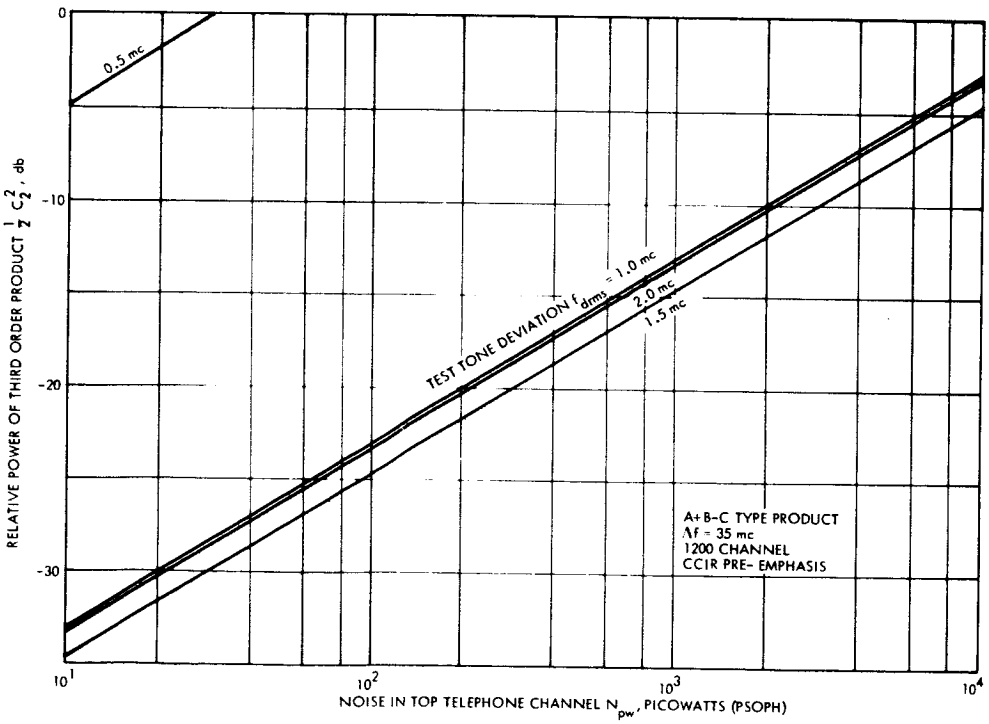

Figure 5-20. Noise Due to Interference Between Carrier and Third Order Product

Table 5-1. Total Intermodulation Noise in the Worst Telephone Channel due to Re-entrant Loop (6-carrier systems)

Relative Power of (A + B - C) Type Product	6 db per Octave Pre-emphasis Test Tone Deviation, f_{drms}			
	0.5 mc	1.0 mc	1.5 mc	2.0 mc
-30 db	> 12,500 pw	1,600 pw	530 pw	240 pw
-25 db	> 39,500 pw	5,170 pw	1,670 pw	750 pw
-20 db	> 125,000 pw	> 15,500 pw	5,280 pw	2,430 pw

Relative Power of (A + B - C) Type Product	CCIR Pre-emphasis Test Tone Deviation, f_{drms}			
	0.5 mc	1.0 mc	1.5 mc	2.0 mc
-30 db	> 11,000 pw	1,710 pw	590 pw	275 pw
-25 db	> 35,000 pw	5,440 pw	1,890 pw	870 pw
-20 db	> 110,000 pw	> 16,500 pw	5,860 pw	2,740 pw

If we arbitarily assign a maximum allowable intermodulation noise of 2,000 pw to the re-entrant loop, we see from Table 5-1 that an operating point must be chosen where the third order intermodulation products are down more than 20 db from the desired carriers. In addition, quite high deviations are necessary. The value of f_{drms} is normally chosen to achieve some specified thermal noise performance for the system; values used in Figures 5-12 through 5-20 correspond to the following qualities at receiver threshold.[5]

[5] J. A. Develet, Jr., "Coherent FDM/FM Telephone Communication," Proc. IRE, September 1962.

f_{drms} (mc)	Thermal Noise in Top Channel
0.5	250,000 pw
1.0	45,000 pw
1.5	16,000 pw
2.0	7,700 pw

In most cases, then, the intermodulation noise compares favorably with the thermal noise at threshold.

With the present system it is necessary to operate at quite low levels to satisfy the requirements on a third order product level. From Figure 4-3 a reasonable operating range of input signal is -60 to -65 dbm. This corresponds to operating 6 to 12 db below P_{SL}. To achieve higher output powers from the loop or more efficient TWT operation, it would be necessary to reduce the number of carriers amplified still further. It is interesting to note that of the two systems considered, the 6-carrier system actually has the greater channel capacity, having 3600 duplex telephone channels to 3000 for the 20-carrier system.

6.0 TWT ANALYSIS

Previous analyses of baseband distortion in the re-entrant TWT transponder have assumed the TWT to be a linear device. An attempt will be made here to introduce terms into the analysis which will account for some of the nonlinear behavior characteristics of a TWT. Gain and delay variations are introduced and results derived by Weiner and Leon[1] concerning the quasi-stationary response of linear time-invariant filters are used.

It is assumed that the nonlinear and filtering actions of the TWT are separable. Although the primary motivation for the assumption is ease of analysis, there is some supporting experimental evidence: delay versus frequency and gain versus frequency curves have the same shape for different input powers. Hence the mathematical model for the TWT we will use is that of a nonlinear amplifier (with power dependent delay) followed by a linear filter.

The first nonlinear term to produce a measurable effect in a TWT would be a cubic term in the input-output relation. Hence we might start with the input-output relation

$$v_o = Kv_i - kv_i^3 \tag{6-1}$$

But this would produce a third harmonic output for a sinusoidal input, which is not observed experimentally. A more realistic start would be

$$v_o(t) = \left(KV_i - \frac{3}{4} kV_i^3\right) \cos \omega_i(t - \tau_{NL}) \tag{6-2}$$

for

$$v_i(t) = V_i \cos \omega_i(t) \tag{6-3}$$

---

[6] Weiner, D. D. and B. J. Leon, "On the Quasi-Stationary Response of Linear Time-Invariant Filters to Arbitrary FM Signals," IEEE Trans. on Circuit Theory, June, 1964.

For a TWT, Beam and Blattner[7] have shown that

$$\tau_{NL} \cong \tau_o - \delta p_i \tag{6-4}$$

where p_i is the input power.

We will assume that

$$\tau_{NL} \cong \tau_o - \delta p_i(t - \tau_o) \tag{6-5}$$

if the input power varies slowly. Rewriting (6-2) as

$$v_o(t) = V_o \cos \omega_i(t - \tau) = \left(KV_i - \frac{3}{4} kV_i^3\right) \cos \omega_i(t - \tau_{NL}) \tag{6-6}$$

it is apparent that what we have done is to write an input-output amplitude equation:

$$V_o = KV_i - \frac{3}{4} kV_i^3 \tag{6-7}$$

If $V_i = V_i(t)$ is a slowly varying function of time, we can use the static relation (6-7) dynamically:

$$V_o(t) = KV_i(t - \tau_{NL}) - \frac{3}{4} kV_i^3(t - \tau_{NL}) \tag{6-8}$$

The complete expression, for slowly varying input amplitude, is

$$v_o(t) = \left[K - \frac{3}{2} k \frac{V_i^2(t - \tau_{NL})}{2}\right] V_i(t - \tau_{NL}) \cos \omega_i(t - \tau_{NL}) \tag{6-9}$$

We mentioned above (6-5) that the delay τ_{NL} is a function of input power. For a slowly varying input amplitude we will take the time varying input power to be

$$p_i(t) = \frac{V_i^2(t)}{2} \tag{6-10}$$

---

[7]Beam, W. R. and D. J. Blattner, "Phase Angle Distortion in Traveling-Wave Tubes," RCA Review, March, 1956.

so that (6-5) becomes

$$\tau_{NL} = \tau_o - \delta p_i(t - \tau_o) = \tau_o - \delta \frac{V_i^2(t - \tau_o)}{2} \qquad (6\text{-}11)$$

By writing the trigonometric function in (6-9) as the sum of two exponentials, we note that an exponential form of the input-output relation can be used:

$$v_{op}(t) = \left[K - \frac{3}{2} k \frac{V_i^2(t - \tau_{NL})}{2}\right] v_{ip}(t - \tau_{NL}) \quad , \quad v_{ip}(t) = V_i(t)\, e^{j\omega_i(t)} \qquad (6\text{-}12)$$

Equation (6-9) is obtained from (6-12) by writing

$$v_o(t) = \frac{v_{op}(t) + v_{op}^*(t)}{2} \qquad (6\text{-}13)$$

Since $\delta p_i(t - \tau_o)$ is usually much smaller than τ_o, (6-12) can be expanded in a Taylor series about the point $t - \tau_{NL} = t - \tau_o$ and only the first two terms retained:

$$\begin{aligned} v_{op}(t) = {} & \left[K - \frac{3}{2} k \frac{V_i^2(t - \tau_o)}{2}\right] V_i(t - \tau_o)\, e^{j\omega_i(t-\tau_o)} \\ & + \delta p_i(t - \tau_o) \left\{ \left[K - \frac{3}{2} k \frac{V_i^2(t - \tau_o)}{2}\right] \left[\dot{V}_i(t - \tau_o) + j\dot{\omega}_i(t - \tau_o)\, V_i(t - \tau_o)\right] \right. \\ & \left. - 3k \frac{V_i^2(t - \tau_o)}{2} \dot{V}_i(t - \tau_o) \right\} e^{j\omega_i(t-\tau_o)} + \cdots \end{aligned} \qquad (6\text{-}14)$$

Since

$$3k \frac{V_i^2}{2} << K - \frac{3}{2} k \frac{V_i^2}{2} \quad ,$$

$$v_{op}(t) \cong \left[K - \frac{3}{2} k \frac{V_i^2(t - \tau_o)}{2}\right]\Big\{V_i(t - \tau_o) + \delta p_i(t - \tau_o)$$

$$\times \left[\dot{V}_i(t - \tau_o) + j\dot{\omega}_i(t - \tau_o) V_i(t - \tau_o)\right]\Big\} e^{j\omega_i(t-\tau_o)}$$

$$\cong \left[K - \frac{3}{2} k\, p_i(t - \tau_o)\right] v_{ip}(t - \tau_o + \Delta\tau) \qquad (6\text{-}15)$$

where

$$\left.\begin{aligned} p_i(t) &= \frac{V_i^2(t)}{2} \\ v_{ip}(t) &= V_i(t)\, e^{j\omega_i(t)} \\ \Delta\tau &= \delta p_i(t - \tau_o) \end{aligned}\right\} \qquad (6\text{-}16)$$

The quantity δ for the MEC TWT can be determined, approximately, from Figure 3-14.

$$\delta \cong 10^{-6.2} \quad , \quad p_i \text{ in watts} \qquad (6\text{-}17)$$

Hence for an average power input of -30 dbm, $|\Delta\tau| \sim 10^{-12}$.

For multiple inputs,

$$v_i(t) = \sum_{n}^{N} V_n(t) \cos \theta_n(t) = \frac{1}{2} \sum_{n}^{N} V_n(t)\, e^{j\theta_n(t)} + \text{c.c.} = \frac{1}{2} V_i(t)\, e^{j\theta_i(t)} + \text{c.c.} \qquad (6\text{-}18)$$

Then

$$v_{ip}(t) = V_i(t)\, e^{j\theta_i(t)} \qquad (6\text{-}19)$$

and

$$p_i(t) = \frac{V_i^2(t)}{2} = \sum_{n'}^{N} \frac{V_n^2(t)}{2} + \sum_{m}^{N} \sum_{n}^{m-1} \frac{V_m(t)\, V_n(t)}{2} \left\{e^{j\left[\theta_m(t) - \theta_n(t)\right]} + \text{c.c.}\right\} \qquad (6\text{-}20)$$

If $\theta_m(t) - \theta_n(t)$ is sufficiently slowly varying, the output is given by (6-15)

$$v_{op}(t) = \sum_{n}^{N} \left[K - \frac{3}{2} kp_i(t - \tau_o) \right] V_n(t - \tau_o + \Delta\tau)\, e^{j\theta_n(t-\tau_o+\Delta\tau)} \qquad (6\text{-}21)$$

For a two tone test, $N = 2$, $V_1 = V_2 = \text{constant}$, $\theta_n(t) = \omega_n(t)$ and (6-21) becomes

$$v_{op}(t) = \left[K - \frac{3}{2} kp_i(t - \tau_o) \right] V \left[e^{j\omega_1(t-\tau_o+\Delta\tau)} + e^{j\omega_2(t-\tau_o+\Delta\tau)} \right] \qquad (6\text{-}22)$$

where

$$p_i(t) = 2\frac{V^2}{2} + \frac{V^2}{2}\left[e^{j(\omega_1-\omega_2)t} + \text{c. c.} \right] \qquad (6\text{-}23)$$

Now

$$e^{j\omega_n(t-\tau_o+\Delta\tau)} \cong e^{j\left[\omega_n(t-\tau_o)+\omega_n\Delta\tau\right]}$$

$$\cong \left[1 + j\omega_n \delta \frac{V_i^2(t - \tau_o)}{2} \right] e^{j\omega_n(t-\tau_o)}$$

represents a narrowband angle modulated signal. At the frequencies and power levels of interest (two tone tests), the extra sidebands produced by the presence of $\Delta\tau$ in (6-22) may be neglected in comparison with those produced by the amplitude nonlinearity. Hence (6-22), with $\Delta\tau = 0$, together with the two-tone test data can be used to evaluate K and k. The approximate value of K for the MEC M5184 is fairly easy to compute, a representative value being $K \cong 10^{1.95}$. The nonlinear coefficient, k, is rather difficult to evaluate accurately. Values calculated from the data lie in the range $10^{6.5} < k < 10^{7.5}$.

For the linear portion of our model, we will use the results derived in Appendix E: the quasi-stationary response of a linear system with response function H(S) due to an input $e_i(t)$ is

$$e_o(t) = H\left[\frac{\dot{R}(t)}{R(t)} + j\,\dot{\theta}(t)\right] R(t)\, e^{j\theta(t)} \tag{6-24}$$

where

$$e_i(t) = R(t)\, e^{j\theta(t)} \tag{6-25}$$

R(t) and θ(t) must be sufficiently slowly varying that the inequality (E-12) of Appendix E is satisfied. We shall take

$$H(j\omega) = e^{\alpha(\omega)+j\,\beta(\omega)} \tag{6-26}$$

If the system power transfer function is expressed in db,

$$G(\omega) = 10\log_{10} HH^* = 10\log_{10} e^{2\alpha(\omega)} = \alpha(\omega)\,(20\log_{10} e) = 8.68\,\alpha(\omega) \tag{6-27}$$

since α(ω) is in nepers. Then

$$H(j\omega) = e^{CG(\omega)+j\beta(\omega)} \quad , \quad C = \frac{1}{\omega \log_{10} e} \cong 0.115 \tag{6.28}$$

If

$$\theta(t) = \omega_c t + \phi(t) + \gamma \quad , \quad \gamma \text{ and } \omega_c \text{ constant} \tag{6-29}$$

and H(jω) is a bandpass function, G(ω) and β(ω) can be represented by a few expansion terms about the carrier frequency ω_c:

$$\left.\begin{aligned} G(\omega) &= G(\omega_c) + g_1(\omega - \omega_c) + g_2(\omega - \omega_c)^2 + g_3(\omega - \omega_c)^3 \quad , \\ \beta(\omega) &= \beta(\omega_c) + b_1(\omega - \omega_c) + b_2(\omega - \omega_c)^2 + b_3(\omega - \omega_c)^3 \end{aligned}\right\} \tag{6-30}$$

Assuming that $G(\omega_c)$, $\beta(\omega_c)$ and $b_1(\omega - \omega_c)$ have been absorbed in K and τ_o of the analysis above, we will use

$$\left.\begin{aligned} G(\omega) &= g_1(\omega - \omega_c) + g_2(\omega - \omega_c)^2 + g_3(\omega - \omega_c)^3 \quad , \\ \beta(\omega) &= b_2(\omega - \omega_c)^2 + b_3(\omega - \omega_c)^3 \end{aligned}\right\} \tag{6-31}$$

Using (6-31) in $H(j\omega)$ and (6-25) for the input, the output is

$$e_o(t) = \exp\left\{C\left[g_1\left(\dot\phi - j\frac{\dot R}{R}\right) + g_2\left(\dot\phi - j\frac{\dot R}{R}\right)^2 + g_3\left(\dot\phi - j\frac{\dot R}{R}\right)^3\right] + j\left[b_2\left(\dot\phi - j\frac{\dot R}{R}\right)^2 + b_3\left(\dot\phi - j\frac{\dot R}{R}\right)^3\right]\right\} R\, e^{j(\omega_c t+\phi+\gamma)} \quad (6\text{-}32)$$

$$= \exp\left[C\left\{g_1\dot\phi + g_2\left[(\dot\phi)^2 - \left(\frac{\dot R}{R}\right)^2\right] + g_3\dot\phi\left[(\dot\phi)^2 - 3\left(\frac{\dot R}{R}\right)^2\right]\right\} + 2b_2\dot\phi\frac{\dot R}{R} + b_3\frac{\dot R}{R}\left[3(\dot\phi)^2 - \left(\frac{\dot R}{R}\right)^2\right] + j\left(C\frac{\dot R}{R}\left\{-g_1 - 2g_2\dot\phi - g_3\left[3(\dot\phi)^2 - \left(\frac{\dot R}{R}\right)^2\right]\right\} + b_2\left[(\dot\phi)^2 - \left(\frac{\dot R}{R}\right)^2\right] + b_3\dot\phi\left[(\dot\phi)^2 - 3\left(\frac{\dot R}{R}\right)^2\right]\right)\right] R\, e^{j(\omega_c t+\phi+\gamma)} \quad (6\text{-}33)$$

The quantity of primary interest is the output phase:

$$\phi_o = \phi - C\frac{\dot R}{R}\left\{g_1 + 2g_2\dot\phi + g_3\left[3(\dot\phi)^2 - \left(\frac{\dot R}{R}\right)^2\right]\right\} + b_2\left[(\dot\phi)^2 - \left(\frac{\dot R}{R}\right)^2\right] + b_3\dot\phi\left[(\dot\phi)^2 - 3\left(\frac{\dot R}{R}\right)^2\right] \quad (6\text{-}34)$$

The output phase can be expressed in terms of input quantities by equating $e_i(t)$, (6-25), to $v_{op}(t)$, (6-15). For the amplitude, we have

$$R(t) = \left[K - \frac{3}{2}k\frac{V_i^2(t-\tau_o)}{2}\right] V_i(t - \tau_o + \Delta\tau)$$

$$\cong \left[K - \frac{3}{2}k\frac{V_i^2(t-\tau_o)}{2}\right]\left[V_i(t-\tau_o) + \delta\frac{V_i^2(t-\tau_o)}{2}\dot V_i(t-\tau_o)\right] \quad (6\text{-}35)$$

and for the phase

$$\theta(t) = \omega_c t + \phi(t) + \gamma$$

or

$$\omega_c t + \gamma + \phi(t) = \omega_i(t - \tau_o + \Delta\tau)$$

$$= \omega_c(t - \tau_o + \Delta\tau) + \phi_i(t - \tau_o + \Delta\tau)$$

$$\cong \omega_c(t - \tau_o) + \delta\omega_c \frac{V_i^2(t - \tau_o)}{2} + \phi_i(t - \tau_o)$$

$$+ \delta \frac{V_i^2(t - \tau_o)}{2} \dot{\phi}_i(t - \tau_o) \qquad (6\text{-}36)$$

Denoting the average value of $V_i^2(t - \tau_o)$ as $\overline{V_i^2}$

$$\omega_c t + \gamma = \omega_c(t - \tau_o) + \delta\omega_c \frac{\overline{V_i^2}}{2} \qquad (6\text{-}37)$$

$$\phi(t) = \phi_i(t - \tau_o) + \delta \frac{V_i^2(t - \tau_o)}{2} \dot{\phi}_i(t - \tau_o) + \delta\omega_c \left[\frac{V_i^2(t - \tau_o)}{2} - \frac{\overline{V_i^2}}{2} \right]$$

Estimates of the magnitude of the coefficients b_2 and b_3 can be obtained from Figure 3-16.

$$|b_2| \cong 0.1 \text{ ns/mc}^2$$

$$|b_3| \cong 0.02 \text{ ns/mc}^3$$

The coefficients g_1, g_2, and g_3 are difficult to estimate but since the TWT appears to be reasonably flat (±0.5 db) in a 50 mc band, g_2 and g_3 are probably negligible compared to g_1. If (6-37) and (6-35) are substituted in (6-34) and terms in δ, g_1, and b_2 only are retained, the output phase is approximated by

$$\phi_o(t) \cong \phi_i(t - \tau_o) + \delta \left\{ \frac{V_i^2(t - \tau_o)}{2} \dot{\phi}_i(t - \tau_o) + \omega_c \left[\frac{V_i^2(t - \tau_o)}{2} - \frac{\overline{V_i^2}}{2} \right] \right\}$$
$$- Cg_1 \frac{\dot{V}_i(t - \tau_o)}{V_i(t - \tau_o)} + b_2 \left[\dot{\phi}_i(t - \tau_o) \right]^2 \qquad (6\text{-}38)$$

Since

$$\lambda = \delta \frac{\overline{V_i^2}}{2} \qquad (6\text{-}39)$$

is a small quantity compared to τ_o,

$$\phi_i(t - \tau_o) + \lambda \dot{\phi}_i(t - \tau_o) \cong \phi_i(t - \tau_o + \lambda) \qquad (6\text{-}40)$$

and (6-38) can be written

$$\phi_o(t) \cong \phi_i(t - \tau_o + \lambda) + \delta \left[\frac{V_i^2(t - \tau_o)}{2} - \frac{\overline{V_i^2}}{2} \right] \left[\omega_c + \dot{\phi}_i(t - \tau_o) \right]$$
$$- Cg_1 \frac{\dot{V}_i(t - \tau_o)}{V_i(t - \tau_o)} + b_2 \left[\dot{\phi}_i(t - \tau_o) \right]^2 \qquad (6\text{-}41)$$

From (6-15), the power input-output relation is

$$\left. \begin{aligned} 10 \log_{10} \frac{p_o}{p_i} &\cong 20 \log_{10} \left(K - \frac{3}{2} k p_i \right) \\ \text{or} \\ P_o - P_i &= 20 \log_{10} K + 8.68 \ln \left(1 - \frac{3}{2} \frac{k}{K} e^{P_i/4.34} \right) \end{aligned} \right\} \qquad (6\text{-}42)$$

where $P = 10 \log_{10} p$. Expanding (6-42) in a Taylor series about some reference power P_r,

$$P_o \cong + P_r + 20 \log_{10} \left(K - \frac{3}{2} k e^{P_r/4.34} \right)$$
$$+ \left(1 - 3 \frac{k}{K} e^{P_r/4.34} \right) (P_i - P_r) - \cdots \qquad (6\text{-}43)$$

Using $P_r = -80$ db, Equation (6-43) for the MEC TWT is

$$P_o \cong -41 + (1 - 3 \times 10^{-3})(P_i + 80) \qquad (6\text{-}44)$$

which indicates that the slope of the $P_o - P_i$ curve (Figure 3-6) is approximately 0.997.

Although the expressions above describe the action of a TWT (in particular, the MEC TWT) reasonably well, caution must be used if these expressions are utilized in re-entrant loop analysis. For example, our model (nonlinear amplifier—linear filter) of the TWT cannot be cascaded in a re-entrant loop analysis. Cascaded, the slope of the loop $P_o - P_i$ curve would be approximately one: the measured slope, Figure 4-1, ranges from 0.82 to 0.9.

Gain compression in the loop is apparently due to the simultaneous presence of a small 6 gc signal and a 4 gc signal several orders of magnitude greater in the nonlinear amplifier of our model. For two inputs to the nonlinear amplifier whose amplitudes are constant (6-21) yields (omitting the arguments of time-varying quantities).

$$v_{op} = \left[K - \frac{3}{4}k\left(V_1^2 + 2V_2^2\right)\right] V_1 e^{j\theta_1} + \left[K_2 - \frac{3}{4}k\left(2V_1^2 + V_2^2\right)\right] V_2 e^{j\theta_2}$$

$$- \frac{3}{4}kV_1^2V_2 e^{j(2\theta_1 - \theta_2)} - \frac{3}{4}kV_1V_2^2 e^{j(2\theta_2 - \theta_1)} \qquad (6\text{-}45)$$

for

$$v_{ip} = V_1 e^{j\theta_1} + V_2 e^{j\theta_2} \qquad (6\text{-}46)$$

Granted license to use the static amplitude relation (6-7), (6-45) can be used to analyze the re-entrant loop by letting V_2 be the amplitude of the 6 gc input and setting

$$V_1 = a\left[K - \frac{3}{4}k\left(2V_1^2 + V_2^2\right)\right] V_2 \qquad (6\text{-}47)$$

where a is the attenuation suffered by the base-band signal during frequency conversion.

The power loss during conversion is about 10 db, so $a \cong 10^{-0.5}$. In (6-47), the amplitude of the 4 gc input is equated to the amplitude of the 6 gc output with conversion loss taken into account. Filtering and delay effects are not included. Solving (6-47) for V_1,

$$V_1 = \frac{-1 + \sqrt{1 + 6a^2 k K v_2^2 \left(1 - \frac{3}{4}\frac{k}{K} V_2^2\right)}}{3akV_2} \qquad (6\text{-}48)$$

Since $V_2^2 = 2 \times 10^{-10}$ for a loop input of -70 dbm, a reasonable approximation to V_1 can be obtained by expanding (6-48) and retaining only the linear and cubic terms in V_2:

$$V_1 \cong aKV_2 - \frac{3}{4} k\left(2a^3K^2\right) V_2^3 \qquad (6\text{-}49)$$

Since V_2 is the amplitude of the 6 gc input, from (6-45) and (6-49) the amplitude of the 4 gc output is

$$V_4 = \left[aK^2 - \frac{3}{2} k\left(3a^3K^3\right) \frac{V_6^2}{2}\right] V_6 \qquad (6\text{-}50)$$

or

$$V_4 = K_L V_6 - \frac{3}{4} k_L V_6^3 \qquad (6\text{-}51)$$

where

$$\left.\begin{aligned} K_L &= aK^2 \\ k_L &= 3a^3K^3k \end{aligned}\right\} \qquad (6\text{-}52)$$

The overall $P_o - P_i$ relation for the loop is identical in form to (6-43), with K and k in (6-43) replaced by K_L and k_L. In order to compare theoretical and experimental loop $P_o - P_i$ curves, we set $P_r = -100$ db:

$$P_4 \cong -32 \text{ db} + \left(1 - 3\frac{k_L}{K_L} \times 10^{-10}\right)(P_6 + 100) \qquad (6\text{-}53)$$

From (6-52)

$$\frac{k_L}{K_L} = 3a^2kK \qquad (6\text{-}54)$$

and since $10^{6.5} < k < 10^{7.5}$, the slope of the $P_4 - P_6$ curve (6-53) lies in the interval

$$0.72 < 1 - 3\frac{k_L}{K_L} \times 10^{-10} < 0.972 \qquad (6\text{-}55)$$

The slopes of the experimental curves, Figure 4-1, vary from 0.84 to 0.9.

We have postulated nonlinear TWT characteristics and derived expressions which are in reasonable agreement with TWT experiments. However, the behavior of a re-entrant loop in which a TWT is used may differ markedly from that anticipated unless great care is taken in the application of the TWT characteristics. The sensitivity of the calculated value of the slope of the $P_4 - P_6$ curve to the value of the TWT nonlinear coefficient k [(6-53) and 6-55)] illustrates the principle conclusion to be drawn here: the slight departures from linearity at low power levels which are always present in a TWT are aggravated by re-entrant operation. Specifically, a total power input (direct and re-entrant inputs) which is about 20 db below P_s, a region in which the TWT would produce about 0.3 percent compression, produces about 15 percent compression in the re-entrant loop. Noticeable increases in other nonlinear effects should also be anticipated.

7.0 CONCLUSIONS

The feasibility of a direct RF to RF transponder using a TWT in a re-entrant mode as the major portion of the amplifier chain has been demonstrated. The system developed uses the re-entrant loop as an intermediate amplification stage with a low noise preamplifier to establish the system noise figure and a power amplifier to enhance the dc to RF conversion efficiency consistent with the distortion requirements for the system. The achieved gain, output power, and noise figure are consistent with the basic requirements for a communication satellite transponder. However, a low power TWT having a noise figure in the 6 to 10 db range could be used in the re-entrant mode and also provide the first stage of amplification, thus eliminating the need for preamplification.

Some desirable characteristics of a TWT to be used for a re-entrant amplifier, predicated upon the results of this study, are as follows:

1) A low noise tube is mandatory if the wide bandwidths available with the re-entrant transponder are to be used efficiently. This requirement is imposed to inhibit system saturation on internally generated noise.

2) A flat gain-frequency characteristic is required over the frequency range occupied, but the down converter appears to present more of a problem than the TWT in this respect. Of the down converters investigated, none were able to completely achieve the conversion loss variation objectives over the entire frequency range.

3) A minimum small signal gain suppression characteristic is desirable to enhance the dc to RF efficiency of the transponder since the usable output power of the re-entrant loop is predicated upon this parameter as discussed in Section 4. This would become particularly important in the case of a high power transponder (40 to 100 watts) where the re-entrant loop was used as the first stage of amplification followed by a single power amplifier.

4) A maximum slope of the TWT power-out/power-in characteristic is desirable to minimize the aggravation of gain compression which takes place when the tube is operated in the re-entrant mode. The effect is not significant for single angle modulated carriers; however, with more than one carrier present in the loop, the envelope variations of the composite signal tend to be smoothed out with a resulting distortion of the output signals. In loop operation, aggravation of the nonlinear effects of the TWT was also noted in the intermodulation measurements. In the case of intermodulation, however, referencing the input power to a normalized reference input power, P_S for the TWT and P_{SL} for the re-entrant loop, results in essentially the same performance for both the tube and loop. In this sense the re-entrant loop may be considered as a single amplifier stage with power transfer and intermodulation characteristics such as those shown in Figures 4-1 and 4-3 respectively. Intermodulation products between the 4 gc and 6 gc signals are higher order and are negligible compared to the products produced by signals in the 4 gc band.

The excellent quality of the television pictures obtained from the re-entrant loop in the TV demonstration tests indicates that the loop may be operated at saturation with a single carrier with no difficulty. The poorer quality of the pictures taken with the signal passed through the entire transponder is due to saturation of the transponder on broadband noise. However, a flyable model of this transponder would exhibit a greater dynamic range, utilize diplexer/preselector filters limiting the noise bandwidth to something less than 500 mc, and would therefore be considerably less affected by this problem.

Operation with a single carrier, while satisfactory, still does not make use of the wide bandwidth capabilities of the re-entrant transponder. The wide bandwidths available suggest multiple access systems as an application for the re-entrant loop amplifier. Intermodulation distortion appears to be the main constraint for this

application. The results obtained in Section 5 show the effect of the amplitude nonlinearities of the loop in producing intermodulation noise at the received baseband. It was determined that the operating point for the loop in the presence of several carriers below the reference input power level P_{SL} can be chosen predicated upon the number of carriers and the amount of intermodulation noise that can be tolerated. It is felt that with more than two carriers, the operating point is sufficiently far below P_{SL} to make distortion due to AM to PM conversion of secondary importance. More detailed analysis and loop measurements are required to fully support this.

Thus, the re-entrant amplifier may be considered as a means of achieving direct wideband RF to RF conversion to facilitate a multiple access system. This can greatly simplify communication satellites, particularly if TWT's become available with sufficiently low noise levels that the re-entrant loop can be made the first stage of amplification.

BIBLIOGRAPHY

1. Beam, W.R. and D.J. Blattner, "Phase Angle Distortion in Traveling Wave Tubes," RCA Review, March 1956.

2. Develet, J.A., Jr., "Coherent FDM/FM Telephone Communication," Proc. IRE, September 1962.

3. Develet, J.A., Jr., "Selected Topics on Modulation Systems for an Active Wideband Communication Satellite," STL 8949-0006-NU-000, 23 April 1961.

4. Putz, J.L., Private Communications, August 1963, General Electric Power Tube Division, Palo Alto, California.

5. Weiner, D.D. and B. J. Leon, "On the Quasi-Stationary Response of Linear Time-Invariant Filters to Arbitrary FM Signals," IEEE Trans. on Circuit Theory, June 1964.

APPENDIX A

DEFINITION OF TERMS
STUDY OF SPACECRAFT TRANSPONDER POWER AMPLIFIER

APPENDIX A

DEFINITION OF TERMS
STUDY OF SPACECRAFT TRANSPONDER POWER AMPLIFIER

1. Intermodulation (cross-modulation)

The nonlinear process by which two or more frequency components generate new components. The same nonlinear process generally will produce harmonics of individual frequency components. This is usually termed harmonic distortion rather than intermodulation.

It is clear from the basic definition that in a communication system this phenomenon can take place in many devices and various frequency regions. In particular, amplifiers at baseband, modulators and demodulators at baseband and intermediate frequency, i-f amplifiers and r-f mixers and amplifiers - - all are possible sources of intermodulation. If it is desired to further specify the type of intermodulation under consideration, the terms r-f intermodulation, i-f intermodulation, and baseband intermodulation may be used.

2. Intermodulation noise

The unintelligible products formed by intermodulation between channels in a multi-channel frequency division multiplex (FDM) system. The term can also be generalized to include such products formed by intermodulation between television video material and an audio subcarrier, for example.

Intermodulation noise basically refers to an effect observed at baseband. Therefore, the term is not usually applied to r-f or i-f intermodulation in which two or more communication carriers interact. Rather the term is reserved for noise produced in the baseband of a single carrier because of a nonlinear transfer characteristic at baseband, intermediate or radio frequency. For the latter two frequency regimes, it is the noise generated by the nonlinearity as seen by the modulation about an operating point on either the gain or delay (phase) transfer characteristic for amplitude and angle modulation, respectively. See differential gain and differential phase. This type of noise might be called intramodulation noise, meaning intermodulation within the modulation components of a single carrier. However, it seems undesirable to create such a terminology which would be peculiar to this project.

3. Crosstalk

a. Intelligible Crosstalk

The phenomenon by which a voice channel in an FDM system is transferred to a baseband channel of another carrier in such fashion as to be intelligible to the listener in that channel. If the talker talks and listens in the same baseband channel location (complementary channel operation), intelligible crosstalk may be manifested as echo.

In an FDM/FM system intelligible crosstalk arises from FM-to-AM conversion followed by AM-to-PM conversion or by direct adjacent channel interference (DACI).

b. Unintelligible Crosstalk

See Intermodulation Noise.

4. Baseband Distortion (Modulation Distortion)

a. Linear Distortion

The difference in relative amplitude or phase between frequency components in the input and output basebands. Linear distortion is caused by lack of a flat gain-or delay-frequency characteristic (or linear phase-frequency characteristic) over the frequency range of interest.

In a wideband, high deviation FM system linear distortion is principally caused by the baseband equipment. However, certain nonlinear processes such as FM-to-AM and AM-to-PM conversion occurring in r-f or i-f can produce linear distortion as here defined.

b. Nonlinear Distortion

The creation of new baseband frequency components through nonlinear processes. Examples of nonlinear distortion are harmonic distortion and intermodulation noise.

5. Band

A range of frequencies often without exact specification of limits.

a. Baseband

The low-frequency region occupied by the modulating signal or basic information.

6. Bandwidth

The difference between the upper and lower frequency limits of a band. The bandwidth of interest is simply the bandwidth under consideration at the moment. Also sometimes used in the sense of the bandwidth required for a certain quality of transmission.

a. 3 db Bandwidth

The bandwidth between points at which the gain-frequency characteristic of a transmission network is 3 db down from the maximum gain or the gain at center frequency of the band.

Note: Gain could be more than 3 db down within the 3 db bandwidth.

b. Shape Factor (of a filter)

The ratio of the bandwidths at two different points on the gain-frequency characteristic, e.g., the 6-db bandwidth to the 60-db bandwidth.

c. Equivalent Noise Bandwidth

The rectangular bandwidth (B_N) which when multiplied by either the maximum network power gain or the gain at center frequency (G_o), gives the total area under the gain-frequency characteristic of a network. Thus when noise (or a signal) of uniform power density (ρ) in watts/cps is applied to the input of the network, the noise (or signal) output is simply $G_o \rho B_N$.

In symbols

$$B_N = \frac{1}{G_o} \int_{-\infty}^{\infty} G(\omega) \, df$$

where

B_N = equivalent noise bandwidth, cps(two sided)

G_o = reference power gain, either the maximum or center frequency value

$G(\omega)$ = two sided gain frequency characteristic in power

d. One Sided (Two Sided) Bandwidth

The bandwidth excluding (including) the response at negative frequencies.

7. Spectrum Occupancy

The band of frequencies occupied by the signal energy. For example, it may be defined in terms of the band within which 99% of the signal energy lies. Or, for an FM system a rule-of-thumb which is often used to estimate the spectrum occupancy of the modulated carrier is

$$\text{Spectrum occupancy} = 2 f_p + 2 f_m,$$

where

f_p = peak frequency deviation

f_m = highest modulation frequency

8. Spectrum Efficiency

The ratio of the band occupied by the signal(s) (spectrum occupancy) to the total band, including guard bands, required to be allocated to the signal(s) in order to provide protection against distortion, interference, intermodulation, etc.

9. Multiple-access Communication Satellite

A satellite in which two or more independent r-f signals can simultaneously be amplified in the repeater(s).

10. Threshold

The point(s) at which a characteristic of a transmission system is outside of a previously defined allowable limit. Generally, the signal-to-noise ratio (SNR) is the characteristic of most interest.

a. Breaking Threshold (FM Improvement Threshold)

The region in an FM system at which the curve of post-detection vs. pre-detection SNR in decibels departs from linearity. This threshold is a function of the nature of the modulating signal, the deviation used, and the type of demodulator. If an input-output SNR curve is available for a particular application, precise input SNR can be defined as threshold on the basis of a prescribed amount of departure from linearity.

b. FM Performance Threshold

Generally the pre- or post-detection SNR at which system noise performance drops below a prescribed limit. The threshold behavior may be abrupt or not, depending on whether the performance threshold coincides with the breaking threshold in an FM system, for example.

c. Dynamic Range

May be defined as the range of values that a characteristic takes on between threshold points, e.g., the range of input signal power determined by sensitivity on the lower limit and intermodulation requirements on the upper limit.

11. Sensitivity

The least input signal for which the system will produce a prescribed output indication. Typically, the sensitivity is defined as the signal power level which just equals the noise power, that is, which produces a doubling of the observed output power.

If the sensitivity is denoted S_{min}, then

$$S_{min} = KT_s B_N = KT_o B_N (F-1) + KT_B B_N$$

where

F = system noise figure

K = Boltzmann's constant, 1.38×10^{-23} joules/degree

T_o = reference temperature, 290^o K.

B_N = equivalent noise bandwidth, cps

T_s = system noise temperature

T_B = input noise temperature

12. Noise Figure

a. Noise Factor (noise figure)of a linear system at a selected input frequency, (is) the ratio of (1) the total noise power per unit bandwidth (at a corresponding output frequency) available at the output terminals, to (2) the portion thereof engendered at the input frequency by the input termination, whose noise temperature is standard (290° K.) at all frequencies (IRE Receiver Standards, 1952).

$$F = \frac{G\,k\,T_o + \rho_n}{G\,k\,T_o}$$

where

G = gain at the frequency of interest

ρ_n = network noise density, watts/cps

k, T_o as in definition of sensitivity

13. Spurious Response

The response of a system to any other than the desired signal(s). The response may be measured in terms of baseband signal degradation, such as distortion, intermodulation, noise interference, etc. In a system employing heterodyning, responses to higher order products of the local oscillator and incoming desired or interfering signals result in spurious responses.

a. Image Response

The response of the system to signals appearing in the image band centered at $2 f_{LO} - f_{SIG}$, where f_{LO} = local oscillator and f_{SIG} = center frequency of the desired signal band.

b. Adjacent Channel Response

The response of the system to the immediately adjacent signal channel.

14. Interference

The presence of extraneous frequency component(s) in the band occupied by the signal of interest. Interference may enter the r-f, i-f or baseband of the desired signal and will produce different effects accordingly. Generally, the effects will be evaluated at baseband.

a. Direct Adjacent Channel Interference (DACI)

A phenomenon in which, for an FM system, the adjacent r-f channel causes intelligible crosstalk in the baseband of the channel of interest.

b. Intra-system Interference

Interference which originates within the system under study.

c. Inter-system Interference

Interference from external sources such as other systems.

15. Differential Gain

The difference between (a) the ratio of the output amplitudes of a small, high-frequency sinewave signal at two stated levels of a low-frequency signal on which it is superimposed, and (b) unity. (IRE, 1960)

16. Differential Phase

The difference in output phase of a small, high-frequency sinewave signal at two stated levels of a low-frequency signal on which it is superimposed. (IRE, 1960)

17. Differential Delay

The departure of the derivative of phase with respect to frequency from a flat characteristic. For example, at i-f this differs from differential time delay at baseband, previously defined in the linear distortion section, in that a non-flat delay-frequency characteristic at i-f can cause non-linear distortion, as well for an angle modulation system.

18. AM-PM Conversion

Phase modulation generated in the output signal as a result of amplitude variations (amplitude modulation) of the input signal.

19. FM-AM Conversion

Amplitude modulation generated in the output signal as a result of frequency variations (frequency-modulation) of the input signal due to a non-flat gain-frequency characteristic.

20. Matched (Impedance Matched)

a. For Maximum Power Transfer

A circuit (generator) is said to be matched to its termination (load) when the impedances are such that maximum power transfer occurs. This is accomplished by making the load impedance the conjugate of the generator impedance; thus, the magnitude and phase angles are both equal, but the phase angles are of opposite sign.

b. For Image Match

The circuit may also be said to be matched when the load impedance is made identical to (the image of) the generator impedance. In this case the magnitude and phase angles of the impedances are equal and the phase angles have the same sign; however, this type of match does not in general result in a maximum power transfer.

21. Gain Suppression

The reduction in gain of an amplifier at one frequency due to the presence of a signal at some other frequency. In TWT's, this effect usually occurs as one of the signals approaches saturation.

22. Homodyne

Homodyne refers to a particular detector system in which a synchronous detector is used to beat the incoming carrier down to zero frequency. This is accomplished by injecting a local oscillator signal into the synchronous detector, with the local oscillator derived from, or phase locked to the incoming carrier.

23. Synchrodyne

Synchrodyne refers to a type of modulation in which the phase shift through the modulator is made to vary simusoidally. By adjusting the amplitude of the modulation frequency the output at the carrier frequency may be made to go through zero. The zeros of carrier output correspond to the zeros of the Bessel function $J_o(\Delta\phi)$, where $\Delta\phi$ is the peak phase shift introduced by the modulator. The output spectrum is symmetrical about the carrier frequency.

24. Serrodyne

Serrodyne refers to a type of modulation in which the phase shift through the modulator is made to vary in a sawtooth fashion. By adjusting the amplitude of the modulation sawtooth the output of the carrier frequency may be made to go through zero. For a perfectly linear sawtooth with zero flyback time and with the amplitude adjusted so the phase shift introduced is given by $\Delta\phi = 2n\pi$ where n is an integer; the only output is a single frequency given by X $f_{out} = f_{in} + nf_{saw}$. The output frequency can be higher or lower than the input frequency depending upon whether the ramp portion of the sawtooth causes the phase shift of the modulator to decrease or increase respectively.

25. TWT Gain-Fine Structure

For a traveling-wave tube, fine grain structure is defined as periodic variations in the gain of the tube with respect to frequency. The frequency period of the variations is normally in the order of 200 mcs or less. The complete definition of fine grain structure requires that the amplitude and frequency period be stated.

APPENDIX B

TESTING TECHNIQUES
STUDY OF SPACECRAFT TRANSPONDER POWER AMPLIFIER

APPENDIX B

TESTING TECHNIQUES

STUDY OF SPACECRAFT TRANSPONDER POWER AMPLIFIER

TEST — ENVELOPE DELAY DISTORTION **(Preferred Method)**

PURPOSE — To measure the differential phase or envelope delay of a system.

DESCRIPTION — Envelope delay is proportional to the derivative of phase with respect to angular velocity. If the time of transmission is constant for all frequencies, that is, if the ϕ-versus-ω curve is perfectly linear, the derivative is a constant. It is the departure of this variable from a flat characteristic which causes distortion.

PROCEDURE — A sawtooth wave V(t) and a small high frequency signal ω_h are summed, then supplied to an FM deviator. The output of the deviator is supplied to the system under test, thence to an FM discriminator, filter, amplitude limiter and phase detector, where the phase shift ϕ of the high frequency signal ω_h is determined. The output of the high frequency signal generator at ω_h is supplied as the reference to the phase detector through a phase shifter which is used for calibration. The output of the phase detector $K\phi$ is displayed on the oscilloscope versus the sawtooth sweep amplitude V(t) which corresponds to the frequency deviation. It has been shown,[1] that

$$\phi = \tan^{-1}\left(\omega_h \frac{d\beta}{d\omega_i}\right),$$

where β is a phase-shift introduced at the output as a function of the input frequency deviation ω_i. Since the phase shift is usually small

$$\tan\phi \simeq \phi = \omega_h \frac{d\beta}{d\omega_i},$$

where $\frac{d\beta}{d\omega}$ is called the envelope delay.

TEST EQUIPMENT

1. Sawtooth Generator
2. Summer
3. High Frequency Signal Generator
4. FM Deviator
5. FM Discriminator
6. Filter
7. Limiter
8. Phase Detector
9. Phase Shifter
10. Oscilloscope

PRECAUTIONS The frequency of ω_h should be adjusted to yield good resolution on the scope presentation and also to yield

$$\tan \phi \simeq \phi \lesssim 10^{\circ}.$$

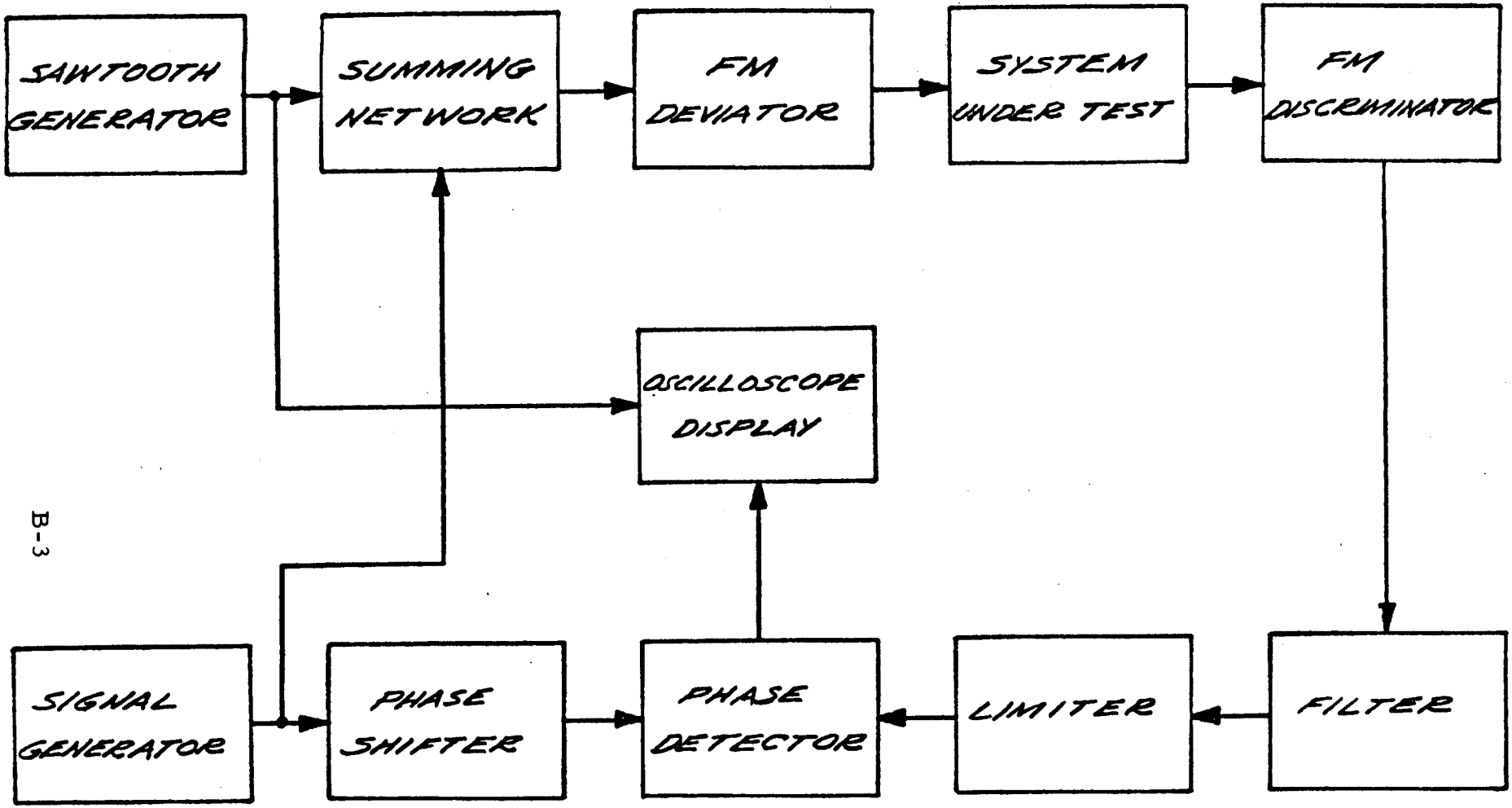

DIFFERENTIAL PHASE
(ENVELOPE DELAY)
MEASUREMENT BLOCK DIAGRAM

TEST — ENVELOPE DELAY DISTORTION

PURPOSE — To measure the phase non-linearities of the TWT, or Envelope Delay.

DESCRIPTION — Envelope delay is the measurement of the slope of the phase versus frequency curve, also called group delay. It is the first derivative of the phase angle with respect to angular velocity. If the time of transmission is constant for all frequencies, that is, if the ϕ-versus-f curve is perfectly linear, the derivative is a constant. The basic theory involved in the measurement of envelope delay relates to the phase shift produced in a signal consisting of the frequencies spaced $\omega = 2\pi\Delta f$ apart. If such a signal is passed through a system, the two frequencies will appear at the output with their phases shifted according to the phase shift at each frequency caused by the system. It is possible to show that the envelope delay time

$$T_e = \frac{d\phi}{d\omega} = \frac{\Delta\phi}{2\pi\Delta f} = \frac{\phi_2 - \phi_1}{2\pi(f_2 - f_1)}$$ Where

ϕ_1 and ϕ_2 are the phase of the frequencies f_1 and f_2 respectively.

PROCEDURE — The output of a signal generator is fed to an envelope generator which employs a balance modulator. Both the carrier and the modulating frequency are suppressed. The output contains two side bands, $f_o + \Delta f/2$ and $f_o - \Delta f/2$ which are amplified and used to modulate a slowly sweeping transmitter whose output is fed to the input of the TWT where the side-bands will suffer phase shifts ϕ_1 and ϕ_2 and amplitude variation A_1 and A_2 in passing through it. The output of the TWT is fed to a receiver and a detector, the output of which contains the original frequencies $f_o - \Delta f/2$ and $f_o + \Delta f/2$, harmonics of these frequencies, the difference frequency Δf and harmonics of the difference frequency. The detector is followed by an amplifier tuned to Δf, which eliminates all other components. The remaining

signal, Δf is shifted in phase with respect to the envelope generator signal by $\Delta \phi$. The phase shift, $\Delta\phi$ is measured by comparing Δf to a reference signal from the envelope generator. This is accomplished by a phase detector whose output is proportional to $\sin \Delta \phi$.

TEST EQUIPMENT

1. Signal Generator
2. Envelope Generator
3. Transmitter
4. Envelope Detector
5. Pad (2 each)
6. Phase Detector
7. Oscilloscope

PRECAUTIONS

1. To prevent amplitude from affecting the envelope delay measuring circuits, the detected signal is fed through an amplitude limiter.

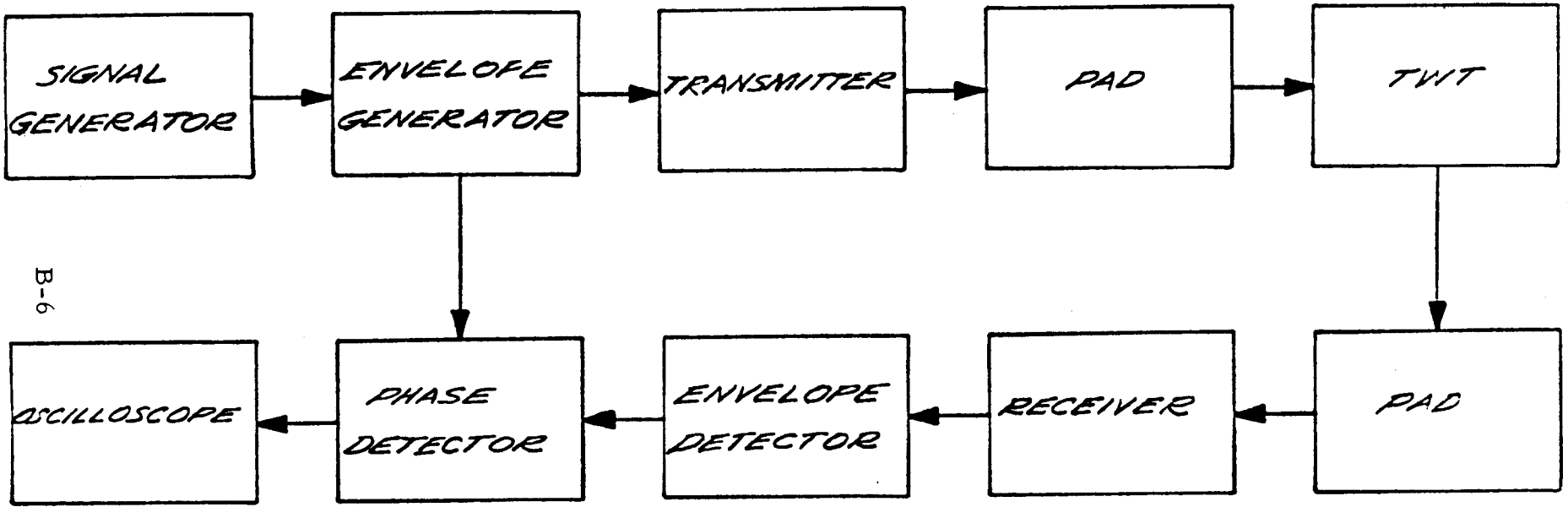

ENVELOPE DELAY DISTORTION
MEASUREMENT BLOCK DIAGRAM

TEST — FM TO AM DISTORTION

PURPOSE — To measure amplitude modulation at the output resulting from frequency modulation of the input signal.

DESCRIPTION — Amplitude modulation which is a result of a frequency modulated signal being amplified by a TWT is a form of distortion.

PROCEDURE — The output of an FM signal generator is supplied through a variable attenuator to the TWT under test. The output of the TWT is fed through a properly terminated directional coupler, a variable attenuator, and an RF filter to a detector. The detector is monitored with an oscilloscope for any amplitude modulation caused by the TWT.

TEST EQUIPMENT

1. FM Signal Generator
2. Variable Attenuator (2 each)
3. Directional Coupler and Termination
4. RF Filter
5. Detector
6. Oscilloscope
7. RF Switch (2 each)

PRECAUTION

1. A small deviation must be used to preclude generation of AM within the generator.

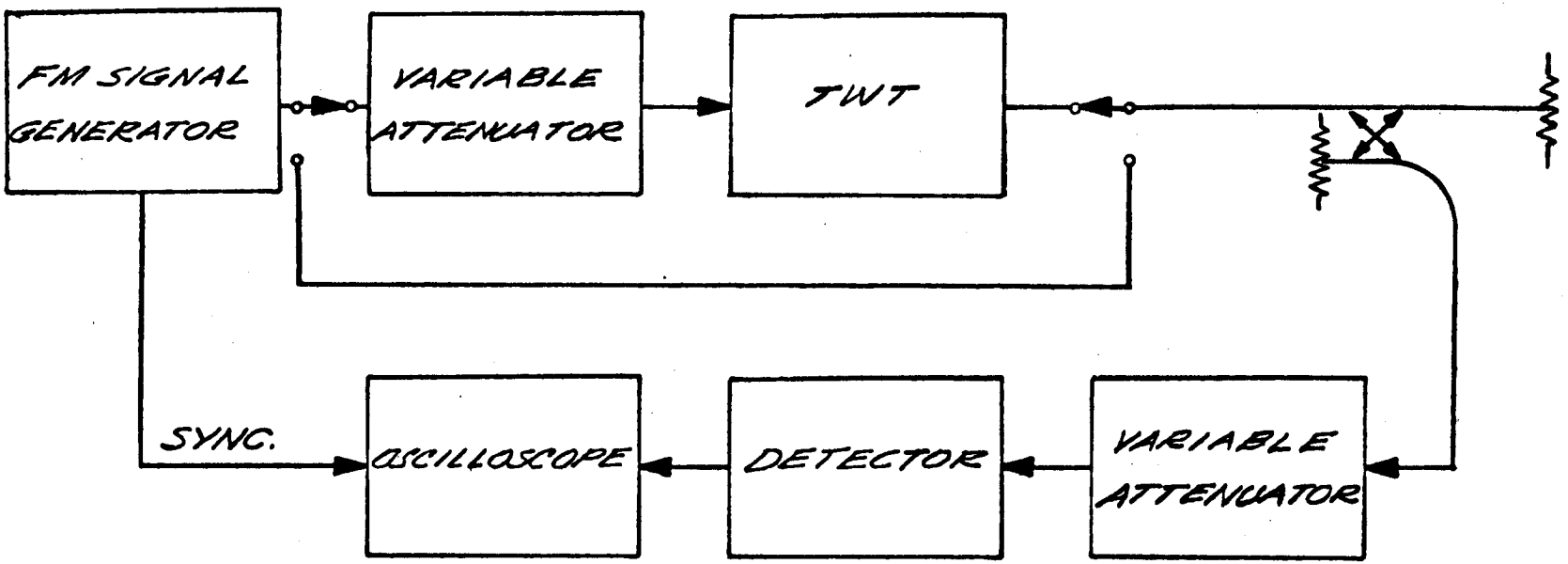

FM TO AM DISTORTION
MEASUREMENT BLOCK DIAGRAM

TEST GAIN SUPPRESSION

PURPOSE To measure the gain suppression of a signal in a TWT resulting when one or more additional signals are introduced.

DESCRIPTION Gain suppression in a TWT is defined as the reduction in gain of one signal due to the presence of another signal at some other frequency.

PROCEDURE The outputs of the signal generators are summed in a directional coupler and applied to the input of the TWT through a single-pole double-throw switch and a pad. The output of the TWT passes through another pad, switch, a tunable bandpass filter and a variable attenuator to a power meter. The switches permit calibration of the power levels.

TEST EQUIPMENT

1. Signal Generator (2 each)
2. Pad (2 each)
3. Directional Coupler
4. Tunable Bandpass Filter
5. Variable Attenuator
6. Power Meter

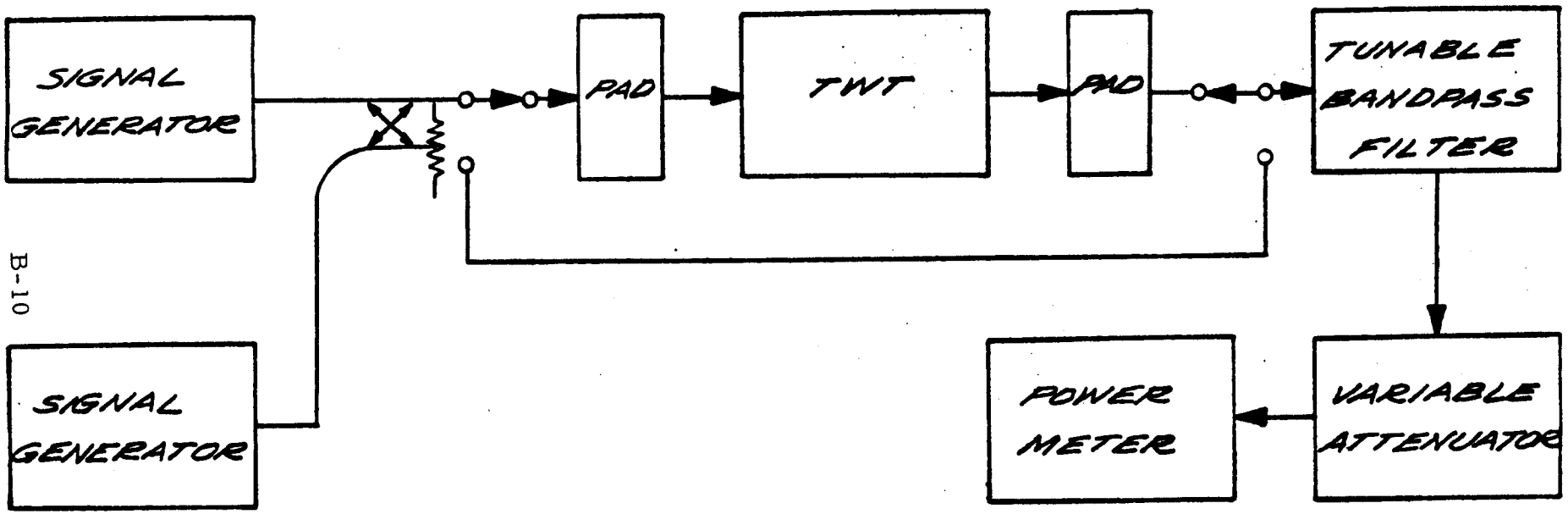

GAIN SUPPRESSION
MEASUREMENT BLOCK DIAGRAM

TEST INTELLIGIBLE CROSS-TALK

PURPOSE To determine the intelligible crosstalk produced between two signals being amplified by a TWT.

DESCRIPTION Intelligible cross-talk results from system non-linearities and is evidenced by the transfer of modulation from one carrier to another.

PROCEDURE The outputs of a frequency modulated signal generator and an unmodulated signal generator are combined in a directional coupler and supplied to the TWT through an attenuator pad. The output of the TWT is supplied through a pad to a receiver which is used to determine the modulation level on the unmodulated carrier.

TEST EQUIPMENT

1. FM Signal Generator
2. Signal Generator
3. Directional Coupler
4. Attenuator (2 each)
5. Receiver
6. Tunable Bandpass Filter

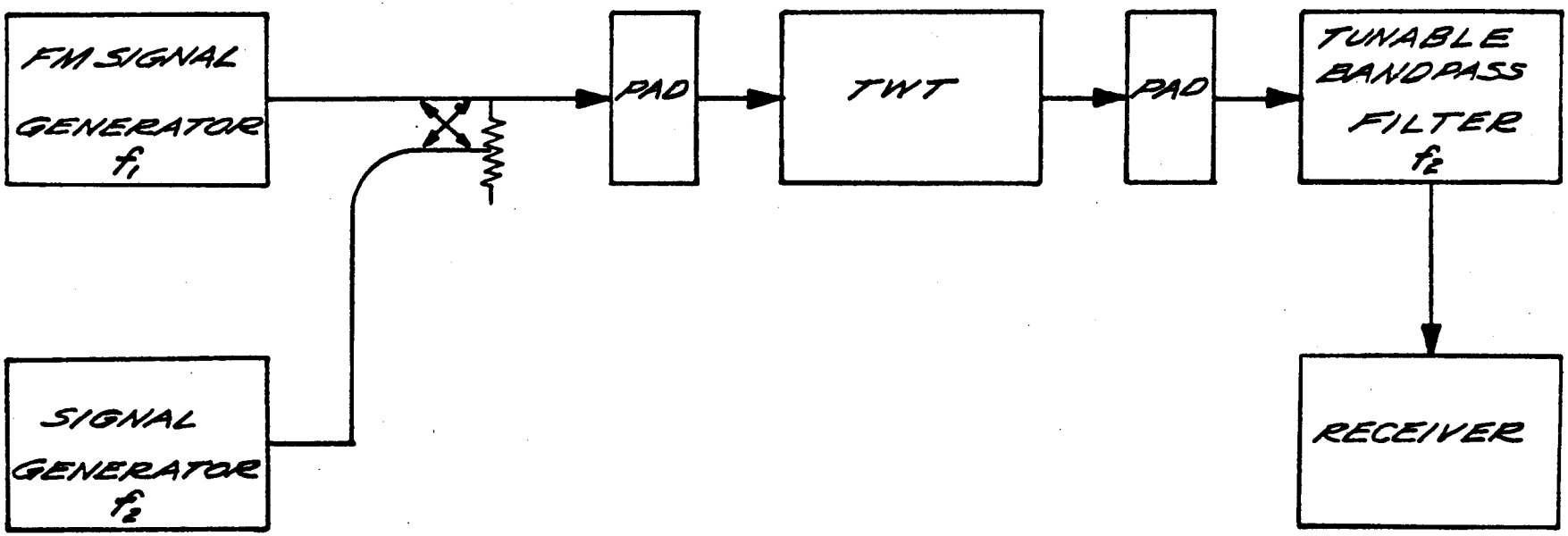

INTELLIGIBLE CROSS-TALK MEASUREMENT BLOCK DIAGRAM

TEST TWT IMPEDANCE

PURPOSE To measure the input and output impedance of the TWT

DESCRIPTION The impedance match between the input and output couplers and the helix determines not only the rf power applied to and extracted from the helix, but also the power reflected from the input coupler back to the driving source, and the power reflected to the helix by the output coupler.

PROCEDURE The output of the signal generator, with appropriate modulation is fed through a pad to the slotted line. The input or output of the TWT under test is connected to the output of the slotted line. A matched load is connected to the other terminal of the TWT. The output of the slotted line probe is coupled to the standing wave indicator. The SWR is then measured and the shift of a minimum is noted when the TWT and load are replaced with a short. The normalized impedance can then be computed from a Smith chart.

ACCURACY The accuracy is dependent upon the type of slotted line and the VSWR range.

TEST EQUIPMENT

1. Signal Generator
2. Pad
3. Slotted Line
4. Probe and Carriage
5. Standing Wave Indicator
6. Matched Load
7. Calibrated Short

PRECAUTIONS 1. The penetration of the sampling probe into the line must be kept at a minimum to avoid setting up any reflections and to insure that the crystal is not driven out of its square law region.

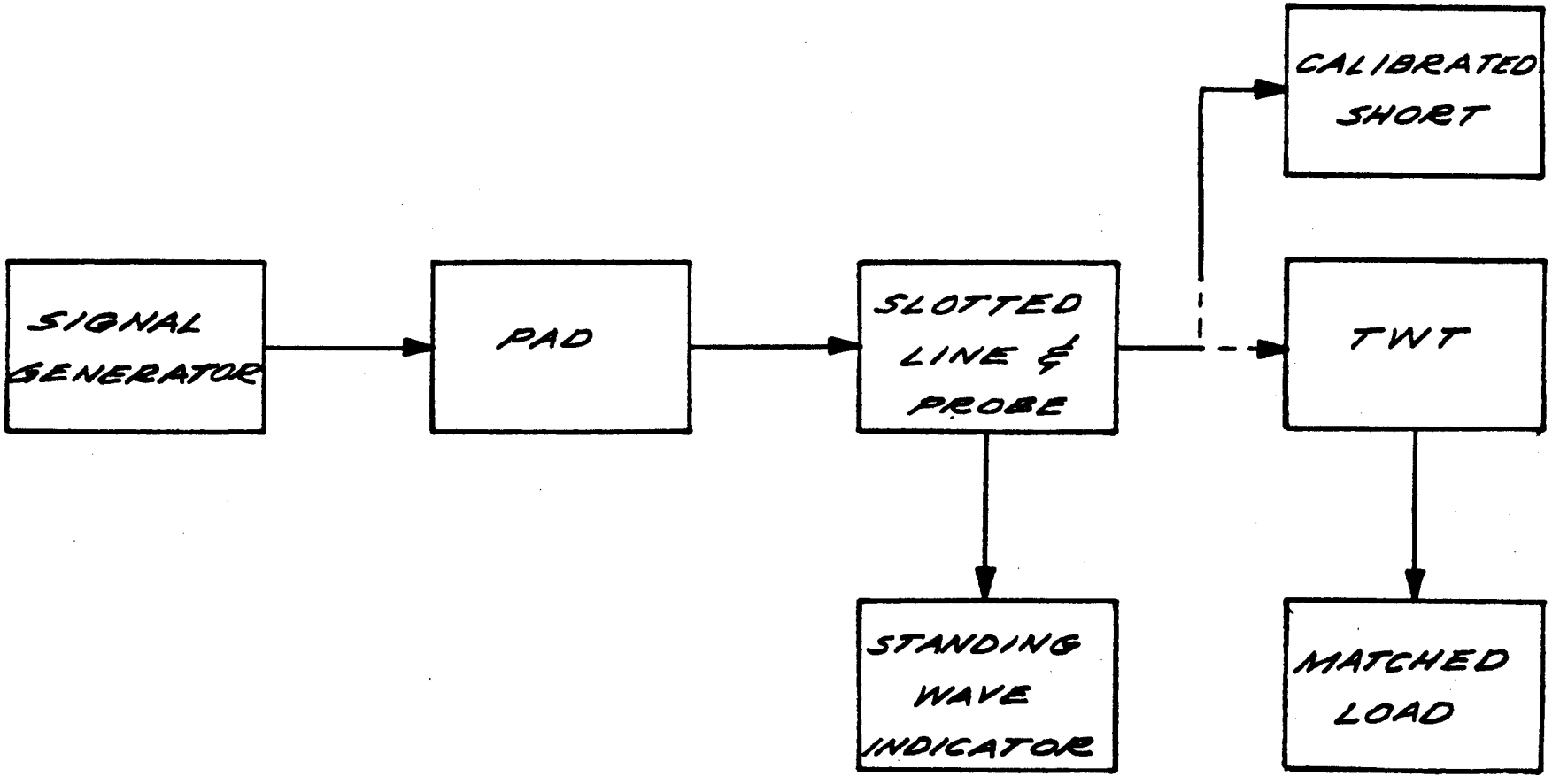

TWT IMPEDANCE MEASUREMENT BLOCK DIAGRAM

TEST TWT INTERMODULATION

PURPOSE To measure the products resulting from two or more input frequencies to the TWT.

DESCRIPTION The non-linearity of the TWT gain characteristics can result in the generation of unwanted signals when one or more legitimate signals are present.

PROCEDURE The outputs of the signal generators are summed in a directional coupler and applied to the input of the TWT through a single-pole double throw switch and a pad. The output of the TWT passes through another switch, a tunable bandpass filter and a variable attenuator to a spectrum analyzer. The switches permit calibration of the power levels. The two signal generators are set for the desired frequencies and their power output increased until an intermodulation product is observed on the spectrum analyzer and its level noted. The tunable bandpass filter precludes the development of other products in the front end of the spectrum analyzer. The TWT is then bypassed and one of the signal generators is tuned to the intermodulation frequency and adjusted to the level noted for it. This process is then repeated for all the desired frequencies and levels.

TEST EQUIPMENT

1. Signal Generator (2 each)
2. Pad (2 each)
3. Tunable Bandpass Filter
4. Spectrum Analyzer
5. rf SPDT Switch (2 each)
6. Directional Coupler
7. Variable Attenuator

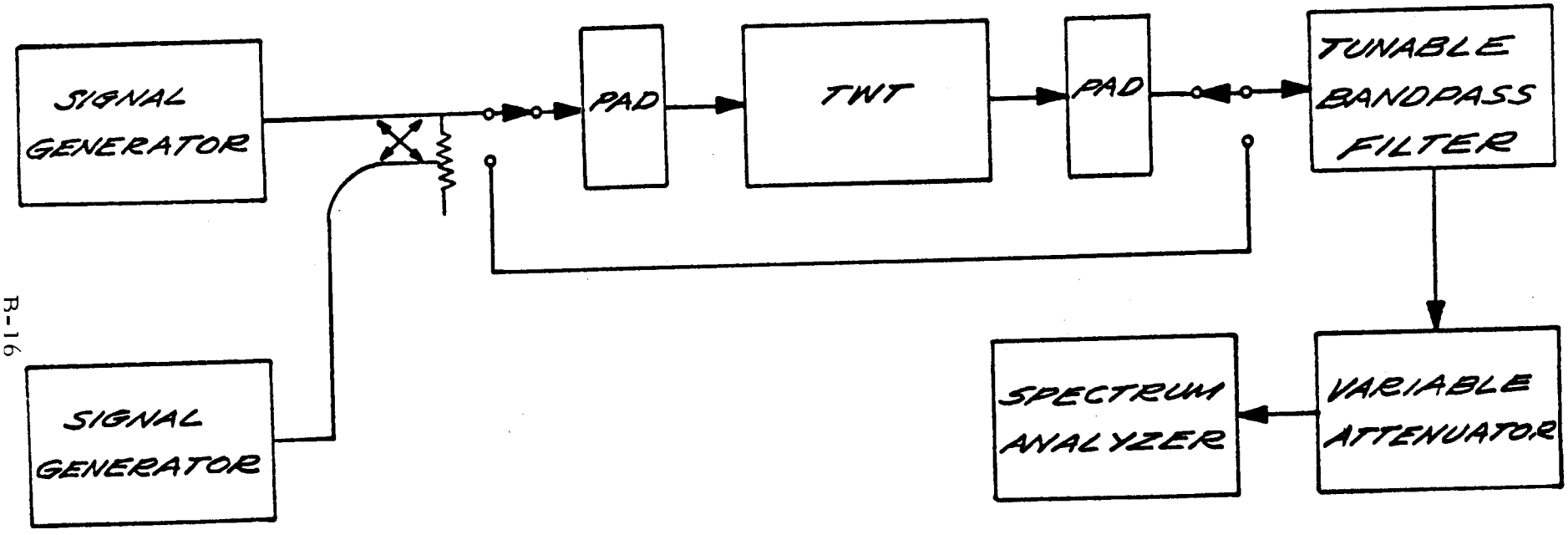

INTERMODULATION MEASUREMENT BLOCK DIAGRAM

TEST TWT NOISE FIGURE

PURPOSE To determine the noise figure of the TWT at a desired point in the band.

DESCRIPTION Noise figure is the ratio of the signal to noise power ratio at the input of an amplifier to the signal to noise power ratio at its output.

PROCEDURE The output of the noise source is fed to the input of the TWT through a single-pole double-throw switch. The output of the TWT is mixed with the output of the local oscillator, which has been tuned to the desired frequency. The mixer output is then fed through a variable attenuator, and an I-F amplifier to a power detector and power meter. With the noise source operating, the attenuator is adjusted until the power meter reads approximately full scale. The input is then switched to the matched load and the attenuator adjusted until the power meter again indicates full scale. The difference in the two attenuator settings, P in db may then be converted to a power ratio and substituted in the following equation:

$$N.F.(\text{in db}) = 10 \log \frac{37K}{\frac{P_1}{P_2} - 1}$$ Where

$$\frac{P_1}{P_2} = \log^{-1} 0.1\,P$$ and K is a

small number less than 1.0 which accounts for any cable loss between the noise source and the tube. It is the cable loss in db converted to a power ratio (eg., for a cable loss of one db K=0.794). The 37 is valid only for a noise source whose level is 15.8 db above thermal noise.

ACCURACY The accuracy of this measurement depends upon the mixer linearity.

TEST EQUIPMENT

1. Argon Noise Source
2. Matched Load
3. Crystal Mixer
4. Signal Generator (L.O.)
5. I-F Amplifier
6. Power Detector
7. Power Meter
8. RF Switch

PRECAUTIONS

1. The local oscillator signal must be large enough to produce linear mixing.
2. The time between the two readings must be short so as to preclude power meter drift from affecting the results.

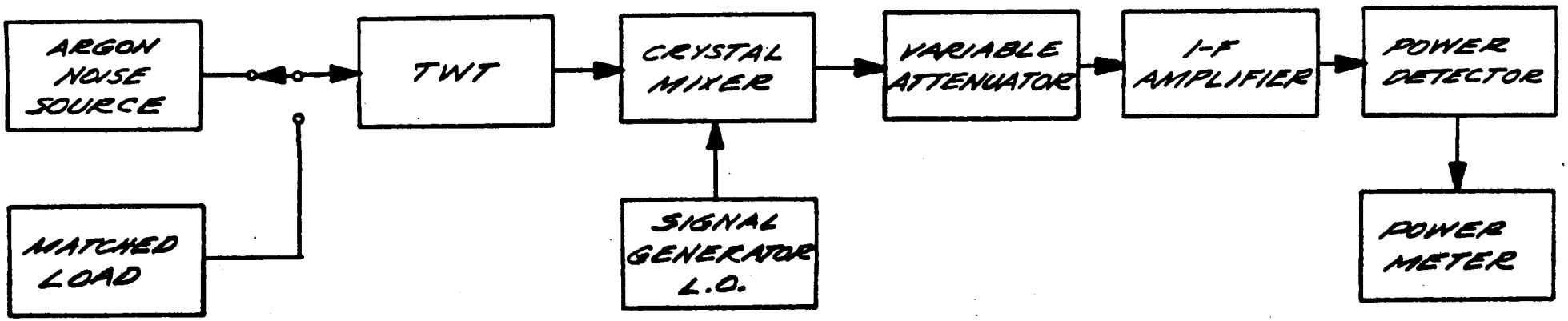

TWT NOISE FIGURE MEASUREMENT BLOCK DIAGRAM

TEST — TWT PHASE CHARACTERISTICS

PURPOSE — To measure TWT phase shifts as a function of operating parameters.

DESCRIPTION — The rf phase shift through a traveling wave tube is related to its electron beam transit time, accelerating voltages, gain, input power and output VSWR. Since a change in helix voltage produces a relative phase shift, it is desirable to know the extent of this phase shift with all other operating conditions held constant. Further, as a consequence of the inter-action between the electron beam and the helix fields, because of the transfer of energy from electron beam to the rf wave, there results a shift in phase of the output signal for different drive levels.

PROCEDURE — The output of the signal generator is fed through a pad to the TWT, then through another pad and a variable attenuator to a slotted line. The output of the signal generator is also fed through an attenuator directly to the opposite end of the slotted line. The probe in the slotted section is adjusted to the position of a minimum, and the voltage on the electrode under investigation is changed by an incremental amount. The probe is then adjusted to the new position of the minimum. The angular phase shift is given by the following relationship:

$$\phi = (2L)\ \ (360)/\lambda_g$$

Where ϕ is the change in phase angle in degrees,
L is the change in position of the minimum in millimeters, and
λ_g is the guide wavelength of the signal in millimeters.

TEST EQUIPMENT

1. Signal Generator
2. Variable attenuator (2 each)
3. Slotted line
4. Probe and carriage
5. Standing-wave indicator
6. Pad (2 each)

PRECAUTIONS

1. Voltage regulation of the power supply for the TWT under test must be very good to avoid random errors resulting from it.
2. Probe depth must be maintained at a minimum.

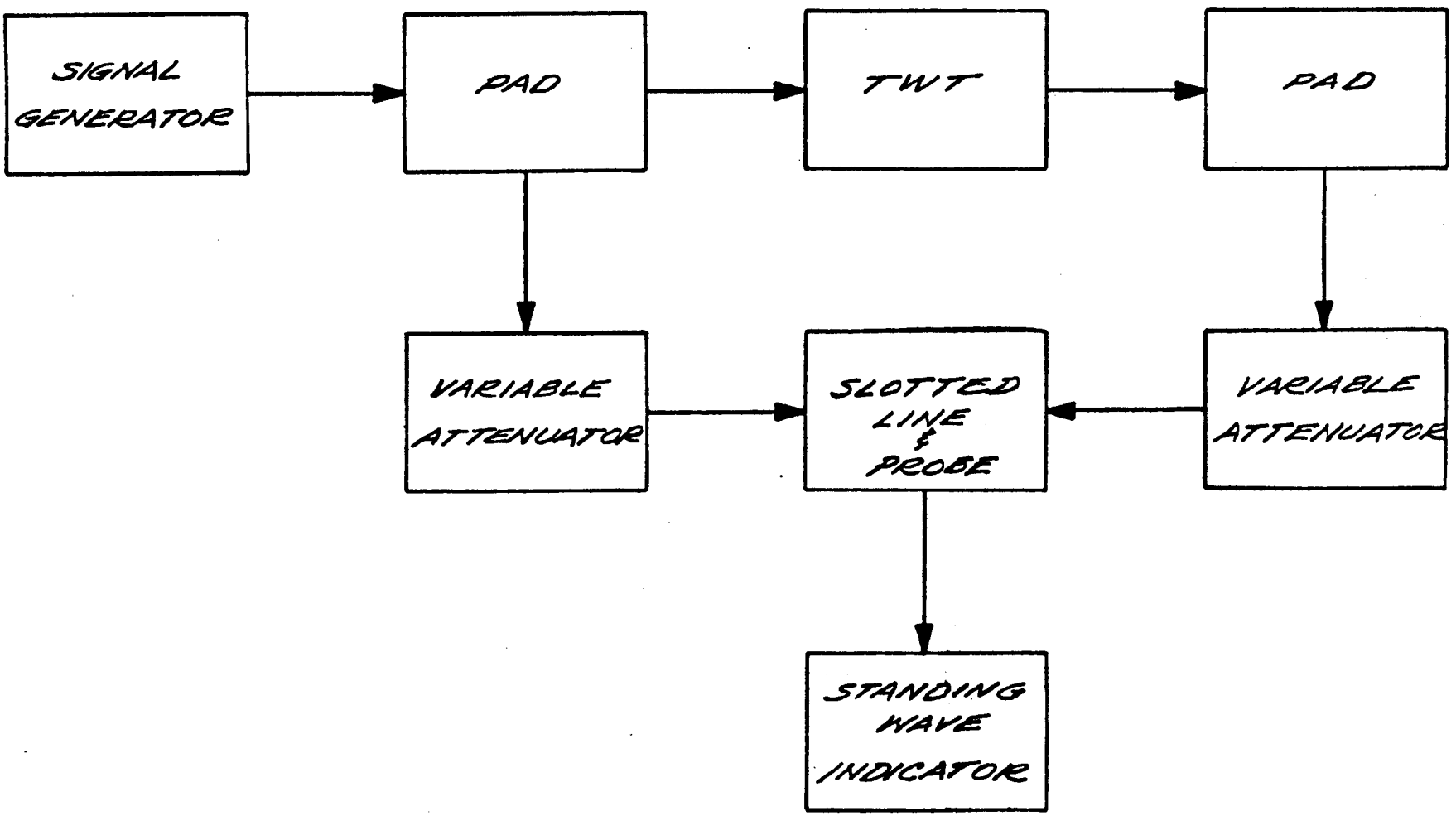

TWT PHASE CHARACTERISTICS MEASUREMENT

TEST — TWT SATURATION GAIN

PURPOSE — To determine the saturation gain of the TWT

DESCRIPTION — An rf signal is applied to the TWT input. The ratio of the maximum output obtainable to the input power that produced it, represents the saturation gain of the TWT.

PROCEDURE — The signal generator output is fed to the input of the TWT through an attenuator pad and an af single-pole double-throw switch. The TWT output is fed through another rf switch, a lowpass filter (to exclude harmonics) and an attenuator pad to the detector. The output of the detector is fed to the standing wave indicator. The TWT is by-passed when the switches are thrown to the calibration position.

ACCURACY — This method does not require a knowledge of the detector characteristrics nor an absolute power calibration of the signal generator; its accuracy depends only upon the calibration accuracy of the signal generator output attenuator.

TEST EQUIPMENT

1. Signal Generator
2. RF Detector
3. SPDT RF Switch (2 each)
4. Attenuator (2 each)
5. Standing Wave Indicator
6. Lowpass Filter

PRECAUTIONS

1. Minimize line length between coax switches on Position 2, (calibrate position).
2. The switches used must have a low VSWR and very low crosstalk.
3. Attenuator pads should be at least 6 db.

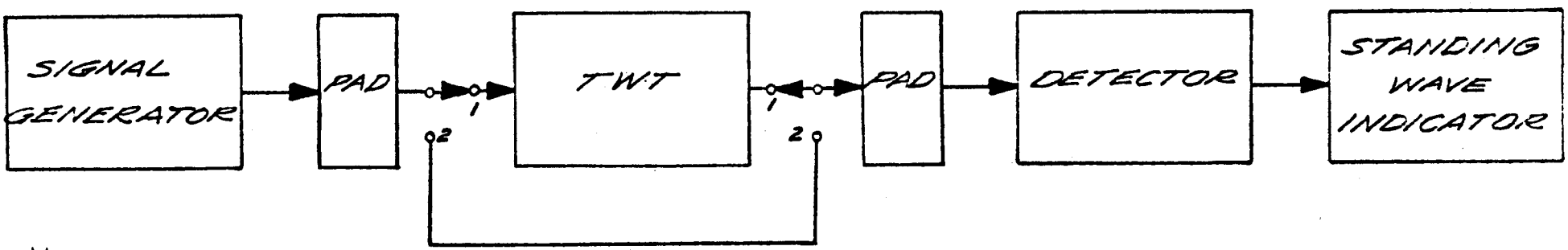

SATURATION GAIN
MEASUREMENT BLOCK DIAGRAM

TEST — TWT SMALL SIGNAL GAIN

PURPOSE — To determine the small signal gain of the TWT.

DESCRIPTION — An rf signal, small enough to insure operation in the linear gain region of the TWT, is applied at the input. The ratio of output to input power represents the small signal gain of the amplifier.

PROCEDURE — The signal generator output is fed to the input of the TWT through an attenuator pad and an rf single-pole double-throw switch. The TWT output is fed through another rf switch and an attenuator pad to the detector. The output of the detector is fed to the standing wave indicator. The TWT is bypassed when the switches are thrown to the calibration position.

ACCURACY — This method does not require a knowledge of the detector characteristics nor an absolute power calibration of the signal generator; its accuracy depends only upon the calibration accuracy of the signal generator output attenuator.

TEST EQUIPMENT

1. Signal Generator
2. RF Detector
3. SPDT Switch (2 each)
4. Attenuator (2 each)
5. Standing Wave Indicator

PRECAUTIONS

1. Minimize line length between coax switches on Position 2, (calibrate position).
2. The switches used must have a low VSWR and very low crosstalk.
3. Attenuator pads should be at least 6 db.

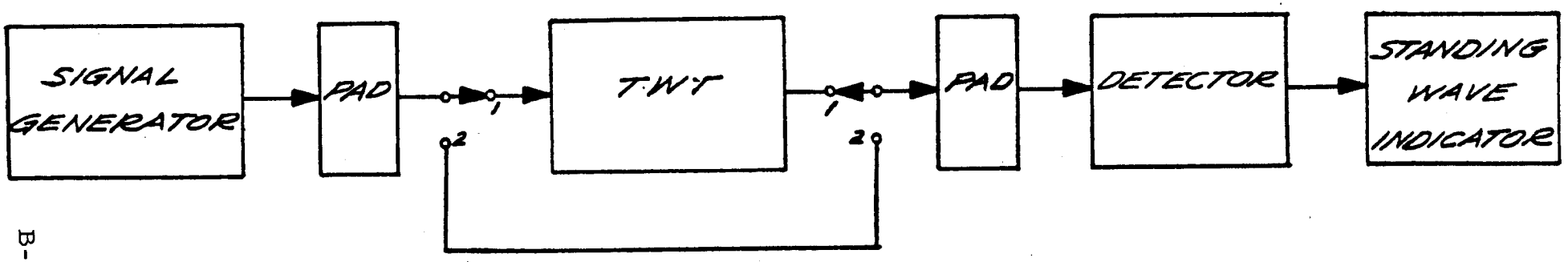

SMALL SIGNAL GAIN
MEASUREMENT BLOCK DIAGRAM

TEST — TWT VSWR

PURPOSE — To determine the VSWR of the TWT

DESCRIPTION — Incident and reflected waves, on a transmission line that is not terminated in its characteristic impedance, combine to form standing waves of current and voltage. The ratio of the voltage maximum to the voltage minimum is the voltage standing wave ratio.

PROCEDURE — The output of the signal generator, with appropriate modulation, is fed through a pad to the slotted line. The input or output of the TWT under test is connected to the output of the slotted line. The VSWR should be measured with the TWT beam on and off. The probe is mounted on the probe carriage and adjusted for minimum penetration into the slotted line. The output of the probe is coupled to the standing wave indicator.

ACCURACY — The accuracy is dependent upon the type of slotted line and the VSWR range.

TEST EQUIPMENT

1. Signal Generator
2. Pad
3. Slotted Line
4. Probe and Carriage
5. Standing Wave Indicator
6. Matched Load

PRECAUTIONS

1. The penetration of the sampling probe into the line must be kept at a minimum to avoid setting up any reflections and to insure that the crystal is not driven out of its square law region.

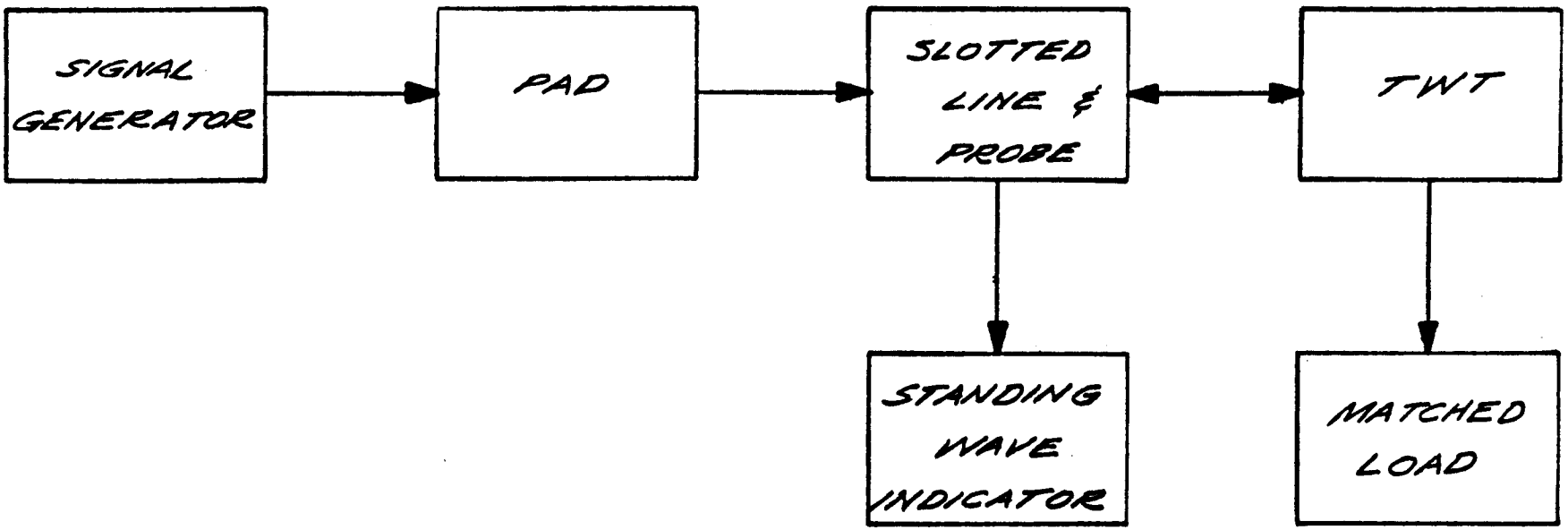

TWT VSWR MEASUREMENT BLOCK DIAGRAM

APPENDIX C

DERIVATION OF UPLINK NOISE CONTRIBUTION

APPENDIX C

DERIVATION OF UPLINK NOISE CONTRIBUTION

Consider the communication link shown

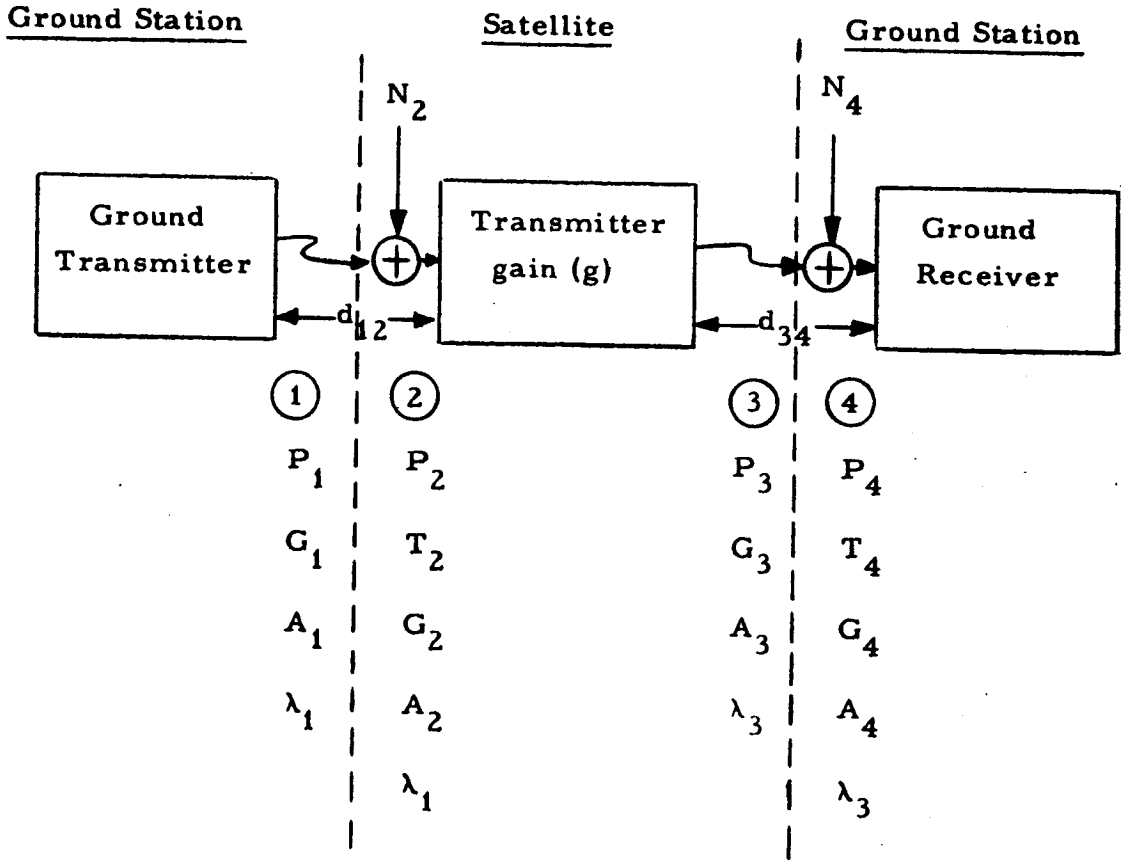

Communication Link

where P_i = total effective power (signal and noise) at each point

$G_i = \frac{4\pi A_i}{\lambda_i^2}$ antenna gain at each point

A_i = antenna capture area at each point

λ_i = wavelength at each point

d_{ij} = range between points

T_i = total effective noise temperature at each point

Noise enters the link at two points, N_2 at the input to the satellite and N_4 at the input of the ground receiver, and is assumed to be additive thermal noise with noise densities kT_2 and kT_4, respectively. (k = Boltzmann's constant) Then, the signal power at the spacecraft is given by:

$$S_2 = \frac{A_1 A_2 P_1}{d_{12}^2 \lambda_1^2}$$

and the total power at the spacecraft is

$$P_2 = S_2 + N_2$$

If the transponder operates as a linear repeater, the power transmitted by the satellite differs from that received only by a gain factor g. That is

$$P_3 = g P_2 = g(S_2 + N_2)$$

$$= S_3 + N_3$$

where it is assumed that the signal and noise are uncorrelated.

Note: The gain of the transponder may be a variable, e.g., because of ideal AGC.

The total power received at the ground is given by:

$$P_4 = \frac{A_3 A_4 P_3}{d_{34}^2 \lambda_3^2} + N_4 = \frac{A_3 A_4}{d_{34}^2 \lambda_3^2} (S_3 + N_3) + N_4$$

$$= S_4 + N_T$$

where

$$S_4 = \frac{A_3 A_4 g S_2}{d_{34}^2 \lambda_3^2} \quad \text{received signal power}$$

$$N_T = \frac{A_3 A_4 g N_2'}{d_{34}^2 \lambda_3^2} + N_4 \quad \text{total noise power}$$

where N_2' is the satellite noise N_2 measured in the ground receiver bandwidth. Therefore, the total system signal-to-noise ratio is

$$(S/N)_T = \frac{S_4}{N_T} = \frac{A_3 A_4 g S_2}{A_3 A_4 g N_2' + d_{34}^2 \lambda_3^2 N_4}$$

The signal-to-noise ratio due to the down-link alone is determined by setting $N_2' = 0$ in the above expression.

$$(S/N)_D = (S/N)_T \Big|_{N_2' = 0}$$

$$= \frac{A_3 A_4 g S_2}{d_{34}^2 \lambda_3^2 N_4}$$

Then, the effect of the up-link thermal noise is expressed by the ratio of the down-link to total system signal-to-noise ratios.

$$\text{(Effect of up-link)} = \frac{(S/N)_D}{(S/N)_T} = 1 + \frac{A_3 A_4 g N_2'}{d_{34}^2 \lambda_3^2 N_4}$$

$$= 1 + \frac{S_4}{S_2} \frac{N_2'}{N_4} = 1 + \frac{(S/N)_4}{(S/N)_2'} \qquad \text{(A-1)}$$

Since noises N_2' and N_4 are measured in the same bandwidth, this expression may be written in terms of noise temperatures as:

$$\frac{(S/N)_D}{(S/N)_T} = 1 + \frac{(S/T)_4}{(S/T)_2}$$

and substituting for S_2 and S_4

$$= 1 + \frac{d_{12}^2 \lambda_1^2 T_2 A_3 A_4 S_3}{A_1 A_2 P_1 T_4 d_{34}^2 \lambda_3^2} \qquad \text{(A-2)}$$

If the same ground antenna is used for transmit and receive and the spacecraft antenna is gain limited (e.g., isotropic), then

$$A_1 = A_4$$

$$G_2 = G_3$$

$$d_{12} = d_{34}$$

and (2) simplifies to

$$\frac{(S/N)_D}{(S/N)_T} = 1 + \frac{S_3 T_2}{P_1 T_4}$$

$$= 1 + \frac{P_3 T_2}{P_1 T_4} \cdot \frac{N_3 T_2}{P_1 T_4} \approx 1 + \frac{P_3 T_2}{P_1 T_4}$$

Or, using the notation of equation (2-1) Section 2.3

$$\frac{(S/N)_D}{(S/N)_T} = 1 + \frac{(S/N)_g}{(S/N)_s} \approx 1 + \frac{P_s T_s}{P_g T_g}$$

The essential approximation, then, is that the satellite transmitted power (P_3) consists solely of signal $S_3 = g S_2$, or that transmitted spacecraft noise is negligible. Clearly, this is a necessity for an efficient transponder and highlights the need for some form of bandwidth limiting in the spacecraft receiver. Preferably, this bandwidth would not appreciably exceed that of the ground receiver.

APPENDIX D
INTERMODULATION NOISE ANALYSIS

APPENDIX D

INTERMODULATION NOISE ANALYSIS

In Section 5, expressions were required for the effective noise due to intermodulation. This noise, as seen at baseband, was expressed as the amount of psophometrically weighted noise present in any telephone channel due to interfering spectra which arise from intermodulation products. In this Appendix we develop formulas for the spectral density of the intermodulation products of RF and the resulting interference spectrum at baseband. A practical method of computing the interference products, due to Curtis,[1] is used in deriving these expressions. Finally, expressions for the amount of psophometrically weighted intermodulation noise in any telephone channel are obtained for both 6 db per octave and CCIR[2] pre-emphasis and this quantity calculated for the worst channel.

Consider an input signal to a nonlinear amplifier consisting of a sum of N independent angle modulated carriers.

$$v_i(t) = \sum_{n=1}^{N} A_n \cos\left[\omega_n t + \phi_n(t) + \alpha_n\right] \qquad \text{(D-1)}$$

where the A_n and ω_n are constants, the α_n are random variables uniformly distributed on $[-\pi, \pi]$, and the $\phi_n(t)$ are sample functions of independent wide-sense stationary gaussian random processes having zero means, and are taken to represent multichannel FDM signals. Expressing the output signal of the nonlinear amplifier in a power series we may then write

$$v_o(t) = g_1 v_i(t) + g_2 v_i^2(t) + g_3 v_i^3(t) + \ldots \qquad \text{(D-2)}$$

$$= g_1 \sum_{n=1}^{N} A_n \cos\beta_n + g_2 \sum_{m=1}^{N} \sum_{n=1}^{N} A_m A_n \cos\beta_m \cos\beta_n$$

$$+ g_3 \sum_{l=1}^{N} \sum_{m=1}^{N} \sum_{n=1}^{N} A_l A_m A_n \cos\beta_l \cos\beta_m \cos\beta_n$$

$$+ \ldots \qquad \text{(D-3)}$$

where $\cos\beta_n = \cos\left[\omega_n t + \phi_n(t) + a_n\right]$

Taking N = 3 for simplicity and writing only those terms which possibly fall within the passband, expression (D-3) becomes*

$$v_o(t) = \left[g_1 A_1 + \frac{3}{4} g_3 A_1 (A_1^2 + 2A_2^2 + 2A_3^2)\right] \cos\beta_1 + \left[g_1 A_2 + \frac{3}{4} g_3 A_2 (A_2^2 + 2A_1^2 + 2A_3^2)\right] \cos\beta_2$$

$$+ \left[g_1 A_3 + \frac{3}{4} g_3 A_3 (A_3^2 + 2A_1^2 + 2A_2^2)\right] \cos\beta_3 +$$

$$+ \frac{3}{4} g_3 \left[A_1 A_2^2 \cos(2\beta_2 - \beta_1) + A_1 A_3^2 \cos(2\beta_3 - \beta_1) + A_2 A_1^2 \cos(2\beta_1 - \beta_2)\right.$$

$$\left. + A_3 A_1^2 \cos(2\beta_1 - \beta_3) + A_2 A_3^2 \cos(2\beta_2 - \beta_3) + A_3 A_2^2 \cos(2\beta_3 - \beta_2)\right]$$

$$+ \frac{3}{2} g_3 A_1 A_2 A_3 \left[\cos(\beta_1 + \beta_2 - \beta_3) + \cos(\beta_1 - \beta_2 + \beta_3) + \cos(\beta_1 - \beta_2 - \beta_3)\right] \qquad \text{(D-4)}$$

Expression (D-4) above gives the frequency location and amplitude of the modulation products in the passband.

The power spectral density of any one of the terms may now be found from the Fourier transform of its covariance function, $R_k(\tau)$.

$$R_k(\tau) = K^2 E\left\{\cos\theta_k(t) \cos\theta_k(t + \tau)\right\} \qquad \text{(D-5)}$$

where the k's designate the kth term and K is the coefficient of the kth term.

---

*Actually in the case of the re-entrant TWT, even order products can fall within the passband of the tube, i.e., 4th and 6th order products between 6 gc and 4 gc signals. However, these products are of a lower order of magnitude and are not considered in the present analysis.

Third order product terms of two types are of interest in Equation (D-4).

(1) for $\theta_k = 2\beta_m - \beta_n$

(2) for $\theta_k = \beta_l + \beta_m - \beta_n$

It can be shown that the autocorrelation function of a single angle modulated carrier is given by[3]:

$$R(\tau) = \frac{A_n^2}{2} e^{-\left[R_{\phi_n}(o) - R_{\phi_n}(\tau)\right]} \cos \omega_n \tau \qquad \text{(D-6)}$$

where $R_{\phi_n}(\tau)$ is the autocorrelation function of the modulating gaussian random process $\phi_n(t)$.

Then for terms of the first type

$$s_k(t) = K \cos (2\beta_m - \beta_n);\ m \neq n$$

$$= K \cos \left[2\omega_m t - \omega_n t + 2\phi_m - \phi_n + 2a_m - a_n\right] \qquad \text{(D-7)}$$

where

$$K = \frac{3}{4} g_3 A_n A_m^2$$

and the autocorrelation function is

$$R_{s_k}(\tau) = \frac{K^2}{2} e^{\left[-R_\psi(o) + R_\psi(\tau)\right]} \cos (2\omega_m - \omega_n)\tau$$

where

$$R_{\psi}(\tau) = E\left\{\left[2\phi_m(t) - \phi_n(t)\right]\left[2\phi_m(t+\tau) - \phi_n(t+\tau)\right]\right\}$$

$$= 4R_{\phi_m}(\tau) + R_{\phi_n}(\tau) \qquad \text{(D-8)}$$

$$\therefore R_{s_k}(\tau) = \frac{K^2}{2}\exp\left\{-4\left[R_{\phi_m}(o) - R_{\phi_m}(\tau)\right] - \left[R_{\phi_n}(o) - R_{\phi_n}(\tau)\right]\right\}\cos(2\omega_m - \omega_n)\tau, \qquad \text{(D-9)}$$

The power spectral density is

$$S_{s_k}(f) = \frac{K^2}{2}e^{-\left[4R_{\phi_m}(o) + R_{\phi_n}(o)\right]}\int_{-\infty}^{\infty} e^{\left[4R_{\phi_m}(\tau) + R_{\phi_n}(\tau)\right]}\cos(2\omega_m - \omega_n)\tau e^{-j\omega\tau}\,d\tau \qquad \text{(D-10)}$$

$$= \frac{K^2}{4}e^{-\left[4R_{\phi_m}(o) + R_{\phi_n}(o)\right]}F\left\{e^{\left[4R_{\phi_m}(\tau) + R_{\phi_n}(\tau)\right]}\right\} * \left\{\delta\left[f - (2f_m - f_n)\right] + \delta\left[f + (2f_m - f_n)\right]\right\} \qquad \text{(D-11)}$$

where $F\{\ \}$ is the Fourier transform and * denotes a convolution operation.

A simple way of determining the power spectrum given by (D-11) will now be demonstrated.

Consider

$$R_{2\omega_m}(\tau) = \frac{K_1^2}{2} e^{-4\left[R_{\phi_m}(o) - R_{\phi_m}(\tau)\right]} \cos 2\omega_m \tau \qquad \text{(D-12)}$$

$$S_{2\omega_m}(f) = \frac{K_1^2}{4} e^{-4R_{\phi_m}(o)} F\left\{e^{4R_{\phi_m}(\tau)}\right\} * \left\{\delta(f - 2f_m) + \delta(f + 2f_m)\right\} \qquad \text{(D-13)}$$

and

$$R_{\omega_n}(\tau) = \frac{K_2^2}{2} e^{-\left[R_{\phi_n}(o) - R_{\phi_n}(\tau)\right]} \cos \omega_n \tau \qquad \text{(D-14)}$$

$$S_{\omega_n}(f) = \frac{K_2^2}{4} e^{-R_{\phi_n}(o)} F\left\{e^{R_{\phi_n}(\tau)}\right\} * \left\{\delta(f - f_n) + \delta(f + f_n)\right\} \qquad \text{(D-15)}$$

Now if the autocorrelation functions given by (D-12) and (D-14) are multiplied together we obtain

$$R_{2\omega_m}(\tau)\, R_{\omega_n}(\tau) = \frac{K_1^2 K_2^2}{8} e^{-4\left[R_{\phi_m}(o) - R_{\phi_m}(\tau)\right]} e^{-\left[R_{\phi_n}(o) - R_{\phi_n}(\tau)\right]}$$

$$\left[\cos\left(2\omega_m - \omega_n\right)\tau + \cos\left(2\omega_m + \omega_n\right)\tau\right]$$

$$= R_{s_k}(\tau)(\text{for } 2\omega_m - \omega_n) + R_{s_k}(\tau)\ (\text{for } 2\omega_m + \omega_n) \qquad \text{(D-16)}$$

where

$\frac{K_1^2 K_2^2}{8}$ has been set equal to $\frac{K^2}{2}$.

The power spectrum is then

$$F\left\{R_{2\omega_m}(\tau)\, R_{\omega_n}(\tau)\right\} = S_{2\omega_m}(f) * S_{\omega_n}(f) = S_{2\omega_m-\omega_n}(f) + S_{2\omega_m+\omega_n}(f) \qquad \text{(D-17)}$$

Thus, it is seen that the power spectrum of the terms at $(2\omega_m \pm \omega_n)$ may be found simply by convolving the spectra at $2\omega_m$ and ω_n if the coefficients are properly adjusted. The actual power of these terms is determined by measurement or from an assumed nonlinearity. This convolution actually gives the spectra at the sum and difference frequencies at once, in a sum form, although only the difference term is of interest for the present problem.

In a similar manner the autocorrelation function and power spectral density of the second type of third order product may be determined. The resulting expressions are

$$s_k(t) = K\cos(\beta_1 + \beta_m - \beta_n)\ ;\ 1 \neq m \neq n$$

$$= K\cos\left[\omega_1 t + \omega_m t - \omega_n t + \phi_1 + \phi_m - \phi_n + a_1 + a_m - a_n\right] \qquad \text{(D-18)}$$

$$R_{s_k}(\tau) = \frac{K^2}{2}\, e^{-\left[R_{\phi_1}(o) - R_{\phi_1}(\tau)\right]} e^{-\left[R_{\phi_m}(o) - R_{\phi_m}(\tau)\right]} e^{-\left[R_{\phi_n}(o) - R_{\phi_n}(\tau)\right]}$$

$$\cos(\omega_1 + \omega_m - \omega_n)\,\tau \qquad \text{(D-19)}$$

$$S_{s_k}(f) = \frac{K^2}{4}\, e^{-\left[R_{\phi_l}(o) + R_{\phi_m}(o) + R_{\phi_n}(o)\right]} F\left\{e^{\left[R_{\phi_l}(\tau) + R_{\phi_m}(\tau)\right]}\right\} *$$

$$\left\{\delta\left[f - (f_l + f_m - f_n)\right] + \delta\left[f + (f_l + f_m - f_n)\right]\right\} \qquad \text{(D-20)}$$

which may be found by multiplying the autocorrelation functions for ω_l, ω_m, and ω_n together and adjusting the coefficients.

$$R_{\omega_l}(\tau)\, R_{\omega_m}(\tau)\, R_{\omega_n}(\tau) = R_{s_k}(\tau)\,(\text{for } \omega_l) + R_{s_k}(\tau)\,(\text{for } \omega_m) + R_{s_k}(\tau)\,(\text{for } \omega_n) \qquad \text{(D-21)}$$

$$S_{\omega_l}(f) * S_{\omega_m}(f) * S_{\omega_n}(f) = S_{\omega_l + \omega_m + \omega_n}(f) + S_{\omega_l + \omega_m - \omega_n}(f) + S_{\omega_l - \omega_m + \omega_n}(f)$$

$$+ S_{\omega_l - \omega_m - \omega_n}(f) \qquad \text{(D-22)}$$

where $\dfrac{K_1^2 K_2^2 K_3^2}{32} = \dfrac{K^2}{2}$ for this case.

Note that $K = \dfrac{3}{2} g_3 A_l A_m A_n$ now.

By carrying out the power series expression indicated in (D-3) to more terms, similar expressions for higher order product terms may be obtained if so desired.

For high deviation systems, the RF spectrum of the modulated carrier wave will be gaussian in shape if the modulating signal $\phi(t)$ is a gaussian random process.[4]

$$S_{\omega_n}(f) = \frac{A_n^2/2}{\sqrt{2\pi}\, f_{D_n}} \exp\left[-\frac{(f - f_n)^2}{2 f_{D_n}^2}\right] \qquad \text{(D-23)}$$

where

f_{D_n} = rms frequency deviation of carrier at ω_n

f_n = carrier frequency

$\frac{A_n^2}{2}$ = power in the wave

Also

$$S_{2\omega_m}(f) = \frac{B_m^2/2}{\sqrt{2\pi}\, 2 f_{D_m}} \exp\left[-\frac{(f-2f_m)^2}{8 f_{D_m}^2}\right] \qquad \text{(D-24)}$$

Then the spectrum at $2\omega_m - \omega_n$ is determined by convolving (D-23) and (D-24)

$$S_{2\omega_m - \omega_n}(f) = \frac{A_n^2 B_m^2}{16\sqrt{2\pi}\,\sigma} e^{-\frac{f^2}{2\sigma^2}} * \left\{\delta\left[f-(2f_m - f_n)\right] + \delta\left[f+(2f_m - f_n)\right]\right\} \qquad \text{(D-25)}$$

where $\sigma^2 = (f_{D_n}^2 + 4 f_{D_m}^2)$

We will assume that both signals have the same rms deviation f_D such that $\sigma^2 = 5 f_D^2$ and the single-sided spectral density is

$$S_{2\omega_m - \omega_n}(f) = \frac{C^2/2}{\sqrt{2\pi}\sqrt{5}\, f_D} \exp\left[-\frac{\left[f-(2f_m - f_n)\right]^2}{10 f_D^2}\right] \qquad \text{(D-26)}$$

where the power has been re-normalized to $C^2/2$, which is the power in the third order product at $(2\omega_m - \omega_n)$ relative to the desired carrier.

Similarly, the spectrum at $\omega_1 + \omega_m - \omega_n$ is determined by convolving three terms such as (D-23). Again assuming equal deviations and normalizing to $C^2/2$

$$S_{\omega_1+\omega_m-\omega_n}(f) = \frac{C^2/2}{\sqrt{2\pi}\sqrt{3}f_D} \exp\left[-\frac{\left[f-(f_1+f_m-f_n)\right]^2}{6f_D^2}\right] \qquad \text{(D-27)}$$

Equations (D-26) and (D-27) are the expressions for the power spectral density of the two types of third order product respectively. We now wish to determine the effect of these intermodulation products on the received baseband signal; hence we require an expression for the interference spectrum which appears at baseband due to these products. This spectrum is necessary to determine the location of the worst channel and the actual interference (intermodulation) noise present in that channel.

To calculate this interference spectrum we formulate a slightly different problem. Consider the input to a linear system to be made up of the original modulated carriers plus the intermodulation products. Since the system is now assumed linear we may calculate the effect of each product on a single carrier separately and treat the individual carriers one at a time. Then, as the carriers and intermodulation products are uncorrelated, the total noise at baseband is just the sum of the individual contributions due to each product.

Therefore, consider the sum of a single modulated carrier and a distortion product, both angle modulated.

$$A_1 \cos\left[\omega_1 t + \phi_1(t) + a_1\right] + A_2 \cos\left[\omega_2 t + \phi_2(t) + a_2\right]$$

where the variables are as previously defined with the exception that the subscript 2 now refers to the intermodulation product. The sum can be expressed in the well-known alternative form

$$A(t) \cos\left[\omega_1 t + a_1 + \phi_1(t) + \theta(t)\right] \qquad \text{(D-28)}$$

where $\phi_1(t)$ is now assumed to be the desired information-bearing signal and, for $A_2/A_1 << 1$,

$$\theta(t) = \frac{A_2}{A_1} \sin \left[(\omega_2 - \omega_1)\, t + \alpha + \phi_2(t) - \phi_1(t) \right] \qquad \text{(D-29)}$$

where $\alpha = \alpha_2 - \alpha_1$.

After perfect limiting and phase detection, the output signal is $\alpha_1 + \phi(t_1) + \theta(t)$. The power spectral density of this composite random process can be found, if it exists, as the Fourier transform of the covariance function of the process.

For the baseband power spectrum to exist, the process must be at least second-order stationary. We examine the first mean of the process $\alpha_1 + \phi_1(t) + \theta(t)$ for stationarity:

$$E\left[\alpha_1 + \phi_1(t) + \theta(t) \right] = E\,\alpha_1 + E\,\phi_1(t) + E\,\theta$$

$$= E\,\theta(t)$$

$$= E \frac{A_2}{A_1} \sin \left[(\omega_2 - \omega_1)\, t + \alpha + \phi_2(t) - \phi_1(t) \right]$$

$$= \frac{A_2}{A_1} \left\{ E \sin \left[\Delta\omega t + \phi_2 - \phi_1 \right] E \cos \alpha + E \cos (\Delta\omega t + \phi_2 - \phi_1)\, E \sin \alpha \right\}$$

$$= 0 \quad \text{since } E \cos \alpha = E \sin \alpha = 0$$

Note that $\omega_2 - \omega_1$ has been redefined as $\Delta\omega$. The desired process is therefore at least first order stationary.

Since the first mean of the process is zero, the covariance function and the autocorrelation function are identical. Therefore,

$$R(t_1, t_2) = E\left[a_1 + \phi_1(t_1) + \theta(t_1)\right] \quad \left[a_1 + \phi_1(t_2) + \theta(t_2)\right]$$

$$= E\,\phi_1(t_1)\,\phi_1(t_2) + E\,\phi_1(t_1)\,\theta(t_2) + E\,\phi_1(t_2)\,\theta(t_1)$$

$$+ E\,\theta(t_1)\,\theta(t_2) + E\,a_1^2 \qquad \text{(D-30)}$$

$$= R_{\phi_1}(t_1, t_2) + R_{\phi_1\,\theta}(t_1, t_2) + R_{\theta\phi_1}(t_1, t_2)$$

$$+ R_{\theta}(t_1, t_2) + E\,a_1^2$$

since $E\,a = 0$ and a is independent of $\phi_1(t)$ and $\theta(t)$. The first term is the autocorrelation function of the desired information process $\phi_1(t)$ and it should be noted that $R_{\phi_1}(t_1, t_2) = R_{\phi_1}(t_1 - t_2) = R_{\phi_1}(\tau)$, because $\phi_1(t)$ is assumed stationary. The remaining terms represent various forms of distortion due to the interfering signal. The cross-correlation terms take the form

$$R_{\phi_1\,\theta}(t_1, t_2) = E\left\{\phi_1(t_1)\,\frac{A_2}{A_1}\,\sin\left[\Delta\omega t_2 + a + \phi_2(t_2) - \phi_1(t_2)\right]\right\}$$

$$= \frac{A_2}{A_1}\,E\cos a\,E\left\{\phi_1(t_1)\,\sin\left[\Delta\omega t_2 + \phi_2(t_2) - \phi_1(t_2)\right]\right\}$$

$$+ \frac{A_2}{A_1}\,E\sin a\,E\left\{\phi_1(t_1)\,\cos\left[\Delta\omega t_2 + \phi_2(t_2) - \phi_1(t_2)\right]\right\}$$

$$= 0$$

That is, the processes $\phi_1(t)$ and $\theta(t)$ are uncorrelated. The only distortion term is therefore $R_{\theta}(t_1, t_2)$. This term may be evaluated as follows:

$$R_\theta(t_1, t_2) = \left(\frac{A_2}{A_1}\right)^2 E\left\{\sin\left[\Delta\omega t_1 + a + \phi_2(t_1) - \phi_1(t_1)\right]\right.$$
$$\left.\sin\left[\Delta\omega t_2 + a + \phi_2(t_2) - \phi_1(t_2)\right]\right\}$$

$$= \frac{1}{2}\left(\frac{A_2}{A_1}\right)^2 E\left\{\cos\left(\Delta\omega t + \Delta\phi_2 - \Delta\phi_1\right)\right. \qquad \text{(D-31)}$$
$$\left. - \cos\left[\Delta\omega(t_1 + t_2) + 2a + \Sigma\phi_2 - \Sigma\phi_1\right]\right\}$$

$$= \frac{1}{2}\left(\frac{A_2}{A_1}\right)^2 E\cos\left(\Delta\omega\tau + \Delta\phi_2 - \Delta\phi_1\right)$$

in which $\tau = t_1 - t_2$, $\Delta\phi = \phi(t_1) - \phi(t_2)$, $\Sigma\phi = \phi(t_1) + \phi(t_2)$
The last result (D-31) can be conveniently evaluated by noting that

$$E\cos\left(\Delta\omega\tau + \Delta\phi_2 - \Delta\phi_1\right) = \frac{1}{2}e^{i\Delta\omega\tau}\, E\exp\left(i\Delta\phi_2\right) E\exp\left(-i\Delta\phi_1\right)$$
$$+ \frac{1}{2}e^{i\Delta\omega t}\, E\exp\left(-i\Delta\phi_2\right) E\exp\left(i\Delta\phi_1\right)$$
$$= \frac{1}{2}e^{i\Delta\omega t}\, M_2(i\,1, -i\,1)\, M_1(-i\,1, i\,1)$$
$$+ \frac{1}{2}e^{-1\Delta\omega t}\, M_2(-i\,1, i\,1)\, M_1(i\,1, -i\,1)$$
$$= M_1(i\,1, -i\,1)\, M_2(i\,1, -i\,1)\cos\Delta\omega\tau$$

(D-32)

In the above, the joint characteristic function of the random variables $\phi(t_1)$ and $\phi(t_2)$ has been introduced:

$$M(iV_1, iV_2) = E\exp i\left[V_1\,\phi(t_1) + V_2\,\phi(t_2)\right]$$

For gaussian random variables[5] with zero means and variances σ_1^2, σ_2^2,

$$M(iV_1, iV_2) = \exp - \frac{1}{2}\left[\sigma_1^2 V_1^2 + 2\sigma_1\sigma_2\rho V_1 V_2 + \sigma_2^2 V_2^2\right],$$

and

$$M(i\,1, -i\,1) = \exp - \sigma^2(1-\rho) = \exp - \left[R(o) - R(\tau)\right].$$

Finally, then, we have for the distortion term,

$$R_\theta(\tau) = \frac{1}{2}\left(\frac{A_2}{A_1}\right)^2 \exp - \left[R(o) - R(\tau)\right] \cos \Delta\omega\tau, \qquad \text{(D-33)}$$

where $R(\tau) = R_{\phi_1}(\tau) + R_{\phi_2}(\tau)$ and $R_{\phi_1}(\tau)$, $R_{\phi_2}(\tau)$ are the autocorrelation functions of the processes $\phi_1(t)$, $\phi_2(t)$.

The autocorrelation function of the random phase process of the equivalent carrier has therefore been shown to be stationary. Furthermore, the desired phase information $\phi_1(t)$ and the phase distortion $\theta(t)$ have been shown to be uncorrelated processes. The autocorrelation function of the phase output or baseband signal is $R_{\phi_1}(\tau) + R_\theta(\tau)$.

The power spectral density of the interference can now be found as the Fourier transform of $R_\theta(\tau)$.

$$S_I(f) = \frac{1}{2}\left(\frac{A_2}{A_1}\right)^2 e^{-R(o)} \int_{-\infty}^{\infty} e^{R(\tau)} \cos\Delta_{\omega\tau} e^{-j\omega\tau}\, d\tau \qquad \text{(D-34)}$$

Thus, in principle, if the autocorrelation functions of the baseband processes $\phi_1(t)$ and $\phi_2(t)$ are known the spectrum of the interference as manifested at baseband can be calculated from (D-34). However, it is more practical to calculate the interference spectrum using the method of multiplying the autocorrelation functions as was done previously where $R(\tau)$ is given by (D-6). Then multiplying the autocorrelation functions of the two RF signals one obtains

$$R_1(\tau)\,R_2(\tau) = \frac{A_1^2 A_2^2}{4}\, e^{-\left[R(o) - R(\tau)\right]} \cos\omega_1\tau \cos\omega_2\tau$$

$$= \frac{A_1^2 A_2^2}{8}\, e^{-\left[R(o) - R(\tau)\right]} \left[\cos\Delta\omega\tau + \cos(\omega_1+\omega_2)\,\tau\right] \qquad \text{(D-35)}$$

where $R(\tau) = R_{\phi_1}(\tau) + R_{\phi_2}(\tau)$.

If we now take (D-35) to be a new autocorrelation function, and solve for the power spectrum, we find

$$S(f) = \frac{A_1^2 A_2^2}{8}\, e^{-R(o)} \int_{-\infty}^{\infty} e^{R(\tau)} \cos\Delta\omega\tau\, e^{-j\omega\tau}\, d\tau$$

$$+ \frac{A_1^2 A_2^2}{8}\, e^{-R(o)} \int_{-\infty}^{\infty} e^{R(\tau)} \cos(\omega_1+\omega_2)\,\tau\, e^{-j\omega\tau}\, d\tau \qquad \text{(D-36)}$$

If the desired carrier power is normalized to unity $\left(A_1^2/2 = 1\right)$, then the first term of (D-36) is seen to be just the result achieved in (D-34) for the power um spectrum of the baseband interference. The second term yields that portion of the power spectrum located at the frequency

$$(\omega_1 + \omega_2)/2\pi$$

which is of no interest in the baseband interference problem and may be disregarded. The importance of this result is that it allows the calculation of the baseband interference spectrum by the convolution of the spectra of the RF signals as demonstrated.

The RF spectra of interest to be used in calculating the baseband interference spectrum given by (D-34) are, re-writing expressions (D-23), (D-26), and (D-27), the spectrum at the carrier frequency

$$S_c(f) = \frac{A^2/2}{2\sqrt{2\pi}\,\sigma_c} e^{-\frac{f^2}{2\sigma_c^2}} * \left\{\delta(f - f_c) + \delta(f + f_c)\right\} \qquad \text{(D-37)}$$

the spectrum of the $2\beta_m - \beta_n$ type product

$$S_1(f) = \frac{C_1^2/2}{2\sqrt{2\pi}\,\sigma_1} e^{-f^2/2\sigma_1^2} * \left\{\delta\left[f - (f_c - \Delta f)\right] + \delta\left[f + (f_c - \Delta f)\right]\right\} \qquad \text{(D-38)}$$

and the spectrum of the $\beta_l + \beta_m - \beta_n$ type product

$$S_2(f) = \frac{C_2^2/2}{2\sqrt{2\pi}\,\sigma_2} e^{-f^2/2\sigma_2^2} * \left\{\delta\left[f - (f_c - \Delta f)\right] + \delta\left[f + (f_c - \Delta f)\right]\right\} \qquad \text{(D-39)}$$

where

$\frac{A^2}{2}$ = 1 is the normalized desired carrier power

$\frac{C^2}{2}$ = power of the third order product relative to the desired carrier

σ_c = f_D the rms frequency deviation of the carrier

σ_1 = $\sqrt{5}\, f_D$

σ_2 = $\sqrt{3}\, f_D$

Δf = difference between the desired carrier frequency and the frequency location of the intermodulation product being considered

Thus, the baseband interference spectrum due to $S_1(f)$ is determined by convolving $S_c(f)$ and $S_1(f)$

$$S_c(f) * S_1(f) = \frac{C_1^2/2}{4\sqrt{2\pi}\,\sigma} e^{-f^2/2\sigma^2} * \left\{\delta(f-\Delta f) + \delta(f+\Delta f)\right\} * \left\{\delta\left[f-(2f_c-\Delta f)\right] + \delta\left[f+(2f_c-\Delta f)\right]\right\}$$

where

$$\sigma^2 = \sigma_c^2 + \sigma_1^2 = f_D^2 + 5f_D^2 = 6f_D^2$$

Therefore:

$$S_{I_1}(f) = \frac{C_1^2/2}{4\sqrt{2\pi}\sqrt{6}\,f_D} e^{-f^2/12f_D^2} * \left\{\delta(f-\Delta f) + \delta(f+\Delta f)\right\} \qquad \text{(D-40)}$$

or writing in single-sided form

$$S_{I_1}(f) = \frac{C_1^2/2}{2\sqrt{2\pi}\sqrt{6}\,f_D} e^{-(f-\Delta f)^2/12f_D^2} \qquad \text{(D-41)}$$

Similarly, the interference spectrum due to $S_2(f)$ is

$$S_{I_2}(f) = \frac{C_2^2/2}{4\sqrt{2\pi}\,f_D} e^{-(f-\Delta f)^2/8f_D^2} \qquad \text{(D-42)}$$

With (D-41) and (D-42) it is now possible to compute the equivalent amount of noise in any telephone channel due to third order products. The flat-weighted noise in any channel is

$$N_F = k S_I(f)\, B, \text{ watts} \qquad \text{(D-43)}$$

where B is the channel bandwidth and k is a proportionality constant which relates radian deviations to watts. This factor is necessary as $S_I(f)$ has the dimensions of rad^2/cps. When (D-43) is expressed in terms of psophometrically weighted noise the flat weighted noise in a 3.1 kc bandwidth must be reduced by 2.5 db. The factor k is found from f_{drms}, the rms frequency deviation produced by a 0 dbm0, 800 cps test tone without pre-emphasis.

$$k = \frac{1 \text{ mw}}{f_{drms}^2 \; I(f)/f^2}, \quad \frac{\text{mw}}{\text{rad}^2} \qquad \text{(D-44)}$$

where I(f) is the pre-emphasis improvement factor at frequency f. Therefore, the psophometrically weighted noise in the channel located at f is given by

$$N_{pw} = \frac{3100}{10^{0.25}} \; \frac{f^2 \; S_I(f)}{f_{drms}^2 \; I(f)}, \text{ mw (psoph. weighted)} \qquad \text{(D-45)}$$

A multichannel FDM signal can be represented by a band of white gaussian noise extending from f_o to f_m, the minimum and maximum base-band frequencies respectively. CCIR has recommended that the power level of this equivalent noise signal be given by:[6]

$$P_{eq} = -15 + 10 \log N, \text{ dbm0 for } N \geq 240 \qquad \text{(D-46)}$$

where N_c is the number of telephone channels. Since f_{drms} corresponds to a 0 dbm0 test tone, the total rms deviation for N channels may be expressed in terms of P_{eq} and f_{drms}.

$$f_D = \sqrt{P_{eq}}\, f_{drms} \tag{D-47}$$

The only term in equation (D-45) left to be determined is the pre-emphasis factor I(f). Two pre-emphasis characteristics are considered here; 6 db per octave and CCIR. For 6 db per octave, I(f) has the simple form

$$I(f) = \frac{3f^2}{f_m^2 + f_m f_o + f_o^2} = \frac{f^2}{f_d^2} \tag{D-48}$$

where f_o and f_m are as previously defined and f_d is the mean baseband frequency; i.e., that frequency which produces the same deviation with and without pre-emphasis. Substituting (D-48), (D-47), and (D-41) into (D-45) we obtain N_{pw} due to the $2\beta_m - \beta_n$ type product.

$$N_{pw} = \left[\frac{3.1 \times 10^{12} f_d^2 C_1^2/2}{10^{0.25} f_{drms}^3 \, 4\sqrt{3\pi}\sqrt{P_{eq}}}\right] \exp\left[-\frac{(f-\Delta f)^2}{12 P_{eq} f_{drms}^2}\right] \text{pw (psoph)} \tag{D-49}$$

Similarly, using (D-42) instead of (D-41), N_{pw} for the $\beta_l + \beta_m - \beta_n$ type is

$$N_{pw} = \left[\frac{3.1 \times 10^{12} f_d^2 C_2^2/2}{10^{0.25} f_{drms}^3 \, 4\sqrt{2\pi}\sqrt{P_{eq}}}\right] \exp -\left[\frac{(f-\Delta f)^2}{8 P_{eq} f_{drms}^2}\right], \text{pw (psoph)} \tag{D-50}$$

From (D-49) and (D-50) it is seen that with 6 db per octave pre-emphasis, the worst channel is located where $(f - \Delta f)$ is smallest, the rest of the expression depending only on the number of channels, deviation chosen and the relative amplitude $C^2/2$.

The expression for CCIR pre-emphasis is more complex; however, a good approximation is obtained by representing the characteristic as a rising exponential.

$$I(f) = \alpha e^{\gamma f/f_m} \qquad \text{(D-51)}$$

where $\alpha = 0.288$, $\gamma = 2.14$, and f_m is the maximum baseband frequency as before. Using the approximation given by (D-51) in equation (D-45), an expression for the equivalent noise in the telephone channel located at frequency f is found for CCIR pre-emphasis

$$N_{pw} = \frac{X_i f^2}{\alpha} e^{-\gamma f/f_m} e^{-y_i (f - \Delta f)^2} \qquad \text{(D-52)}$$

where

$$X_i = X_1 = \frac{3.1 \times 10^{12}}{10^{0.25}} \frac{C_1^2/2}{4\sqrt{3\pi}\sqrt{P_{eq}} f_{drms}^3}$$

$$y_i = y_1 = \frac{1}{12 P_{eq} f_{drms}^2}$$

for the $2\beta_m - \beta_n$ type product, and for the $\beta_1 + \beta_m - \beta_n$ type product

$$X_i = X_2 = \sqrt{\frac{3}{2}} \frac{C_2^2}{C_1^2} X_1$$

$$y_i = y_2 = \frac{3}{2} y_1$$

The location of the worst channel is not immediately apparent from (D-52) but may be found by maximizing N_{pw} with respect to frequency. However, it is easier to maximize $\ln N_{pw}$.

$$\ln N_{pw} = \ln \frac{X_i}{a} + 2 \ln f - \frac{\gamma f}{f_m} - y_i (f - \Delta f)^2$$

$$\frac{d \ln N_{pw}}{df} = \frac{2}{f} - \frac{\gamma}{f_m} - 2 y_i (f - \Delta f) = 0 \qquad \text{(D-53)}$$

Solving (D-53) for f

$$f_w = - \frac{1}{2} \left(\frac{\gamma}{2 y_i f_m} - \Delta f \right) + \left[\frac{1}{4} \left(\frac{\gamma}{2 y_i f_m} - \Delta f \right)^2 + \frac{1}{y_i} \right]^{1/2} \qquad \text{(D-54)}$$

Hence, the location of the worst channel is seen to be a function of the number of channels and test tone deviation (as y_i is) and the separation, Δf, between the desired carrier and interfering product. This is in contrast to the 6 db per octave case which was a function of the separation only. Given the number of channels and f_{drms}, (D-54) may be solved for the worst channel for each Δf of interest and the corresponding pre-emphasis factor, $I(f_w)$, substituted back in equation (D-52) to determine the actual intermodulation noise.

If desired, the above results may be readily extended to include higher order products. The resulting expressions for the interference spectra and equivalent baseband noise will have the same form as (D-41) and (D-45), differing only by a multiplying constant and the deviation, σ, used in the calculations.

REFERENCES

1. H. E. Curtis, "Interference Between Satellite Communication Systems and Common Carrier Surface Systems," Conference Paper CP 62-343, presented at AIEE Winter General Meeting, January 1961, p. 11.

2. International Radio Consultative Committee (CCIR), "Documents of the IXth Plenary Assembly, Los Angeles, 1959 (Second Impression 1960)," Volume I, Recommendations, p. 238.

3. D. Middleton, "The Distribution of Energy in Randomly Modulated Waves," Phil. Mag., Vol. 42, July 1952, pp. 689-707.

4. _____, Introduction to Statistical Communication Theory, McGraw-Hill, 1960, p. 624.

5. W. B. Davenport, Jr., and W. L. Root, An Introduction to the Theory of Random Signals and Noise, McGraw-Hill, 1958, p. 149.

6. CCIR, p. 268.

APPENDIX E

QUASI-STATIONARY RESPONSE OF LINEAR TIME-INVARIANT SYSTEMS TO ARBITRARY INPUT SIGNALS

APPENDIX E

QUASI-STATIONARY RESPONSE OF LINEAR TIME-INVARIANT SYSTEMS TO ARBITRARY INPUT SIGNALS

Following Weiner and Leon's treatment (PGCT, June 1964, pp. 308-309), let

$$e_i(t) = \begin{cases} R_o\, e^{j\omega_c t} & t < 0 \\ R(t)\, e^{j\theta(t)} = R(t)\, e^{j\int_o^t \omega(u)\,du} & t \geq 0 \end{cases} \qquad \text{(E-1)}$$

R_o and $R(t)$ real and non-negative, be the input to a linear system with system response function

$$H(S) = \frac{A_m S^m + \cdots + A_o}{(S + S_1)(S + S_2)\cdots(S + S_n)}\,, \quad m < n\,, \quad S_i \neq S_j \qquad \text{(E-2)}$$

$$= \sum_{y'}^{n} \frac{K_y}{S + S_y}\,, \quad S_y = a_y + j\omega_y\,, \quad a_y > 0 \qquad \text{(E-3)}$$

The system impulse response is

$$h(t) = \sum_{y'}^{n} K_y\, e^{-S_y t} \qquad \text{(E-4)}$$

The system response to the input $e_i(t)$ is

$$e_o(t) = \int_{-\infty}^{t} h(t-\tau)\, e_i(\tau)\, d\tau = \int_{-\infty}^{o} h(t-\tau)\, e_i(\tau)\, d\tau + \int_{o}^{t} h(t-\tau)\, e_i(\tau)\, d\tau$$

$$= \sum_{y'}^{n} \frac{R_o K_y}{S_y + j\omega_c} e^{-S_y t} + \sum_{y'}^{n} \int_o^t K_y\, e^{-S_y(t-\tau)}\, R(\tau)\, e^{j\theta(\tau)}\, d\tau\,, \quad t > 0 \qquad \text{(E-5)}$$

The formula for integration by parts is

$$\int_a^b f\,dg = fg\Big|_a^b - \int_a^b g\,df \tag{E-6}$$

For each of the integrals in (E-5), let

$$f = \frac{K_y R(\tau)}{R'(\tau) + R(\tau)\left[S_y + j\theta'(\tau)\right]} \tag{E-7}$$

and

$$dg = \left[R'(\tau) + (S_y + j\theta'(\tau))\,R(\tau)\right]\, e^{-S_y(t-\tau)}\, e^{j\theta(\tau)}\, d\tau$$

Then

$$df = \frac{d}{d\tau}\left\{\frac{K_y R(\tau)}{R'(\tau) + R(\tau)\left[S_y + j\theta'(\tau)\right]}\right\} d\tau \tag{E-8}$$

and

$$g = R(\tau)\, e^{-S_y(t-\tau)}\, e^{j\theta(\tau)}$$

Evaluating the integrals in (E-5)

$$e_o(t) = \sum_{y'}^{n} \frac{K_y R(t)^2}{R'(t) + R(t)\left[S_y + j\theta'(t)\right]}\, e^{j\theta(t)}$$

$$+ \sum_{y'}^{n} K_y \left\{\frac{R_o}{S_y + j\omega_c} - \frac{R^2(o)}{R'(o) + R(o)\left[S_y + j\omega(o)\right]}\right\} e^{-S_y t}$$

$$- \sum_{y'}^{n} \int_o^t \frac{d}{d\tau}\left\{\frac{K_y R(\tau)}{R'(\tau) + R(\tau)\left[S_y + j\theta'(\tau)\right]}\right\} R(\tau)\, e^{-S_y(t-\tau)}\, e^{j\theta(\tau)}\, d\tau$$

(E-9)

Equation (E-9) can be written

$$e_o(t) = H\left[\frac{R'(t)}{R(t)} + j\theta'(t)\right] R(t)\, e^{j\theta(t)}$$

$$+ \sum_{y'}^{n} K_y \left\{ \frac{R_o}{S_y + j\omega_c} - \frac{R^2(o)}{R'(o) + R(o)\left[S_y + j\omega(o)\right]} \right\} e^{-S_y t}$$

$$- \sum_{y'}^{n} \int_o^t \frac{d}{d\tau} \left\{ \frac{R(\tau)}{R'(\tau) + R(\tau)\left[S_y + j\theta'(\tau)\right]} \right\} K_y R(\tau)\, e^{-S_y(t-\tau)}\, e^{j\theta(\tau)}\, dt \qquad \text{(E-10)}$$

Hence

$$e_o(t) \cong H\left[\frac{R'(t)}{R(t)} + j\theta'(t)\right] R(t)\, e^{j\theta(t)} \quad , \quad t >> 0 \qquad \text{(E-11)}$$

if

$$\left| \frac{d}{d\tau} \left\{ \frac{R(\tau)}{R'(\tau) + R(\tau)\left[S_y + j\theta'(\tau)\right]} \right\} \right| << 1 \qquad \text{(E-12)}$$